MULTI-OBJECTIVE OPTIMIZATION OF RESIDENTIAL BUILDINGS FOR IMPROVING INDOOR THERMAL COMFORT WHILE REDUCING ENERGY CONSUMPTION

A Thesis Submitted to
the Graduate School of Engineering and Sciences of
İzmir Institute of Technology
in Partial Fulfillment of the Requirements for the Degree of

MASTER OF SCIENCE

in Architecture

by
Ece ÖZYILMAZ

June 2024
İZMİR

We approve the thesis of **Ece ÖZYILMAZ**

Examining Committee Members:

Assoc. Prof. Dr. Zeynep DURMUŞ ARSAN
Department of Architecture, Izmir Institute of Technology

Prof. Dr. Mustafa Emre İLAL
Department of Architecture, Izmir Institute of Technology

Prof. Dr. Gülsu ULUKAVAK HARPUTLUGİL
Department of Architecture, Çankaya University

12 June 2024

Assoc. Prof. Dr. Zeynep DURMUŞ ARSAN
Supervisor, Department of Architecture
Izmir Institute of Technology

Prof. Dr. Koray KORKMAZ
Head of the Department of Architecture

Prof. Dr. Mehtap EANES
Dean of the Graduate School of
Engineering and Science

ACKNOWLEDGMENTS

First of all, my dear advisor, Associate Professor Dr. Zeynep Durmuş Arsan, I would like to thank you for the support, effort, encouragement, guidance, and time.

This thesis study was supported within the scope of The Scientific and Technological Research Council of Türkiye (TUBITAK) Directorate of Science Fellowships and Grant Programmes (BİDEB) 2210/A - Domestic Graduate Scholarship Program. It was also supported within the scope of Izmir Institute of Technology Scientific Research Projects (BAP) with the project number 2023IYTE-1-0010. The program financed the measurement device and the participation fee for the 11th Global Warming Global Conference held at Haliç University on 14-16 June 2023, İstanbul. I want to thank TUBITAK and IZTECH Scientific Research Projects Coordination Office for their contribution to the realization process of this research.

I want to thank the IZTECH Faculty of Architecture, Building Physics Laboratory, for providing the DesignBuilder software student license and measurement equipment.

I want to thank my dear mother, Ayşe Özyılmaz, my dear father, Recai Özyılmaz, and my dear brother, Emre Özyılmaz, for their support and patience.

ABSTRACT

MULTI-OBJECTIVE OPTIMIZATION OF RESIDENTIAL BUILDINGS FOR IMPROVING INDOOR THERMAL COMFORT WHILE REDUCING ENERGY CONSUMPTION

In recent years, residential buildings designed with high window-to-wall ratios regardless of direction have become widespread. These design solutions cause thermal discomfort, especially overheating, and increased energy consumption and cooling load.

The main aim of this study is to determine the most and least sensitive design variables affecting energy consumption and thermal comfort of an existing residential building and to find optimum retrofit solutions reducing energy consumption while improving thermal comfort. The south-facing residential block built in 2019, located in the Mediterranean climate region, was selected as the case. The simulation model created in DesignBuilder was calibrated according to hourly monitored indoor temperature data for eight-months period.

Uncertainty and sensitivity analysis was performed due to eliminate the design variables with low sensitivity. NSGA-II algorithm was performed. Six retrofit scenarios were defined: building envelope features as passive ones, HVAC system features as active ones, and all design variables as combination. While the first three scenarios aim to minimize energy consumption and discomfort hours, the other three scenarios aim to minimize cooling load and discomfort hours.

In conclusion, cooling-heating set point, shading type, infiltration rate, and window-to-wall ratios were defined high sensitivity variables. The heating system operating schedule, cooling system performance coefficient, heating system efficiency, partition wall type, and window frame type variables have low sensitivity for thermal comfort and energy consumption.

Optimum solutions in which all objective functions can be improved compared to the base case were found in the third and sixth scenarios. In these scenarios, it is seen that only active or only passive design variables may be inadequate to solve the overheating problem. By evaluating both active and passive design variables, the overheating problem has been solved.

ÖZET

KONUT BİNALARINDA ENERJİ TÜKETİMİNİ AZALTIRKEN İÇ ISIL KONFORU İYİLEŞTİRMEK İÇİN ÇOK AMAÇLI OPTİMİZASYON

Son yıllarda yön gözetmeksizin yüksek cam-cephe oranı ile tasarlanan konut yapıları yaygınlaşmaktadır. Bu tasarım çözümleri başta aşırı ısınma olmak üzere, ısıl rahatsızlık ile yüksek enerji tüketimi ve soğutma yükü gibi sorunlara yol açmaktadır.

Bu çalışmanın ana amacı, mevcut bir konut binasının enerji tüketimi ve ısıl konforu üzerinde en yüksek ve en düşük hassasiyete sahip tasarım değişkenlerini belirlemek ve enerji tüketimini azaltırken ısıl konforu iyileştiren optimum yenileme çözümlerini bulmaktır. Akdeniz iklim bölgesinde yer alan, 2019 yılında inşa edilmiş, güneye cepheli bir konut bloğu örnek olarak seçilmiştir. DesignBuilder'da oluşturulan model, saatlik iç mekan sıcaklık izleme verilerine göre sekiz aylık bir dönem için kalibre edilmiştir.

Çalışma kapsamında belirsizlik ve duyarlılık analizi yapılmış, analiz sonuçlarına göre duyarlılığı düşük bulunan değişkenler dikkate alınmamıştır. NSGA-II algoritması kullanılmıştır. Altı adet iyileştirme senaryosu tanımlanmıştır. Bunlar, bina zarfı özelliklerini değerlendirmeye yönelik pasif olanlar, HVAC sistemi özelliklerini değerlendiren aktif olanlar ve ilk iki senaryoda alınan tüm tasarım değişkenlerini değerlendiren senaryolar. İlk üç senaryoda enerji tüketimini ve konforsuz saatleri en aza indirmek hedeflenirken, diğer üç senaryoda soğutma yükünü ve konforsuz saatleri en aza indirmek amaçlanmaktadır.

Duyarlılık analizi sonuçlarına göre soğutma-ısıtma ayar noktası, gölgeleme tipi, hava kaçağı, pencere duvar oranları her iki amaç fonksiyonu için de yüksek hassasiyete sahip değişkenlerdir. Isıtma sistemi çalışma takvimi, soğutma sistemi performans katsayısı, ısıtma sistemi verimliliği, iç duvar tipi ve pencere çerçeve tipi değişkenlerinin duyarlılığının düşük olduğu sonucuna ulaşılmıştır.

Üçüncü ve altıncı senaryolarda tüm amaç fonksiyonları mevcut duruma göre iyileşebildiği optimum çözümler bulunmuştur. Bu senaryolarda, yalnızca aktif veya yalnızca pasif tasarım değişkenlerinin aşırı ısınma problemini çözmek için yetersiz olabileceği görülmektedir. Hem aktif hem de pasif tasarım değişkenleri değerlendirilerek aşırı ısınma problemi çözülmüştür.

TABLE OF CONTENTS

LIST OF FIGURES

Figure **Page**

LIST OF TABLES

Table **Page**

LIST OF ABBREVIATIONS

BES: Building Energy Simulation

CDD: Cooling Degree Days

CoP: Coefficient of Performance

DB: DesignBuilder

EPS: Expanded Polystyren Foam

GDM: General Directorate of Meteorology

HDD: Heating Degree Days

HVAC: Heating, Ventilation and Air Conditioning

KS: Kolmogorov-Smirnov

LHS: Latin Hypercube Sampling

MBE: Mean Bias Error

MSE: Mean Squared Error

PCC: Partial Correlation Coefficients

PEAR: Pearson Correlation Coefficient

PRCC: Partial Rank Correlation Coefficient

RMSE: Root Mean Squared Error

SA: Sensitivity Analysis

SHGC: Solar Heat Gain Coefficient

SPEA: Spearman Correlation Coefficient

SRC: Standardised Regression Coefficients

SRRC: Standardized Rank Regression Coefficient

TRNSYS: Transient System Simulation Program

TUBITAK: The Scientific and Technological Research Council of Türkiye

TUIK: Türkiye Statistical Institute

U value: Heat Transfer Coefficient

UA/SA: Uncertainty and Sensitivity Analysis

UA: Uncertainty Analysis

CHAPTER 1

INTRODUCTION

1.1. Problem Statement

The increasing need for energy in the world every year and using non-renewable energy resources to meet this need cause negative consequences. Buildings are responsible for approximately 40% of the energy consumed in the European Union (EU) (European Commission 2020). According to the results of the study conducted by The Republic of Türkiye Ministry of Energy and Natural Resources, this rate is 32.3% in Türkiye (Kabakçı 2017). In addition, buildings cause around 39% of global carbon emissions (Adams et al. 2019). According to these statistics, it is understood that buildings play a crucial role in reducing energy consumption and carbon emissions. The high consumption rates attract attention when focusing on building types, mainly residential buildings. The housing sector causes 17% of total carbon emissions and 25% of energy consumption worldwide (Delmastro et al. 2021; Nejat et al. 2015).

It is predicted that energy consumption and carbon emission rates will increase in the coming years due to the climate crisis, global warming, and increasing population. A study stated that global carbon emissions have increased by an average of 2% annually in the last 20 years and will rise with the increasing population in the coming years (Chen et al. 2017). Temperatures in the world have risen by approximately 1.0 ºC compared to the pre-industrial period, and according to the Intergovernmental Panel on Climate Change report, it is predicted to exceed 1.5 ºC between 2030 and 2052 (IPCC 2018).

Temperature increases cause overheating problems, especially in regions with hot and humid climates, such as the Mediterranean climate. According to the data obtained from The General Directorate of Meteorology for Izmir province, when heating degree days (HDD) and cooling degree days (CDD) were compared for the years between 2000 and 2023, it was calculated that HDD decreased by 32.5% and CDD increased by 4.15% (General Directorate of Meteorology 2024). Figure 1.1 graphically shows the annual HDD and CDD indices for Izmir between 2000 and 2023. It conveys that the CDD indices

are increasing while the HDD indices are decreasing. The trendlines in the figure also get closer to each other over the years. Such changes are observed due to global warming and climate change, and these indices are predicted to be almost equal in the coming years (for further information see 3.1.1).

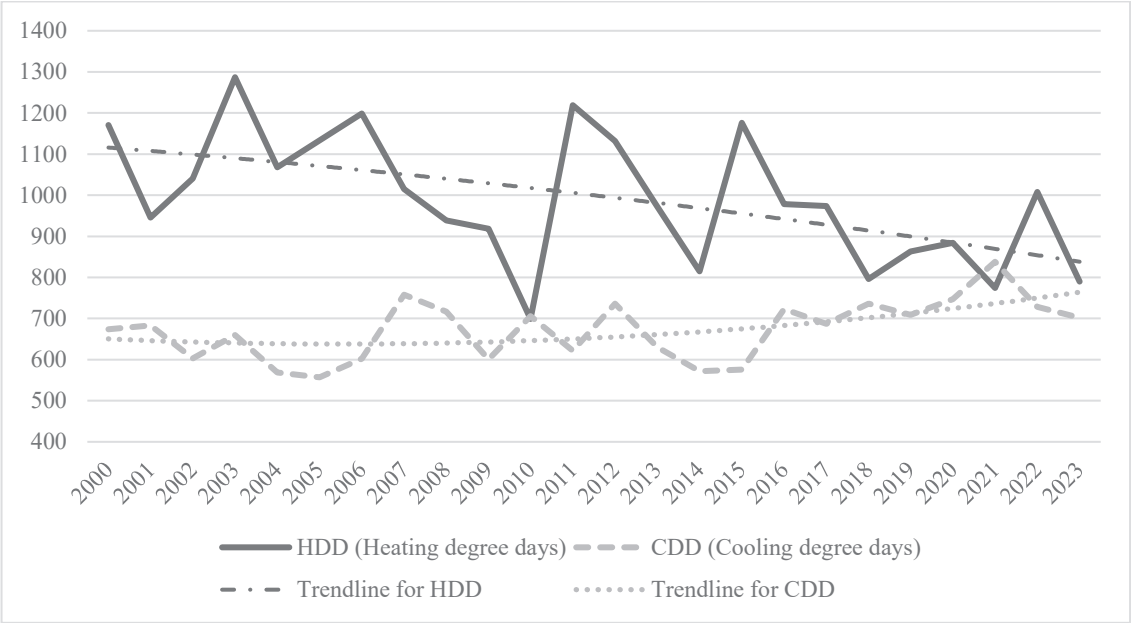

Figure 1.1. Annual Heating-Cooling Degree Days and trendlines for Izmir between 2000-2023 (Source: General Directorate of Meteorology 2024)

Most energy consumption and carbon emissions are caused by ever-increasing heating and cooling demands for better thermal comfort levels (Wan et al. 2011). According to the 'Energy Accounts' research conducted by TUIK (Türkiye Statistical Institute) in 2023, approximately 47% of household energy use is caused by heating and cooling needs (Figure 1.2) (TUIK 2023). At this point, it is understood that thermal comfort and energy consumption should be considered together because focusing on only one of these may result in negative results for the other. Chaudhuri et al. (2019) also emphasized that building energy consumption and carbon emissions should be considered together with indoor thermal comfort.

It is seen that the 1+0, 1+1, and 2+1 flat types in residential buildings, commonly available in recent years, are designed regardless of direction. Designing the same kind of flats with similar openings in all directions causes increased thermal discomfort and energy consumption. High window-to-wall ratios, mainly situated on southern facades, result in overheating problems that require analysis of retrofit scenarios specially

designed for each direction. Determining optimum retrofit solutions may allow for improving thermal comfort while minimizing energy consumption.

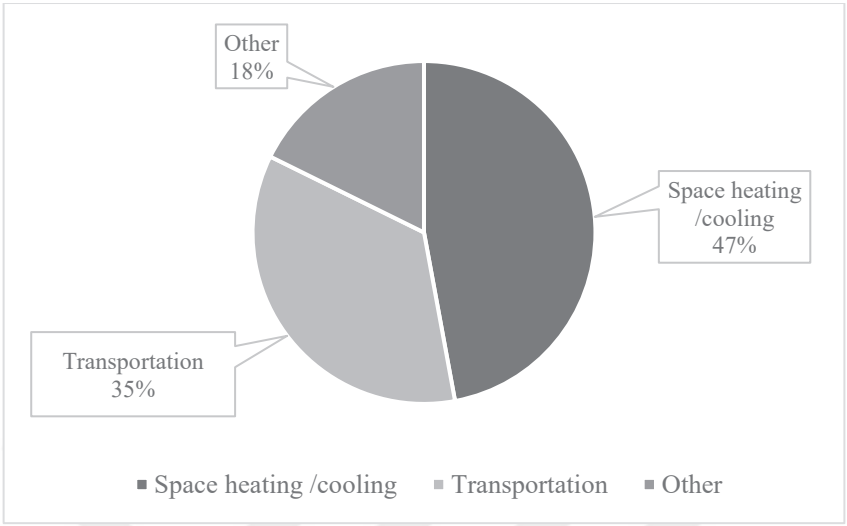

Figure 1.2. Final energy use of households by purpose (Source: TUIK 2023)

1.2. Aim, Scope, and Objectives of the Study

With increasing temperatures day by day, thermal comfort worsens while energy consumption and carbon emissions increase. This thesis study addresses these two contradictory main targets, i.e. energy consumption or cooling load and thermal comfort, and evaluates them through building energy analyses. The main aim of this study is to determine the most and least sensitive variables on energy consumption and thermal comfort of an existing residential building and to find optimum retrofit solutions that improve thermal comfort while reducing energy consumption and cooling loads.

It is considered that energy consumption, cooling load and thermal discomfort hours of existing buildings, especially those in hot and humid climates such as the Mediterranean climate, have risen due to the climate crisis and increasing temperatures, and therefore, developing retrofit solutions is the necessity. According to the research conducted in 2020, the number of residential buildings in existing building stock in Türkiye constitutes 85% of the total number of buildings (Tunç 2021). In addition, existing residential buildings in Türkiye are responsible for 21% of the total final energy consumption (Bayraktar et al., 2023). Due to these high statistical rates, the importance of retrofit scenarios in existing residential buildings is understood.

This thesis focuses on existing residential buildings with their common design problems causing overheating: first, residential buildings with high window-to-wall ratios; second, residential buildings with openings without considering the orientation. Therefore, a residential building in Izmir, where studio-type units with high window-to-wall ratios are frequently seen, was chosen as the case study. A studio-type flat was designed with openings regardless of orientation, plus to high window-to-wall ratios, especially on the south façade. These design decisions cause thermal discomfort and, accordingly, an increase in energy consumption. The problem of overheating is encountered throughout the summer months and expands to the autumn and spring months. It is predicted that this problem may reach more disturbing levels with the possible climate crisis in the coming years. With the selected case study, this thesis proceeded in line with the following research questions:

- What are the design variables and objective functions evaluated in optimization studies in the field of architecture?
- What are the sensitive design variables for thermal comfort and energy consumption in residential buildings located in the Mediterranean climatic region?
- What are the current thermal comfort level and annual energy consumption of a studio-type flat in an existing residential building in Izmir?
- Is it possible to solve the overheating problem seen in residential buildings in the Mediterranean climatic region only with precautions on the building envelope?
- Can high thermal discomfort hours and energy consumption be reduced with reconsidering the properties of heating and cooling systems?
- How much can energy consumption, cooling load and thermal discomfort hours be reduced by implementing solutions both on the building envelope and heating and cooling system requirements? Can the overheating problem be overcome with these related design variables?

1.3. Thesis Method

The methodology of this thesis consists of seven main steps (Figure 1.3). In the first step of the study, a literature review was conducted using the keywords of ‘multi-objective optimization, uncertainty and sensitivity analysis, thermal comfort, energy consumption, Mediterranean climate, and overheating.’ The methodology of the thesis

and the decision on type of case flat were done in the light of this literature review. For the second step of the study, the case building and its surroundings were modeled. Indoor thermal conditions were monitored, and outdoor climatic data were obtained. To increase the accuracy of the simulation model and reduce its deviation, the calibration study was carried out with eight months of monitoring data of indoor air temperatures. During the calibration process, root mean squared error (RMSE) and mean bias error (MBE) indices, determined by ASHRAE Guideline 14, were calculated (ASHRAE Guideline 14 2002). In the third step, the monitoring and simulation model results of the case flat representing current conditions were analyzed. Energy consumption and thermal discomfort hours were calculated through the calibrated simulation model. A psychometric chart was created according to ASHRAE 55 Standards by using monitoring values taken from the case room (ASHRAE 55 2004). The number of discomfort hours obtained from this chart was compared with the data taken from the simulation model. Additionally, the energy consumption bills for heating and cooling of the case flat were stated. In line with these calculations and literature review, in the fourth step, the problem formulation resulted in defining design variables and objective functions.

The fifth step, including the uncertainty and sensitivity analysis processes, was conducted to identify uncertainties that may occur in the objective functions, and to reduce the calculation time and number of design variables. These analyses were run in DesignBuilder energy performance simulation software. Possible deviations in the objective functions were evaluated with the uncertainty analysis. The sensitive design variables were identified with the sensitivity analysis. Therefore, design variables were grouped as having high sensitivity, medium sensitivity, and low sensitivity variables. The design variables with low-level sensitivity were excluded for multi-objective optimization study.

In the sixth step, the multi-objective optimization process, carried out through DesignBuilder, was advanced. Six different retrofit scenarios were performed based on the grouping of design variables and objective functions. The building envelope and its features were evaluated in the first and fourth scenario. The heating and cooling system and its features were evaluated in the second and fifth scenario. Lastly, including building envelope and heating cooling system and its features were evaluated in the third and sixth scenario.

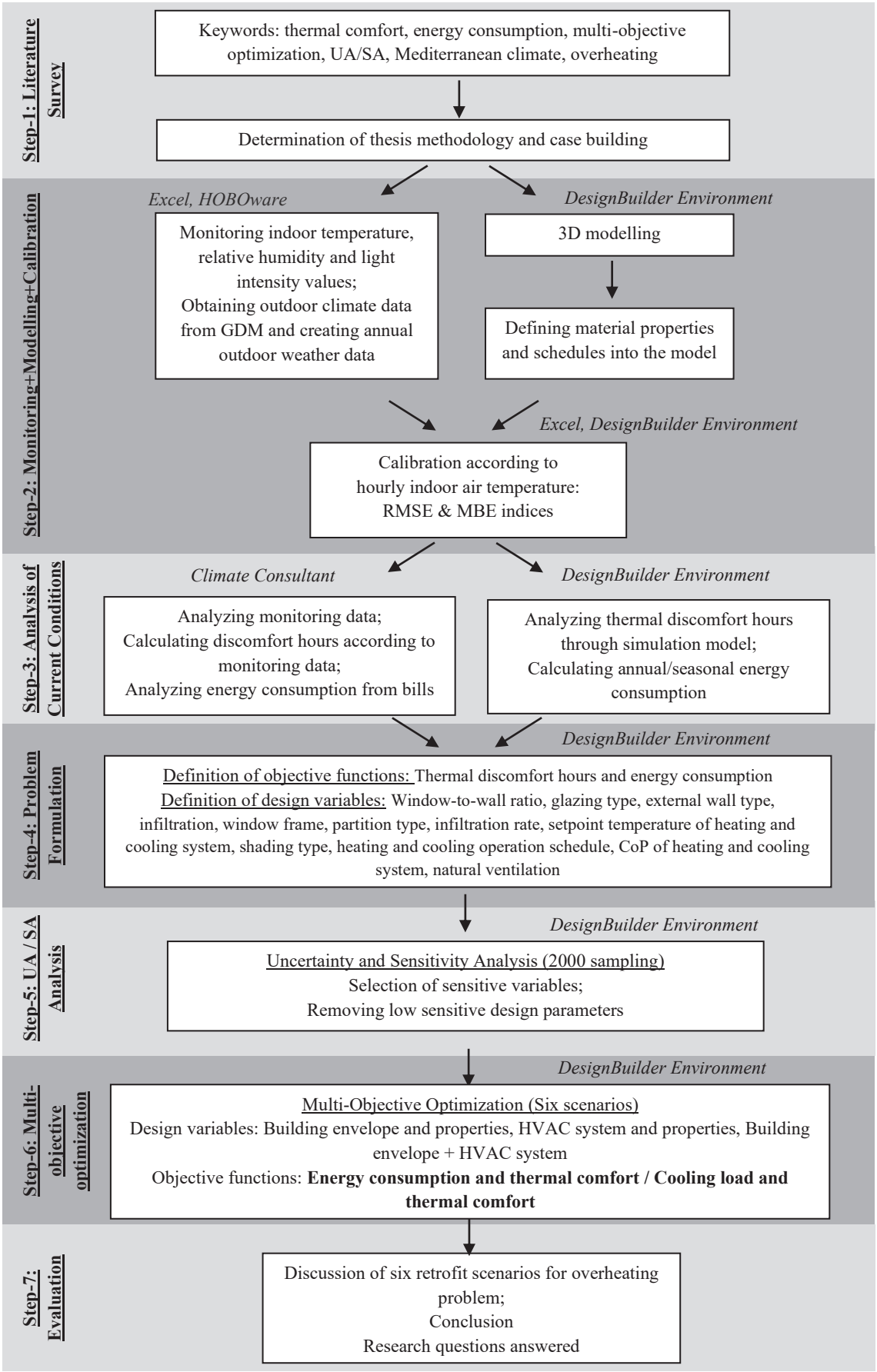

Figure 1.3. Flow chart of the thesis study (*Italics* refers to programs used in the study)

In the last step, the convenience of the six retrofit scenarios considered for the overheating problem was evaluated and optimum solutions that ensure the reduction of both objective functions were listed. The values of the design variables in the optimum results and in the current situation were analyzed. As a result, research questions were answered. Basic recommendations were made for south facing residential buildings in the Mediterranean climate.

1.4. Limitations and Assumptions

There are several limitations and assumptions in the thesis, including the selection of the case flat and the simulation model. Firstly, a south-facing studio-type flat was chosen as the case flat. Because, one of the facades most affected by the overheating problem in Izmir is the south facades. Therefore, the care was taken to choose a flat facing south where the permission for monitoring could be obtained. A studio type flat with a south facade was selected as a case flat.

Secondly, some assumptions arose from using the dynamic building simulation software. While creating three-dimensional model and entering data such as occupancy schedule and material properties closest to the existing situation, some model inputs contain missing information minimized through assumptions. The case flat is modeled as a 'building' block type, while the lower, upper, side, and other flats in the apartment are modeled as an adiabatic block type, assuming that it does not transfer heat beyond their outer surface. Therefore, heat gains and losses from the lower, upper, and side surfaces are not included in the calculations. In addition, since the adjacent flats were modeled as an 'adiabatic block,' the adjacent walls between the side flats and the case flat were modeled as external walls by the software.

1.5. Thesis Outline

There are five main chapters in this thesis: the first chapter explains the problem definition, aim, scope, and research questions of the study. Additionally, information about the thesis method is given.

In the second chapter, the literature review is conducted, which forms the background of the study. The methodologies, design variables and objective functions of

the studies are examined. In the light of the systematic literature review, the methodology of the thesis and case flat are decided.

In the third chapter, information about the case flat, conditions and data of the monitoring process, dynamic simulation model, calibration of the model, and optimization method are explained in detail. Firstly, the location and climate characteristics of the case building, monitoring campaign, and conditions of the case building during the monitoring period are presented. The calibration and simulation processes of the model are mentioned. Additionally, the methods followed for uncertainty and sensitivity analysis and the multi-objective optimization methodology of the thesis are described.

The fourth section includes monitoring, calibration, simulation, UA/SA, and multi-objective optimization results. Sensitive and less sensitive design variables determined as a result of sensitivity analysis. The efficiency of multi-objective optimization scenarios in terms of solving the overheating problem is evaluated. Each of the optimal results that reduce both objective functions is examined in the discussion section. Based on the optimum results, recommendations are developed for south-facing residential buildings in the Mediterranean climate zone. Finally, the fifth chapter underlines the outcomes of multi-objective optimization study, the answers to the research questions, and insights for further study.

CHAPTER 2

LITERATURE REVIEW

The second chapter conveys the literature review on uncertainty-sensitivity analysis, optimization methods, and optimization of design solutions for buildings. The first part is the evaluation of the systematic literature review. In the second part, the purposes of uncertainty and sensitivity analyses, examples, and characteristics of local and global sensitivity analyses are stated. The third part includes modeling and simulation methods in studies on building performance. The fourth part gives information about multi-objective optimization and genetic algorithms used in the literature.

Optimization is searching and comparing all possible situations concerning the targeted objective until the best result or results are found (The Merriam-Webster Dictionary 2024). The targeted objective in the optimization process is called as the objective function, and optimization processes are divided into two according to the number of objective functions: single-objective optimization and multi-objective optimization. Many problems encountered in life have multiple and conflicting goals (Miettinen 1999). Multi-objective optimization problems aim to optimize by considering two or more conflicting goals together, and in multi-objective problems, not a single best result, but a set of best results is obtained (Hwang and Masud 1979; Boyd and Vandenberghe 2004). The set containing these best solutions is called the Pareto-optimal solution set, and no solution has any superiority over the other (Hwang and Masud 1999).

Optimization problems are frequently encountered in all areas of life, and these problems are generally examples of multi-objective optimization with two or more conflicting objective functions (Boyd and Vandenberghe 2004). An engineer's objective of achieving maximum profit with the least cost or aiming for two functions to obtain the maximum value in a mathematical problem can be examples of optimization problems. Optimization problems encountered in every field are also encountered in many processes in the architectural discipline.

Making building design decisions or determining retrofit scenario conditions are complex in architecture. The design decisions made in these processes affect the thermal and visual comfort of the individual living in the building, energy consumption, carbon emissions, life cycle cost, and investment cost. These outputs are decisive and contradictory objectives for the individual, the building, and the building environment.

For this reason, interest in multi-objective optimization studies in architecture has been increasing rapidly, especially in recent years (Abdou et al. 2021; Acar et al. 2021; Albatayneh 2021; Asadi et al. 2014; Ascione et al. 2015; Ascione et al. 2020; Ascione et al. 2023; Badeche and Bouchahm 2020; Baghoolizadeh et al. 2023; Besbas et al. 2022; Bre and Fachinotti 2017; Bre et al. 2016; Chaudhuri et al. 2019; Chen et al. 2022; Chen et al. 2024; D'Agostino et al. 2023; Ekici et al. 2016; Gao et al. 2023; Goua et al. 2018; Hawila and Merabtine 2021; Huo et al. 2024; Hwang and Chen 2022; Kang et al. 2024; Khani et al. 2022; Li and Chen 2023; Long 2023; Lu et al. 2020; Magnier and Haghighat 2010; Mostafazadeh et al. 2023; Mukkavaara and Shadram 2021; Ouanes and Sriti 2024; Özerol and Selçuk 2023; Rosso et al. 2020; Saryazdi et al. 2022; Si et al. 2019; Wang et al. 2023; Wu et al. 2024; Xu et al. 2023; Yaşar and Sumer Haydaraslan 2023; Yigit 2021; Yu et al. 2015; Zhang et al. 2022).

While these conflicting objectives are addressed during the building design or retrofit process, various design variables should be evaluated together. Otherwise, when each design variable is considered separately, the relationship between the inputs will be ignored, which will reduce the accuracy and reliability of the result.

As the number of design variables and objective functions increases, the complexity of the problem and the calculation time required for the solution also proliferate. It is strategically vital to determine sensitive design variables and progress the study with these variables, especially in retrofit scenarios.

2.1. Evaluation of Systematic Literature Review

Various design variables and objective functions are considered in studies regarding optimization, sensitivity analysis, or retrofit scenarios. For this thesis study, sixty journal articles, seven books, ten thesis studies, and eleven review studies were scanned during the literature review. Of the sixty journal articles examined, sensitivity analysis and optimization studies were performed together in fourteen of them, only sensitivity analysis was performed in ten of them, uncertainty and sensitivity analyses were performed together in five, and only optimization studies were performed in thirty-one. Table 2.1 gives the distribution of design variables and objective functions used in these studies.

Table 2.1. Variables and objective functions of the studies identified by systematic literature review

	Design Variables																							Objective Functions				
Author(s)	Infiltration rate	Window wall ratio	Window U value (window-	Window frame type	Number of stories	Weather data	Window SHGC	Efficiency or properties of	Occupancy	Floor type	DHW system	Thermal mass	Window opening control	Natural ventilation	Window shading type	HVAC system (efficiency	Heating/ cooling set-point	Mechanical ventilation	Internal gains	Building layout	Building orientation	Outdoor air flow rate	Roof type	Wall type	Thermal comfort	Energy consumption	Carbon emissions	Cost	Visual comfort
Yigit		+								+				+						+	+		+	+		+			
Yildiz et al.	+	+	+				+			+				+					+				+	+		+			
Carmino et al.	+		+					+		+				+		+	+		+				+	+		+			
Huang et al.			+							+													+	+		+			
Encinas, De Herde	+											+		+	+				+		+				+				
Yu et al.		+	+																		+		+	+	+				
Gercek, Arsan			+			+	+			+					+								+	+		+			
Gou et al.		+	+	+			+						+								+	+	+	+	+				

(cont. on the next page)

Table 2.1(cont.)

	Design Variables																						Objective Functions				
Author(s)	Air infiltration rate	Window wall ratio	Window U value (window-	Window frame type	Number of stories	Weather data	Window SHGC	Efficiency or properties of	Occupancy	Floor type	DHW system	Thermal mass	Window opening control	Natural ventilation	Window shading type	HVAC system (efficiency	Heating/ cooling set-point	Mechanical ventilation	Internal gains	Building layout	Building orientation	Outdoor air flow rate	Roof type	Wall type	Thermal comfort	Energy consumption	Carbon emissions	Cost	Visual comfort
Asadi et al.			+													+							+	+	+		+	
Magnier, Haghighat		+	+							+		+				+									+	+			
Yildiz, Arsan	+	+	+				+			+				+			+			+			+	+		+			
Sarvazdi et al.			+														+		+						+	+	+		
Bre et al.	+		+							+					+						+		+	+	+	+			
Zhang et al.		+													+						+			+					
Mukkavaara,			+							+													+	+		+			
Acar et al.			+							+											+		+	+			+		

(cont. on the next page)

Table 2.1(cont.)

	Design Variables																						Objective Functions				
Author(s)	Air infiltration rate	Window wall ratio	Window U value	Window frame type	Number of stories	Weather data	Window SHGC	Efficiency or properties of	Occupancy	Floor type	DHW system	Thermal mass	Window opening control	Natural ventilation	Window shading type	HVAC system (efficiency	Heating/ cooling set-point	Mechanical ventilation	Internal gains	Building layout	Building orientation	Outdoor air flow rate	Roof type	Wall type	Thermal comfort	Energy consumption	Carbon emissions	Cost	Visual comfort
Hwang, Chen			+			+									+						+				+	+			
Rabani et al.		+	+									+			+	+			+				+	+	+	+			+
Ascione et al.			+					+								+	+								+	+		+	
Rosso et al.			+					+		+														+		+	+	+	
Bre, Fachinotti	+		+							+				+							+		+	+	+	+			
Ascione et al.																	+								+	+			
Baghoolizadeh et al.						+							+		+		+				+				+	+			+
Escandón et al.	+	+	+	+	+					+				+					+	+	+		+	+	+				

(cont. on the next page)

Table 2.1(cont.)

	Design Variables																							Objective Functions				
Author(s)	Air infiltration rate	Window wall ratio	Window U value (window-Window frame type	Number of stories	Weather data	Window SHGC	Efficiency or properties of	Occupancy	Floor type	DHW system	Thermal mass	Window opening control	Natural ventilation	Window shading type	HVAC system (efficiency or	Heating/ cooling set-point	Mechanical ventilation	Internal gains	Building layout	Building orientation	Outdoor air flow rate	Roof type	Wall type	Thermal comfort	Energy consumption	Carbon emissions	Cost	Visual comfort
Gao et al.							+						+			+								+		+		
D'Agostino et al.	+	+	+		+		+	+	+	+	+				+	+	+	+					+	+				
Lu et al.	+							+										+					+	+				
Si et al.			+													+			+				+	+				
Carmino et al.	+		+			+	+		+						+	+		+					+	+				
Rasouli et al.	+	+						+					+					+					+	+		+		
Wetter, Wright	+														+	+		+						+				
Arslan, Oral	+	+	+			+								+									+	+	+			
Long		+	+													+	+	+			+		+	+			+		

(cont. on the next page)

Table 2.1(cont.)

	Design Variables																						Objective Functions				
Author(s)	Air infiltration rate	Window wall ratio	Window U value	Window frame type	Number of stories	Weather data	Window SHGC	Efficiency or properties of	Occupancy	Floor type	DHW system	Thermal mass	Window opening control	Natural ventilation	Window shading type	HVAC system (efficiency	Heating/ cooling set-point	Mechanical ventilation	Internal gains	Building layout	Building orientation	Outdoor air flow rate	Roof type	Wall type	Thermal comfort	Energy consumption	Carbon emissions	Cost	Visual comfort
Badeche, Bouchahm		+	+	+			+								+											+			
Ouanes, Sriti		+	+										+										+	+	+	+			
Yasar, Sumer			+					+			+				+	+				+					+	+	+	+	
Wu et al.	+	+	+				+			+											+		+	+	+	+			+
Li, Chen		+	+												+						+					+			
Huo et al.			+																				+	+	+	+		+	
Chen et al.			+												+					+			+	+	+	+			+
Wang et al.		+					+			+					+								+	+	+	+			
Kang et al.	+	+					+			+					+						+		+	+			+	+	

(cont. on the next page)

Table 2.1(cont.)

	Design Variables																						Objective Functions				
Author(s)	Air infiltration rate	Window wall ratio	Window U value	Window frame type	Number of stories	Weather data	Window SHGC	Efficiency or properties of	Occupancy	Floor type	DHW system	Thermal mass	Window opening control	Natural ventilation	Window shading type	HVAC system (efficiency	Heating/ cooling set-point	Mechanical ventilation	Internal gains	Building layout	Building orientation	Outdoor air flow rate	Roof type	Wall type	Thermal comfort	Energy consumption	Carbon emissions	Cost	Visual comfort
Xu et al.		+	+	+						+					+	+							+	+		+	+	
Chen et al.	+	+	+				+									+	+		+		+	+	+	+	+		+	+	
Chen, Tsay	+	+	+				+		+										+		+	+	+	+	+				
Besbas et al.		+	+							+													+	+	+			+	+
Ekici et al.		+																		+								+	+
Krarti		+	+			+									+						+					+			
Saurbayeva et al.			+																		+		+	+		+		+	
Ioannou, Itard			+	+			+			+											+		+	+	+	+			
Mostafazadeh et			+					+		+							+								+		+	+	

(cont. on the next page)

Table 2.1(cont.)

	Design Variables																						Objective Functions				
Author(s)	Air infiltration rate	Window wall ratio	Window U value	Window frame type	Number of stories	Weather data	Window SHGC	Efficiency or properties of	Occupancy	Floor type	DHW system	Thermal mass	Window opening control	Natural ventilation	Window shading type	HVAC system (efficiency	Heating/ cooling set-point	Mechanical ventilation	Internal gains	Building layout	Building orientation	Outdoor air flow rate	Roof type	Wall type	Thermal comfort	Energy consumption	Carbon emissions	Cost	Visual comfort
Albatayneh	+	+	+								+				+	+						+		+	+		+		
Bagheri-Esfeh.																				+				+	+	+			+
Abdou et al.	+	+	+																			+		+	+	+	+		+
Ascione et al.			+																						+	+	+		
Xu et al.			+													+			+				+	+		+			
Khani et al.		+													+						+				+	+			+
Hawila, Merabtine	+	+	+														+								+	+			

For this thesis study, the words 'multi-objective optimization, optimization, building energy consumption, thermal comfort, sensitivity analysis, uncertainty analysis, overheating' were searched as keywords in the literature review. In total, sixty journal articles, eleven review studies, ten theses, and seven books were examined. Of these sixty journal articles, retrofit scenarios were performed in three, uncertainty analysis in five, sensitivity analysis in twenty-seven, and optimization studies in forty-five. Sensitivity analysis and optimization were discussed together in fifteen studies.

Approximately sixty-two percent of the studies examined, that is, thirty-seven, work on residential buildings (Figure 2.1). Twelve work on office buildings and five work on educational buildings. There are two articles where the building type is not specified. Two articles address commercial buildings, one addresses industrial, and one article addresses health buildings.

In fifteen studies, twenty-five percent of the studies reviewed, the case studies were located in one region of China (Figure 2.2). Nine studies dealt with case buildings in Türkiye and six in Italy. Four studies were conducted to analyze buildings located in more than one country.

Notably, the most frequently used toolbox in studies where UA/SA or optimization analyses are carried out is EnergyPlus (thirty-six articles) (Figure 2.3). The second most commonly used toolbox is MATLAB software. This is followed by DesignBuilder Python and Grasshopper toolboxes, respectively.

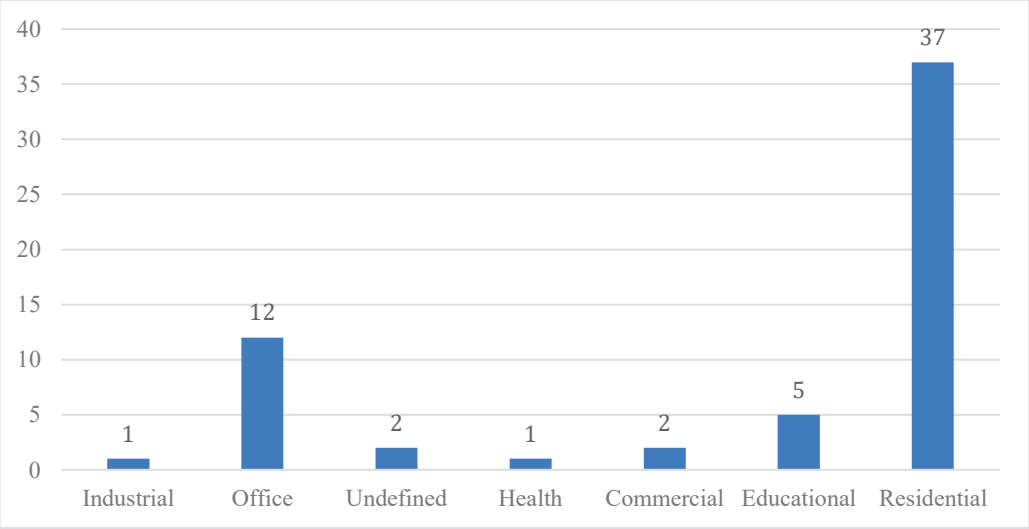

Figure 2.1. Building types in the studies

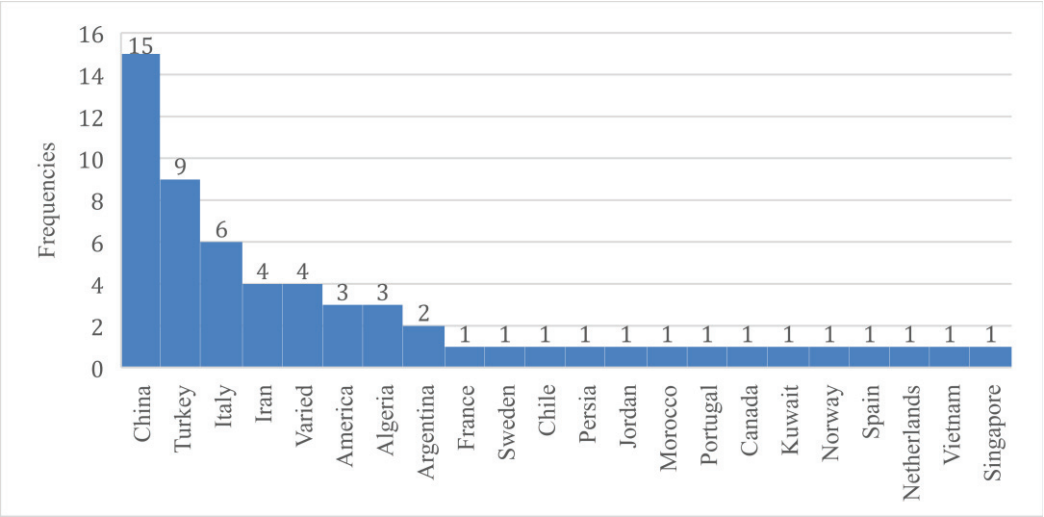

Figure 2.2. Location frequency of case buildings used in the studies

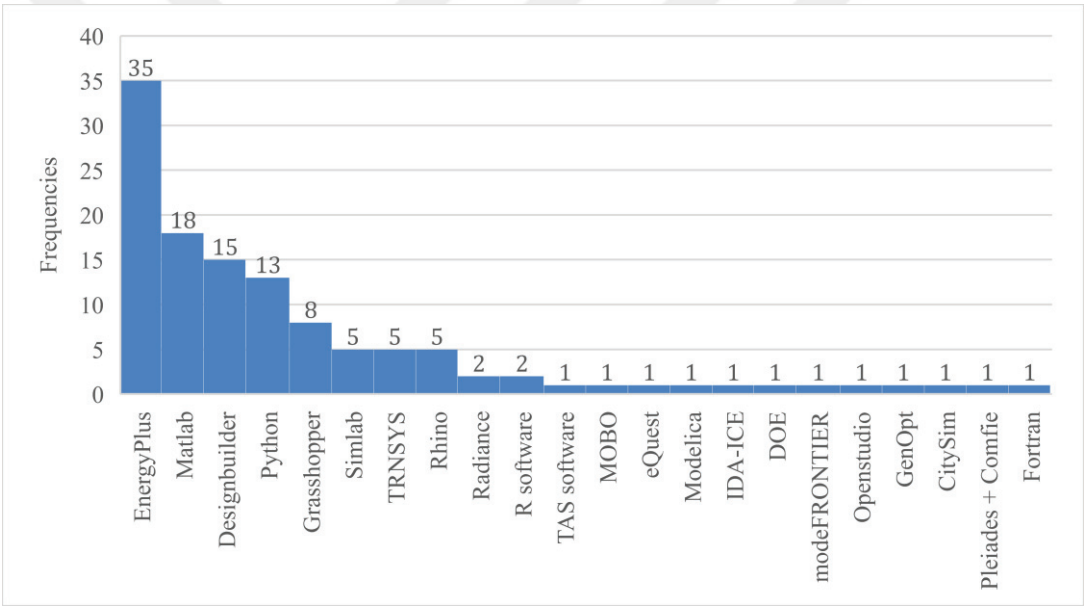

Figure 2.3. Tools used in the studies reviewed

In these studies, different design variables and objective functions are discussed. The design variables and objective functions discussed in Table 2.1 are specified for each study. The frequency of design variables used in the studies is graphed in Figure 2.4. The most common design variables in the studies were glass type and wall type, with fourty-four articles. Roof type is the third most common design variable discussed in thirty-six articles. Roof type is followed by the window-to-wall ratio, floor type, building orientation, air infiltration rate, and shading type. Set points of heating and cooling systems, and internal gains, are discussed in fifteen articles each. The SHGC value of glass and heating-cooling systems is discussed in thirteen articles.

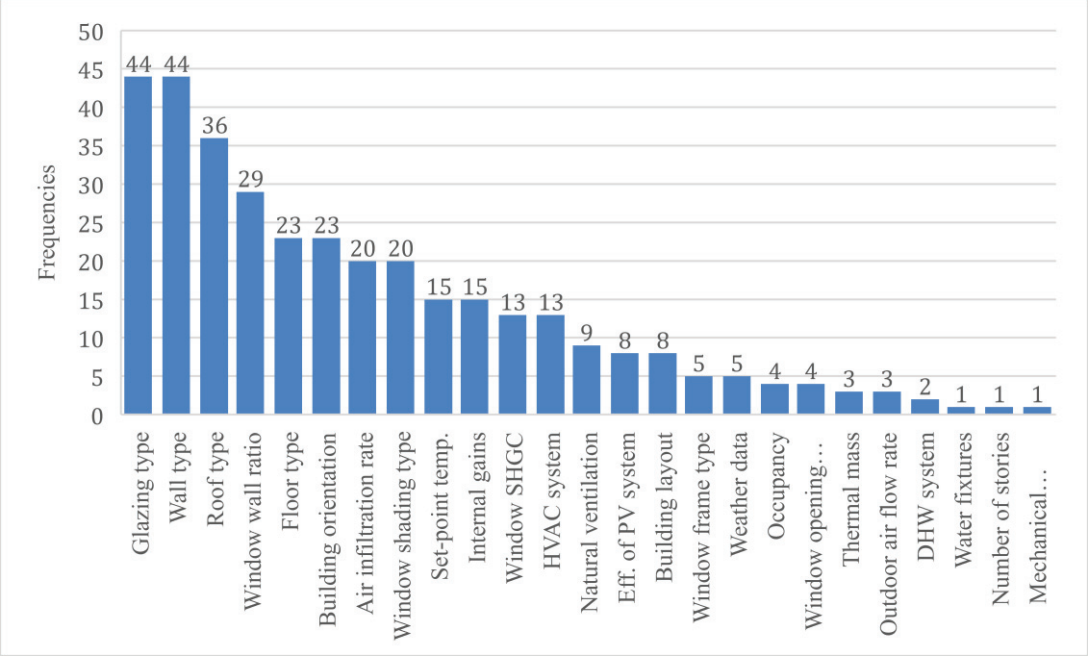

Figure 2.4. Frequency of design variables used in studies

When the objective functions discussed in the studies examined are evaluated, it is seen that thermal comfort and energy consumption outcomes are considered together in twenty-eight percent of the studies (Figure 2.5). The second most common output is energy consumption. These two situations are followed by the situation where energy consumption, thermal comfort, and cost are considered together, the situation where energy consumption and cost are considered, and the situation where energy consumption, thermal comfort, and visual comfort are considered together with seven percent.

Uncertainty and Sensitivity Analysis for Residential Buildings in the Mediterranean Climate Zone: In the literature, there are uncertainty and sensitivity analysis studies for residential buildings located in regions with a Mediterranean climate (Carpino et al. 2022; Encinas and Herde 2013; Escandon et al. 2019; Rosso et al. 2020; Yıldız and Durmuş Arsan 2011; Yıldız et al. 2012). Encinas and Herde (2013) considered summer thermal comfort values, Carpino et al. (2022) regarded as annual energy consumption, Yıldız et al. (2012) and Yıldız and Durmuş Arsan (2011) considered yearly heating and cooling energy loads, Escandon et al. (2019) regarded as thermal comfort as an output for a residential building. When these studies are examined, it is seen that the main design variables considered are air infiltration rate, window-to-wall ratio, glass type,

wall type, natural ventilation, set points of heating-cooling systems, roof type, shading type, and orientation.

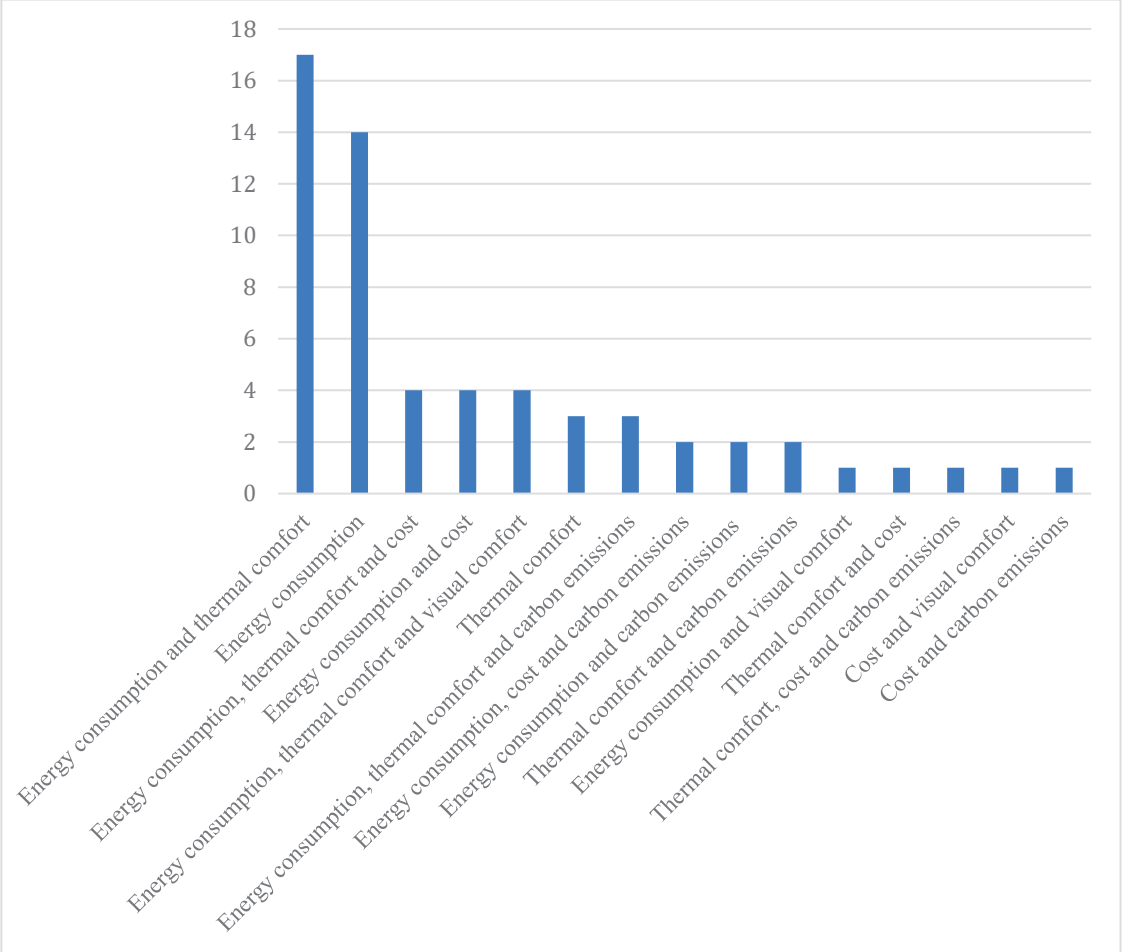

Figure 2.5. Frequency of objective functions used in studies

Multi-Objective Optimization for Residential Buildings in the Mediterranean Climate Zone: Studies are focusing on the problems of overheating, low thermal comfort, high energy consumption, and carbon emissions for residential buildings located in regions with a Mediterranean climate and conducting multi-objective optimization studies to improve these situations (Ascione et al. 2015; Rosso et al. 2020; Ascione et al. 2023; Mostafazadeh et al. 2023; Yiğit 2021). Ascione et al. (2015) pointed out that the overheating problem will increase due to global warming for residents in Mediterranean climates. They stated that high levels of thermal insulation for building envelope will increase the cooling demand. For this reason, it is emphasized that the thermal properties of the building envelope should be chosen carefully.

2.2. Uncertainty and Sensitivity Analysis

Crick et al. (1987) discussed uncertainty and sensitivity analysis as two different analyses determining variable importance and variable sensitivity. While uncertainty analysis analyses variables according to their importance, sensitivity analysis analyses variables according to their sensitivity.

Uncertainty analysis analyses the uncertainties that may occur in the outputs due to the uncertainty of the variables. Sensitivity analysis determines the sensitivity of design variables to these uncertainties (Hensen 2004).

2.2.1. Uncertainty Analysis

Uncertainty analysis determines the range of variations that may occur in building performance due to uncertainties that may occur in design variables and performs risk assessment of the building to achieve the targeted performance. Carpino et al. (2022) analyzed the uncertainties that may arise in the output with uncertainty analysis. They determined that there was a high probability of not achieving the targeted output, and to reduce this uncertainty, they reduced the risks of the sensitive design variables they determined with sensitivity analysis.

Uncertainty analyses applied to building performances in architecture are examined under two categories: forward or direct uncertainty analysis and inverse uncertainty analysis (Carpino et al. 2022; Tian et al. 2018). Forward or direct uncertainty analysis focuses on quantifying and analyzing the uncertainties that may occur in the output because of uncertainties in design variables. Inverse uncertainty analysis, known as calibration, regulates model data according to monitored or energy usage data. Forward uncertainty analysis is divided into probabilistic methods and non-probabilistic methods (Tian et al. 2018). Probability-based uncertainty analysis methods are divided into two: sampling-based and non-sampling approaches. One of the sampling-based approaches is Monte Carlo-based simulation, which is widely used in building performance evaluation studies. In the Monte Carlo-based simulation method, the probability distributions of the variables are determined first. In the second step, one of the methods, such as simple random sampling or Latin Hypercube sampling, is selected and different samples are created where the inputs are in the specified ranges. Outputs are obtained for these

samples, and the outputs' frequencies, averages, and minimum-maximum values are analyzed.

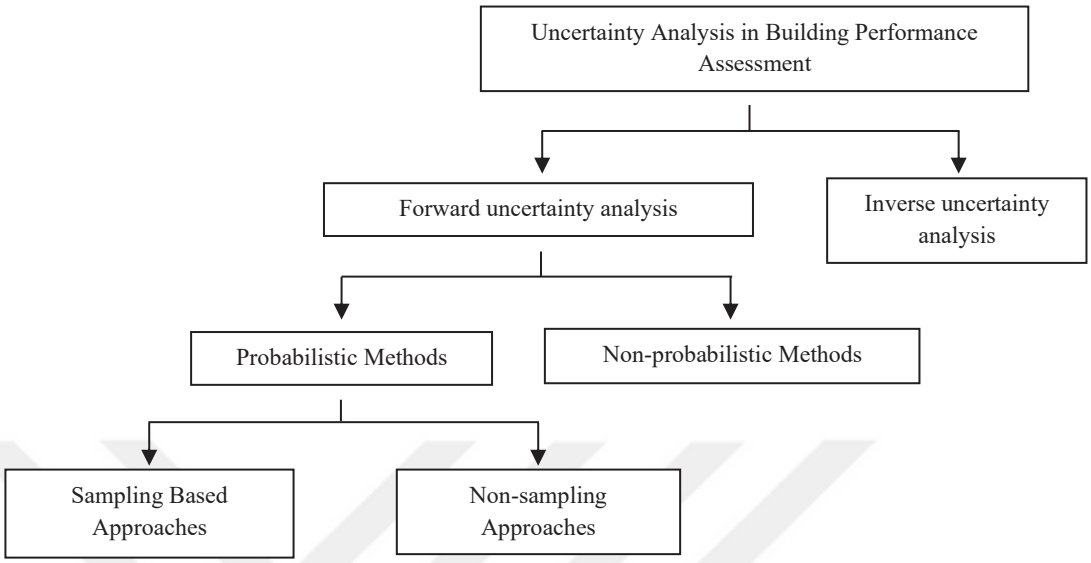

Figure 2.6. Methods of uncertainty analysis in building assessment

There are studies in the literature that increase the accuracy of the model with inverse uncertainty analysis (Escandon et al. 2019; Huang et al. 2020; Hawila and Merabtine 2021). In addition, there are studies examining the distribution and uncertainties that the uncertainties in the design variables will create on the outputs (Yıldız ve Arsan 2011; Gerçek 2016; Escandon et al. 2019).

2.2.2. Sensitivity Analysis

Sensitivity analysis is performed to analyze the sensitivity of variables on the output (Hamby 1994; Saltelli 2007). Sensitivity analysis evaluates the sensitivity of design variables on objective functions. The optimization process is done by considering the sensitive variables, and as the number of variables decreases, the calculation time and complexity of the problem also decrease. There are various studies in which sensitivity analysis is applied to reduce the number of variables before optimization (Albatayneh 2021; Arslan and Oral 2022; Ascione et al. 2020; Baghoolizadeg et al. 2023; Bre et al. 2016; Chen et al. 2022; Gao et al. 2023; Gou et al. 2008; Hawila and Merabtine 2021; Kang et al. 2024; Lu et al. 2020; Mukkavaara and Shadram 2021; Quanes and Sriti 2024; Wang et al. 2023). Especially in research on retrofit scenarios in buildings, it is seen that

sensitivity analysis is applied to identify and reduce potential risks and to ensure that the results are obtained from the retrofit scenario as intended.

Sensitivity analyses, widely applied in building performance analysis, are grouped under two main headings: local and global methods (Tian 2013; Saltelli 2007). While local sensitivity analysis analyzes the effects of design variables on building outputs separately, global sensitivity analysis also considers the interactions of design variables with each other. Global sensitivity analysis is a method that aims to explore many different regions of the input space (Saltelli 1999). Each design variable's minimum and maximum values are determined, and samples are created with different values that the variables can take within these variation ranges for this method. In the final step, the effects of variables on building output are evaluated according to all these samples. Tian examined the different sensitivity analysis methods used in building energy analysis and the steps to be followed in sensitivity analysis (Tian 2013).

In some studies, scenario variables were considered input variables in the sensitivity analysis stage, in addition to design and physical variables (Gerçek and Arsan 2019; Yıldız et al. 2012). In sensitivity analyses conducted with different climate scenarios, such as 2020s, 2050s, and 2080s, using future climate data, it was observed that there may be differences in the sensitivities of design variables with the changes brought about by the climate crisis.

Local Sensitivity Methods

Local sensitivity analysis can also be called the one-factor-at-a-time method. In this method, only one variable is changed to evaluate the sensitivity of the design variables, and all other variables are kept constant (Crick et al. 1987). This process is applied separately for each variable. In the one-factor-at-a-time method, since each input is evaluated separately, the relationship between the inputs is ignored, and the reduced area of the input space around only one base case is examined (Saltelli 1999). For this reason, some studies indicate that local sensitivity analysis is less reliable (Mara and Tarantola 2008; Tian 2013). Advantageously,t local sensitivity analysis is quite simple and easily applicable compared to global sensitivity analysis (Hamby 1994; Tian 2013; Saltelli 1999).

In a study, the effects of window orientation, size, glass type, thermal resistance of shading, and climate on energy consumption for dynamic shades were investigated

(Krarti 2023). With the local sensitivity analysis method, it was stated that dynamic shades performed better than static shades for all window directions, sizes, and glass types. Rasouli et al. also determined that the most sensitive variable for the energy performance of the HVAC system was the ventilation rate using the local sensitivity analysis method (Rasouli et al. 2013).

Global Sensitivity Methods

Global sensitivity analysis analyzes how sensitive each input is to the output, considering the interactions between the inputs (Storlie et al. 2009). Local sensitivity analysis focuses on the base case of uncertain inputs and only points around it, while global sensitivity analysis focuses on all the values uncertain inputs can take (Hamby 1994; Saltelli 1999). Compared to local sensitivity analysis, the longer the calculation time and the more complex of the problem are its disadvantages (Hamby 1994; Tian 2013). Different methods can be applied for global sensitivity analysis: regression method, variance-based method, meta-model-based method, and screening method.

According to Hamby (1994), regression analysis methods provide the most comprehensive sensitivity measure. It is seen in the literature that this method is frequently used in sensitivity analysis for building performance (Table 2.2). The regression method is applied after proceeding with the steps applied in the Monte Carlo-based simulation method. For this method, first, a sampling type is determined. As a sampling method, the Latin hypercube sampling method provides effective classification by dividing the inputs into layers. It is a frequently used method because it allows evaluation with a relatively small number of samples compared to other methods (Helton et al. 2006).

After the samples and their outputs are created, different indicators such as SRC (Standardised Regression Coefficients), PCC (Partial Correlation Coefficients), SRRC (Standardized Rank Regression Coefficient), and PRCC (Partial Rank Correlation Coefficient) are used to evaluate these data. SRC and SRRC indicators are used in standardized regression analysis methods (Helton et al. 1985; Iman and Helton 1988; 1991). In addition, these indicators are the most frequently used method in sensitivity analysis applied for building performance analysis (Albatayneh 2021; Arslan and Oral 2022; Ascione et al. 2020; Carpino et al. 2022; Escandón et al. 2019; Gao et al. 2023;

Gerçek and Arsan 2019; Gou et al. 2018; Ioannou and Itard 2015; Ouanes and Sriti 2024; Yıldız and Arsan 2011; Yıldız et al. 2012).

In many studies, sensitivity analysis is applied to understand the relationship between input and output before the optimization study and to complete the optimization process with fewer design variables by identifying insensitive inputs (Albatayneh 2021; Arslan and Oral 2022; Ascione et al. 2020; Baghoolizadeh et al. 2023; Bre et al. 2016; Chen et al. 2022; Gao et al. 2023; Gou et al. 2018; Kang et al. 2024; Khani et al. 2022; Mukkavaara and Shadram 2021; Ouanes and Sriti 2024). In a study, the number of inputs determined as thirty-seven was reduced to twenty by removing insensitive design variables for thermal comfort and energy consumption outputs using the regression analysis method (Gou et al. 2018). In the study, Albatayneh divided the 12 design variables whose effects on heating and cooling load were investigated into two groups, the high-importance group and the low-importance group, by regression method using the SRC indicator (Albatayneh 2021).

This study examined the sensitivity of ten different inputs to carbon emissions and thermal comfort in a renovated office building located in a hot and humid climate zone (Gao et al. 2023). The results show that the most sensitive variables for both objective functions are the HVAC system heating and cooling set point. Similarly, in a study conducted by Yıldız et al. (2012), a region with a Mediterranean climate was evaluated. Sensitivity analyses were conducted using weather data for the 2020s, 2050s, and 2080s. The most sensitive design variables for each situation are natural ventilation, window area, and the glazing's solar heat gain coefficient (SHGC).

Table 2.2. Specific properties of the UA/SA studies identified by a literature review

Author	Year	Modeling and simulation	SA	Local or Global	Method of SA	Indicator	Sampling Techniques	Tool of SA	UA	Method of UA	Approach	Tool of UA
Albatayneh	2021	Design Builder software	✓	Global	Regression Analysis	Standardized Regression Coefficient (SRC)	Simple Random Sampling	DB software	-	-	-	-
Carpino et al.	2022	Design Builder software	✓	Global	Regression Analysis	Standardized Regression Coefficient (SRC)	Latin Hypercube Sampling method (LHS)	DB software	✓	Forward UA	Sampling-based approach (LHS)	DB software
Ioannou and Itard	2015	Design Builder software	✓	Global	Regression Analysis	Standardised Ranked Regression Coefficient (SRRC)	Simple Random Sampling	Energy Plus, JEPlus	-	-	-	-
Gerçek and Arsan	2019	Design Builder software	✓	Global	Regression Analysis	Standardised Ranked Regression Coefficient (SRRC)	Latin Hypercube Sampling method (LHS)	SimLab	-	-	-	-
Yıldız and Arsan	2011	Energy Plus	✓	Global	Regression Analysis	Standardised Ranked Regression Coefficient (SRRC)	Latin Hypercube Sampling method (LHS)	SimLab	✓	Forward UA	Sampling-based approach (LHS)	SimLab
Saurbayeva et al.	2023	Design Builder software	✓	Global, Local	Regression Analysis, Screening, Local	Standardised Ranked Regression Coefficient (SRRC), Partial rank correlation coefficient(PRCC), Morris	Latin Hypercube Sampling method (LHS), factorial sampling method	R software	-	-	-	-
Gou et al.	2018	Energy Plus	✓	Global	Regression Analysis	Standardised Ranked Regression Coefficient (SRRC)	Latin Hypercube Sampling method (LHS)	SimLab	-	-	-	-
Yıldız et al.	2012	Energy Plus	✓	Global	Regression Analysis	Standardised Ranked Regression Coefficient (SRRC)	Latin Hypercube Sampling method (LHS)	SimLab	-	-	-	-
Saryazdi et al.	2022	Matlab software (ANN Model)	✓		Garson Index Method	-	-	Matlab	-	-	-	-
Bre et al.	2016	Energy Plus	✓	Global	Morris Screening method	The mean and the standard deviation	Undefined	R software	-	-	-	-

(cont. on the next page)

Table 2.2 (cont.)

Author(s)	Year	Modeling and simulation	SA	Local or Global	Method of SA	Indicator	Sampling Techniques	Tool of SA	UA	Method of UA	Approach	Tool of UA
Rasouli et al.	2013	TRNSYS software	✓	Local	Local	-	-	TRNSYS software	✓	Forward UA	Sampling-based approach	TRNSYS software
Mukkavaara and Shadram	2021	Energy Plus	✓	Global	Morris Screening Method and Regression Analysis	The mean and the standard deviation, Standardised Ranked Regression Coefficient (SRRC)	Latin Hypercube Sampling method (LHS)	Python and R software	-	-	-	-
Carpino et al.	2022	Design Builder, Energy Plus	✓	Global	Regression Analysis	Standardized Regression Coefficient (SRC)	Latin Hypercube Sampling method (LHS)	Design Builder	✓	Forward UA	Sampling-based approach	DB software
Chen et al.	2022	Energy Plus	✓	Global	Regression Analysis, Variance-based Sensitivity Analysis	First order, total order, SRC, SRRC, PCC, PRCC, SPEA, PEAR, KS	three sampling methods (FAST extend, Sobol, and LHS)	Undefined	-	-	-	-
Chen and Tsay	2022	Energy Plus	✓	Global	Morris Screening method and Regression Analysis, Variance-based sensitivity analysis	PCC, PRCC, SPEA, PEAR, SRC, SRRC, Sobol (first order and total order), Morris, and KS	Five different Monte Carlo sampling (FASTC, LHS, QRS, RS, and Sobol)	SimLab	-	-	-	-
Ouanes and Sriti	2024	Sketch Up, CitySim	✓	Global	Regression Analysis	Standardized Regression Coefficient (SRC)	Latin Hypercube Sampling method (LHS)	Matlab	-	-	-	-
Hawila and Merabtine	2021	Modelica	✓	Global	Meta-modeling approach	The Analysis of Variance (ANOVA) approach	-	Undefined	✓	Inverse UA		
Krarti	2023	DOE-2.2	✓	Local	Local	-	-	DOE-2.2	-	-	-	-
Kang et al.	2024	Energy Plus	✓	Global	Variance-based sensitivity analysis	Sobol (first order and total order)	Sobol sampling method	SimLab	-	-	-	-

(cont. on the next page)

Table 2.2 (cont.)

Author(s)	Year	Modeling and simulation	SA	Local or Global	Method of SA	Indicator	Sampling Techniques	Tool of SA	UA	Method of UA	Approach	Tool of UA
Ascione et al.	2020	Design Builder software	✓	Global	Regression Analysis	Standardised Ranked Regression Coefficient (SRRC)	Undefined	Matlab	-	-	-	-
Baghoolizadeh et al.	2022	Energy Plus	✓	Global	Morris Screening method	The mean and the standard deviation	Undefined	jEPlus + EA	-	-	-	-
Escandón et al.	2019	Energy Plus	✓	Global	Regression Analysis	Standardised Ranked Regression Coefficient (SRRC)	Latin Hypercube Sampling method (LHS)	Matlab	✓	Forward and inverse UA	Sampling-based approach (LHS)	Matlab
Gao et al.	2023	TRNSYS software	✓	Global	Regression Analysis	Standardized Regression Coefficient (SRC)	Undefined	jEPlus + EA	-	-	-	-
Arslan and Oral	2022	Design Builder, Energy Plus	✓	Global	Regression Analysis	Undefined	Latin Hypercube Sampling method (LHS)	Undefined	-	-	-	-
Gao et al.	2023	TRNSYS software	✓	Global	Regression Analysis	Standardized Regression Coefficient (SRC)	Undefined	jEPlus + EA	-	-	-	-
Arslan and Oral	2022	Design Builder, Energy Plus	✓	Global	Regression Analysis	Undefined	Latin Hypercube Sampling method (LHS)	Undefined	-	-	-	-

2.3. Modelling for Optimization

In building performance evaluations, different modeling methods are used to calculate estimated values of building performance during the optimization phase. A building performance model can be created by entering building data in a building simulation program such as DesignBuilder, TRNSYS, or EnergyPlus. In studies using the simulation-based optimization method, many iterative simulation results are obtained from this model. Figure 2.7 shows the working flow of the simulation-based optimization method. Simulations are made one by one for each sampling, and the results are evaluated in the optimization algorithm. This method is used in most of the studies on building performance (Acar et al. 2021; Ascione et al. 2015; Ascione et al. 2020; Ascione et al. 2022; Baghoolizadeh et al. 2022; Bre et al. 2016; Bre et al. 2017; Gao et al. 2023; Khani et al. 2022).

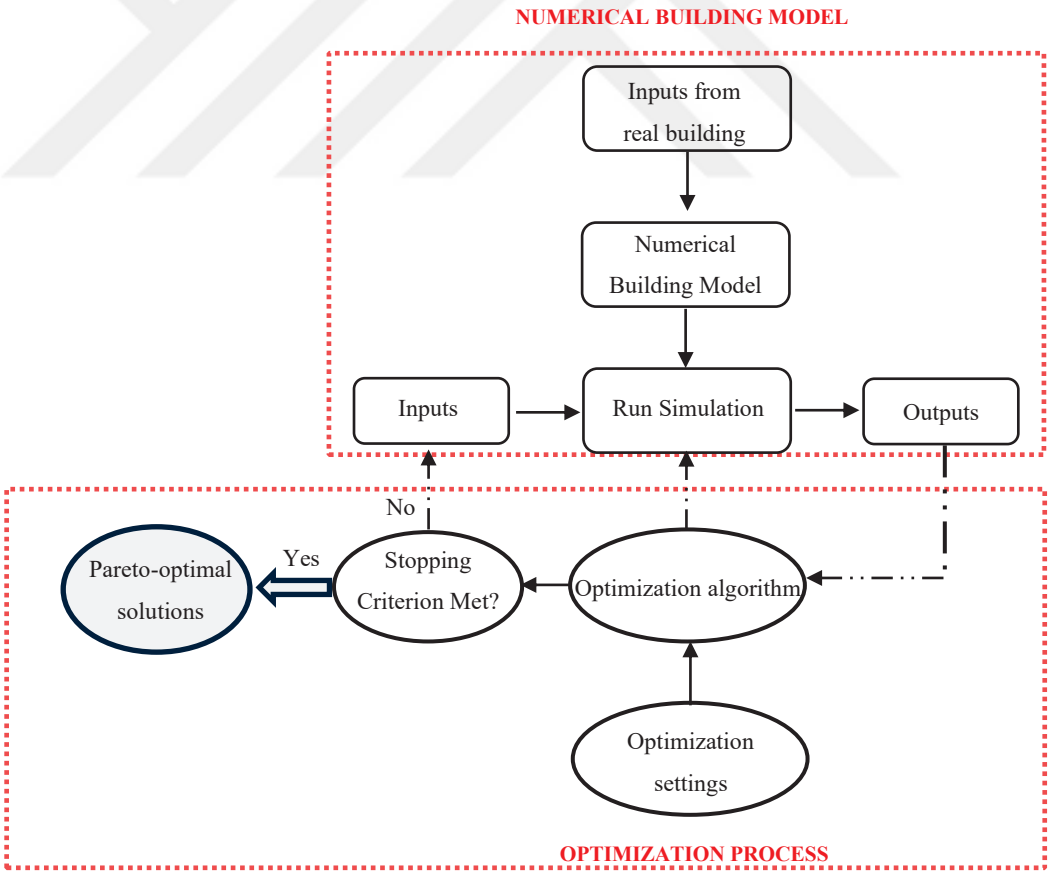

Figure 2.7. Flow chart of simulation-based optimization approach in building performance studies

In the literature, software such as DesignBuilder and Grasshopper have been used for simulation model creation and multi-objective optimization in the simulation-based optimization method (Albatayneh 2021; Taşer 2023). In some studies, models were first created in building simulation programs such as EnergyPlus and Grasshopper and simulation results were obtained (Acar et al. 2021; Ascione et al. 2015; Ascione et al. 2022; Baghoolizadeh et al. 2022; Bre et al. 2016; Brea et al. 2017; D'Agostino et al. 2023; Khani et al. 2022; Mostafazadeh et al. 2023). For multi-objective optimization, a connection was established between genetic algorithms and simulation models using software such as Matlab and Python.

In the literature, it is seen that the surrogate model-based optimization method is also used as an alternative to the simulation-based optimization method in building performance analysis research (Asadi et al. 2014; Bagheri-Esfeh et al. 2022; Ghomeishi et al. 2020; Gou et al. 2018; Magnier et al. 2010; Saryazdi et al. 2022; Sia et al. 2019; Xu et al. 2023; Yu et al. 2015). Many machine learning methods such as linear regression, decision trees, random forest, gradient boosting regression trees, and artificial neural networks have been developed over the years. The method of creating a surrogate model (meta-model) using machine learning methods is widely used. In the surrogate model-based optimization method, the surrogate model is trained with the data set taken from the model, and the relationship between input and output variables is learned, tested, and validated (Fig.2.8). In addition, some studies use monitoring data in surrogate model training as well as numerical data obtained from building energy programs (Kazanasmaz et al. 2009). A connection is established between the validated surrogate model and the optimization algorithm. The optimization algorithm gets the output values from the surrogate model for the input values. The surrogate model quickly predicts output values based on newly given input values, imitating the original model. The output values received are sorted depending on the selected algorithm, and as a result, the Pareto-optimal solution set is determined. Studies indicate that surrogate model-based optimization methods provide advantages by shortening the calculation time (Magnier and Haghighat 2010; Asadi et al. 2014; Sia et al. 2019).

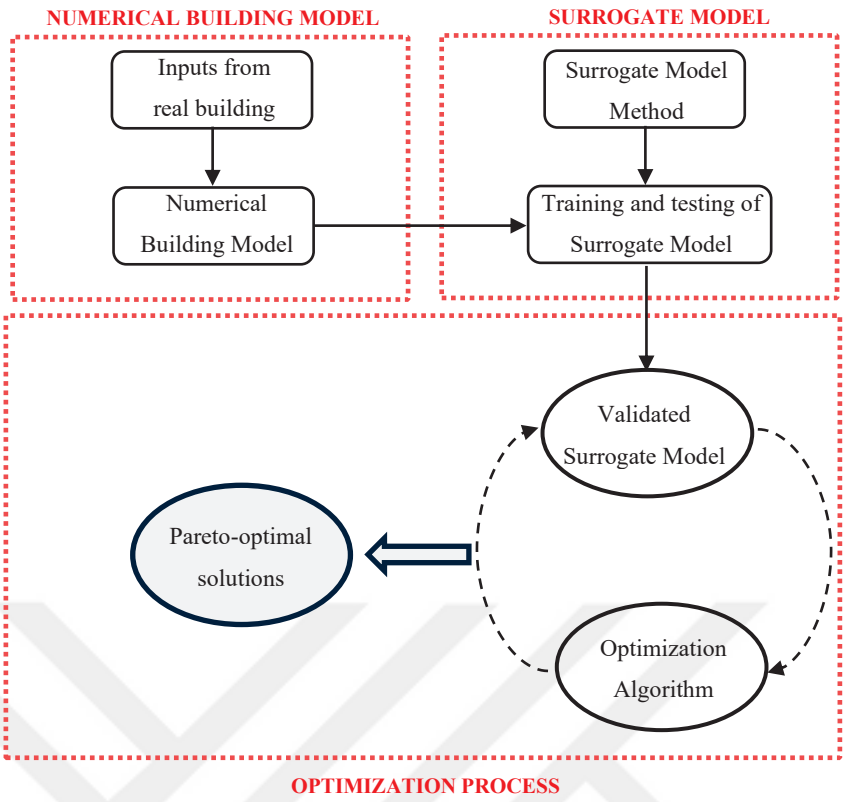

Figure 2.8. Optimization process with surrogate model

2.4. Multi-Objective Optimization Methods

The optimization, on which many relevant studies have been conducted recently, can be done with various methods such as Particle Swarm Optimization, Ant Colony Optimization, Differential Evolution, Gradient-based method, and Genetic Algorithms. Genetic algorithms are used in the majority of optimization studies carried out in the field of architecture (Abdou et al. 2021; Acar et al. 2021; Albatayneh 2021; Asadi et al. 2014; Ascione et al. 2015; Ascione et al. 2022; Bagheri-Eshef and Dehghan 2022; Baghoolizadeh et al. 2022; Bre and Fachinotti 2017; D'Agostino et al. 2023; Gao et al. 2023; Gou et al. 2018; Khani et al. 2022; Magnier and Haghighat 2010; Rosso et al. 2020; Saryazdi et al. 2022; Yu et al. 2015).

Genetic algorithms are a popular meta-heuristic method for multi-objective optimization (Konak et al. 2006). Genetic algorithms are one of the population-based optimization methods and can find many optimal solutions in a single step (Ergül 2010). In addition, they are suitable for parallel calculations, do not get stuck at local optimum points, and can detect global optimum points. Through these features, they have been

preferred in building performance optimization studies (Nguyen et al. 2014; Wetter and Wright 2004).

2.4.1. Genetic Algorithms

Genetic algorithms, one of the evolutionary algorithms, search for the best (optimal) solution by imitating biologically originated functions such as elitism, selection, crossover, and mutation (Tabassum and Mathew 2014). David E. Goldberg's book, in 1989, included many new perspectives, pioneered researchers, and genetic algorithms with different approaches were developed. In the 2000s, studies on this subject increased, and Deb et al. (2002) developed the Non-dominated Sorting genetic algorithm, the foundations of which were laid in 1994, and NSGA-II arose. This method is a Pareto-based method and is widely used in optimization studies in the field of architecture (Abdou et al. 2021; Acar et al. 2021; Albatayneh 2021; Asadi et al. 2014; Ascione et al. 2015; Ascione et al. 2022; Bagheri-Eshef and Dehghan 2022; Baghoolizadeh et al. 2022; Bre and Fachinotti 2017; D'Agostino et al. 2023; Gao et al. 2023; Gou et al. 2018; Khani et al. 2022; Magnier and Haghighat 2010; Saryazdi et al. 2022; Yu et al. 2015).

Si et al. (2019) and Yu et al. (2015) stated in their studies that the NSGA-II algorithm is considered to be the algorithm that provides the most efficient and accurate results among genetic algorithms. In addition, the performances of four different genetic algorithms (NSGA-II, MOPSO, MOSA, and ES) were compared for the multi-objective optimization problem, and the results indicate that the NSGA-II algorithm showed the best performance (Si et al. 2019). In another study, it was stated that the NSGA-II algorithm gave the most accurate results because it efficiently sorted non-dominated solutions, took elitism into account, and gave a set of Pareto-optimal solutions that were well distributed along the Pareto front (Bre and Fachinotti 2017). Saryazdi et al. (2022) chose the NSGA-II algorithm because it provides a well-distributed Pareto-front solution and has a powerful sorting tool.

CHAPTER 3

MATERIALS AND METHOD

The third chapter of the thesis study, which provides information about the study methodology, case building, energy modeling, uncertainty-sensitivity analysis, and multi-objective optimization processes, consists of seven parts. In the first part, the case and the climate characteristics of Izmir, where the residential building is located, are described. The second section explains the monitoring method, the related device, and its technical specifications. While general information about the building energy simulation tool is given in the third part, the energy model and its technical settings are explained in the fourth section. In the fifth part, the problem formulation and determination of objective functions and input variables according to user comments and simulation results are described. The sixth section explains how to conduct the uncertainty and sensitivity analyses for existing buildings according to the determined target outputs, i.e., objective functions. The seventh part contains information about multi-objective optimization study in the simulation tool.

3.1. Case Building

The typical apartment selected as the case study is located in Izmir in the west of Türkiye, next to the Aegean Sea (Figure 3.1). It lies seven meters above sea level with the coordinates of 38°26'55"N 27°11'25" E. Figure 3.2 shows the borders of Bornova district, where the residential building is located.

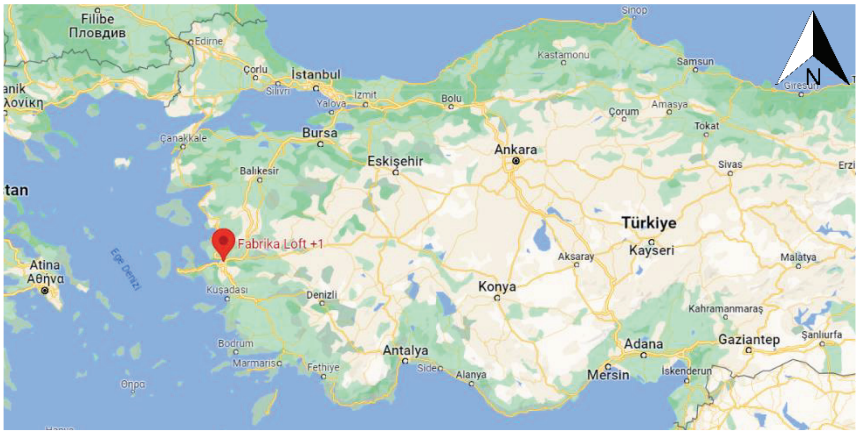

Figure 3.1. Location of Izmir in Türkiye (Source: Google Maps 2024)

Figure 3.2. Borders of Bornova district in Izmir (Source: Yandex Maps 2024)

Bornova district, which has 45 neighborhoods, is considered a predominantly urban region, according to research conducted by the Izmir Development Agency in 2021 (İZKA 2021, 96). According to the census conducted in 2023, the population of Bornova district is 447,553 (TUIK 2023). Kazımdirik neighborhood, where the residential block is located, is the second neighborhood with the highest population in Bornova district. The student population is high since there are two universities in the Bornova district, i.e., Yaşar University and Ege University. Studio types of small houses preferred by students are common. Figures 3.3 and 3.4 show an aerial photograph of the case building and the urban texture of its surroundings. One of the reasons why this residential building was chosen as a case building is that it represents the housing types built in Bornova in recent years.

Figure 3.3. Aerial photo of the urban texture of Bornova district and location of the case building (pointed with a rectangle) (Source: Google Earth 2024)

Figure 3.4. Aerial photo of the surrounding of the case building (pointed with a rectangle) (Source: Google Earth 2024)

There is a metro transportation line to the southeast of the case residential building and residential or office buildings to the southwest, northwest, and northeast. The building positioning deviates 36° from north to west. The apartment building contains residential flats and offices. It was built in 2019 and composed of ten floors. While the areas on the ground and first floors of the block serve for commercial use, two floors of parking in the basement and the other floors are used for residential purposes. The floor height, excluding the ground floor, is 2.80 meters. The gross area of each floor where the residences are located is 355.8 m², and the net area is 261.5 m². There are eight flats on each floor. The 2+1 studio-type flat, considered as the case building, is located on the 4th floor and faces south.

3.1.1. Local Weather Information of Bornova, Izmir

According to the Köppen climate classification, the Izmir region is in the 'Csa' climate classification (Köppen 2011, 351-360). In the ‘Csa' climate class, also known as the hot-summer Mediterranean climate, the summers are hot and dry, and the winters are warm and rainy.

According to the recorded values between 1938 and 2022 by the Republic of Türkiye, Ministry of Environment, Urbanization, and Climate Change, Turkish State Meteorological Service, the annual average temperature for Izmir is 17.9 °C (General Directorate of Meteorology 2022). According to the average temperature values for these years, July was the hottest month with 27.9 °C, while January had the lowest temperatures, i.e. 8.8 °C.

The yearly average of precipitation between 1938-2022 is 709.9 mm (General Directorate of Meteorology 2022). The months with the most and least rainfall is December, with 146.2 mm, and July, with 4.1 mm, respectively.

The dominant wind direction of the Izmir region throughout the year is from the north. When averaged between 2016 and 2024 for Izmir, the windiest month is July with an average hourly speed of 17.7 kmph, while the calmest month is May with an average hourly speed of 12.8 kmph (Weatherspark 2024).

Heating degree days (HDD) and cooling degree days (CDD) indices are the indicators of expected relative differences in heating and cooling energy requirements, respectively, and how these energy requirements will change as the climate warms in the future (Harvey 2020). Considering the outdoor and average room temperatures, the heating degree days index indicates the severity of cold in that specific period. In contrast, the cooling degree days index indicates the severity of heat (Eurostat 2024). The General Directorate of Meteorology (GDM) calculated these indexes according to the standards set by the European Community Statistical Office (Eurostat) (General Directorate of Meteorology 2024). If the daily average outdoor air temperature is less than or equal to 15 °C, the temperature is subtracted from the base temperature of 18 °C, and this value becomes the HDD for that day. When calculating the cooling degree days index, if the daily average outdoor air temperature is equal to or above 24 °C, 21 °C, determined as the base temperature, is subtracted from this value, and the CDD index is calculated.

Table 3.1 shows the HDD and CDD indices for Izmir calculated every month between 2013 and 2023. It is stated that the HDD index reached its highest value of 1176 in 2015 and is at its lowest value of 774 in 2021. The CDD index was calculated at its lowest at 572 in 2014 and at its highest at 838 in 2021. When the index in 2013 and 2023 are compared, it is calculated that HDD decreased by 8.43%, while CDD increased by 11.42%. In 2021, for Izmir, CDD was calculated as 838 and HDD as 774. For 2023, it is seen that CDD is calculated as 702 and HDD is calculated as 790, and these indices are almost equal. In line with the data in Table 3.1, Izmir, which is located in the Mediterranean climate region and has a heating-dominated climate, is increasingly becoming a region where cooling is dominated as well as heating.

Table 3.1. Monthly heating (HDD) and cooling degree days (CDD) for Izmir between 2013 and 2023 (General Directorate of Meteorology 2024)

		Jan	Feb	March	April	May	June	July	Aug	Sept	Oct	Nov	Dec	Annual
2013	HDD	263	182	116	37						16	67	291	972
	CDD				1	44	114	197	210	63	1			630
2014	HDD	186	173	141	24						13	103	175	815
	CDD				1	19	101	180	198	71	2			572
2015	HDD	294	240	203	97							71	271	1176
	CDD					16	56	193	207	100	4			576
2016	HDD	278	109	125		3					3	122	338	978
	CDD				4	16	165	226	215	91	5	1		723
2017	HDD	349	192	123	38						3	103	166	974
	CDD				1	16	126	230	220	92	2			687
2018	HDD	260	155	48							5	64	264	796
	CDD				6	67	128	212	218	105				736
2019	HDD	274	212	114	63							10	190	863
	CDD					35	162	193	233	74	12			709
2020	HDD	290	191	114	46							91	152	884
	CDD					44	101	221	210	145	26			747
2021	HDD	207	175	200	51								141	774
	CDD				7	60	125	268	253	117	6	2		838
2022	HDD	301	210	275	31							57	134	1008
	CDD					46	143	221	209	97	12			728
2023	HDD	206	232	127	45							53	127	790
	CDD					8	101	261	221	102	6	3		702

3.1.2. Layout of Case Flat

The case flat and surrounding blocks can be seen in Figure 3.5. There is a metro line on the south side of the apartment building (Fig.3.6a). Since the case flat is south-facing, no buildings or trees can cast shadows. The case flat is located on the fourth floor of the apartment block. On this floor, there are eight flats: 1+0 (two flats), 1+1 (four flats) and 2+1 (two flats) (Fig.3.6b). The case flat on the south-facing side is a studio type of 2+1 flat. The gross area of the case flat is 45.6 m², and the net area is 43 m². It consists of a bedroom (11.5 m^2), study room (11.5 m^2), kitchen and living area (16 m^2), and bathroom (3.3 m^2) (Fig. 3.7). The window-to-wall ratio of the bedroom and study room is 66.8%, and the living room is 19.5%. There are large openings of 2 m in width and 2.48 m in

height on the facades of the bedroom and study room (Table 3.2). When the entire facade is evaluated, the window-to-wall ratio is 50.3%.

Figure 3.5. Outer picture of case building

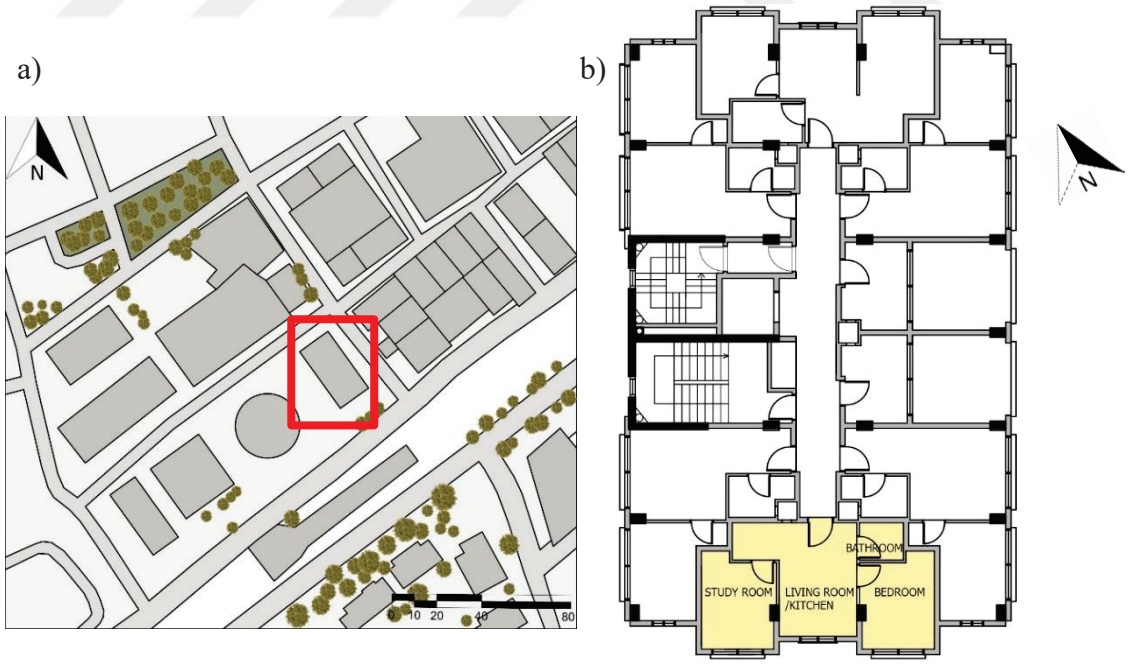

Figure 3.6. a) Site plan: case building and surrounded building blocks in Bornova b) Location of the case flat on the fourth floor

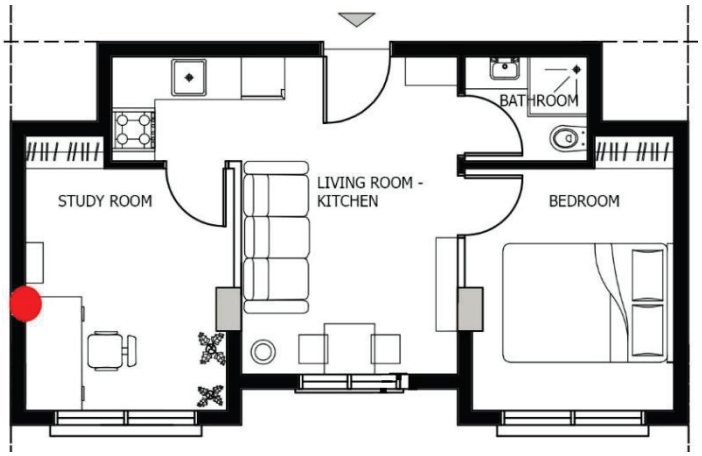

Figure 3.7. The plan of case flat

Table 3.2. Room information of the case flat

Zones	Net Area (m^2)	No. of Window	Dimensions of windows (height x width) (m)	No. of Door
Living room and kitchen	16	1	1.1 x 1.4	3
Bedroom	11.5	1	2.48 x 2	1
Study room	11.5	1	2.48 x 2	1
Bathroom	4	-	-	1

3.1.3. General Information of Case Flat

The flat has a living area, kitchen, bedroom, study room and bathroom. The entrance area includes a living area and kitchen. The kitchen and living area has electrical appliances such as a Wi-Fi device, oven, refrigerator, and dishwasher. There are no electrical appliances in the bedroom or study room. One female person lives in the house. The frequency of use is higher on weekdays than on weekends. The person living in the house does not stay there all year round. Thus, the occupancy of the house may vary from day to day. Lighting is generally used in the living area. There is no balcony in the house.

In the case flat, the heating need is provided by the block's central system with natural gas from the grid through radiators in the bedroom, living room and kitchen, and study room, while the cooling need is provided by the air conditioner with electricity from the grid in the living room and kitchen. There is no mechanical ventilation system.

3.2. Measurements

To analyze the overheating problem observed at home and to complete the calibration of the model, dry bulb temperature, relative humidity, and light intensity values were recorded every ten minutes between 5 May 2023 00:00 and 1 January 2024 00:00. The monitoring campaign was conducted in the study room with a datalogger, hung on the wall at the point indicated by the red circle in Fig.3.8, at a height of 1.4 m from the surface level. It was placed on the southwestern side wall of the case room, away from direct sunlight (Fig.3.8). During the monitoring period; this room was not used; the door to the room was always kept closed, and the thin curtain was always active. No electrical device could cause heat gain in the room. Hourly averages of air temperature and relative humidity values recorded every ten minutes were calculated to use in the calibration process of the model with hourly data.

As stated in Table 3.3, the monitoring device is designed to measure the variables of indoor environmental quality, i.e. air temperature, relative humidity, and light intensity. The air temperature range measured by the datalogger is -20 °C to 70 °C, the relative humidity range is 5%-95%, and the light intensity is 0 to 167.731 lux . The accuracy is ±0.35 °C for temperatures between 0 °C and 50 °C, ±2.5% for relative humidity values between 10% and 90% and . ±10% for light intensity.

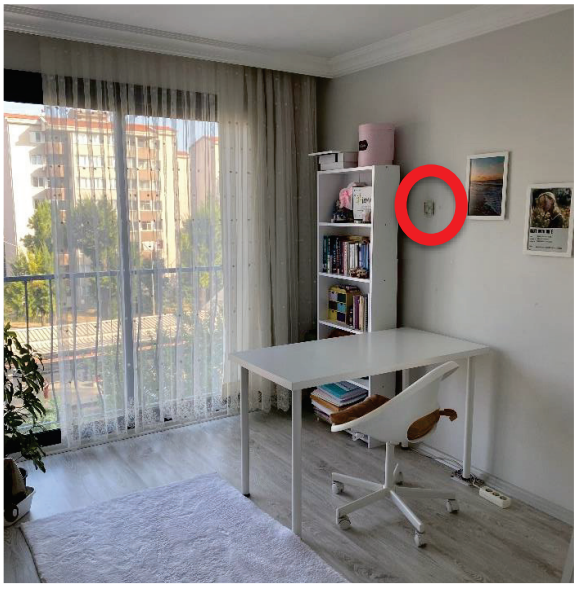

Figure 3.8. Location of datalogger in the study room (pointed with the red circle)

Table 3.3. Specifications of HOBO datalogger (Onset 2023)

Datalogger	**HOBO U12**
Measurement Range	T: -20 °C to 70 °C RH: 5% to 95% Light Intensity: 0 to 167.731 lux
Accuracy	T: ±0.35 °C from 0 °C to 50 °C RH: ±2.5% from 10% to 90% Light Intensity: ±10%

Outdoor weather data were officially retrieved from the GDM's local weather station in The Directorate of Zeytincilik Research Institute in Bornova, Izmir. The station is located 700 m east of the case apartment. The variables of air pressure, relative humidity, wind direction and speed, air temperature, and total global solar radiation were obtained hourly between May 5th, 2023 00:00, and January 1st, 2024 00:00.

3.3. Building Energy Simulation Tool

In this study, DesignBuilder (2024) version 7.0.2 dynamic simulation software was used to prepare the simulation model of the case flat, run the simulations, analyze the uncertainty and sensitivity of energy consumption and thermal comfort, and run the optimization process. It is the state-of-the-art software tool for examining building performance on energy consumption, carbon emissions, and building thermal comfort. It also simplifies the modeling process through its graphical user interface.

DesignBuilder uses the EnergyPlus simulation engine to calculate the energy performance of buildings. In this study, the latest version of EnergyPlus software, version 9.4, was used. It is a whole building energy simulation program that architects, researchers, and engineers use to model both energy consumption and water use in buildings (EnergyPlus 2024).

In this study, visualization, simulation and optimization modules of the software were used via DesignBuilder student license.

3.4. Building Simulation Model

The plan and section drawings of the building were obtained from the Kare Architecture and Engineering Office in Alsancak, Izmir. The floor plan of the fourth floor where the case flat is located, was simplified as seen in Figure 3.9 and 3.10. This simplified plan was converted into dxf format and imported into DesignBuilder as the base for the model. The case flat was modeled separately as a building block, while the remaining part of the building was modeled as an adiabatic component block type. Each of the three rooms in the case housing was modeled as a separate zone, thus all schedules, belonging to occupancy, internal gains, and lighting, were assigned according to the use of each room.

Surrounding buildings, roads, pavements, and trees were also modeled to increase the validity of the model. Surrounding blocks were modeled as standard block type while roads and sidewalks are modeled as ground block type. Table 3.4 presents information about the material, maximum transmittance, and transmittance schedule assigned to the surrounding blocks. Figure 3.11 shows the model along with the sun path diagram for December 21st at noon. Figure 3.12 visualize the close up views of the simulation model.

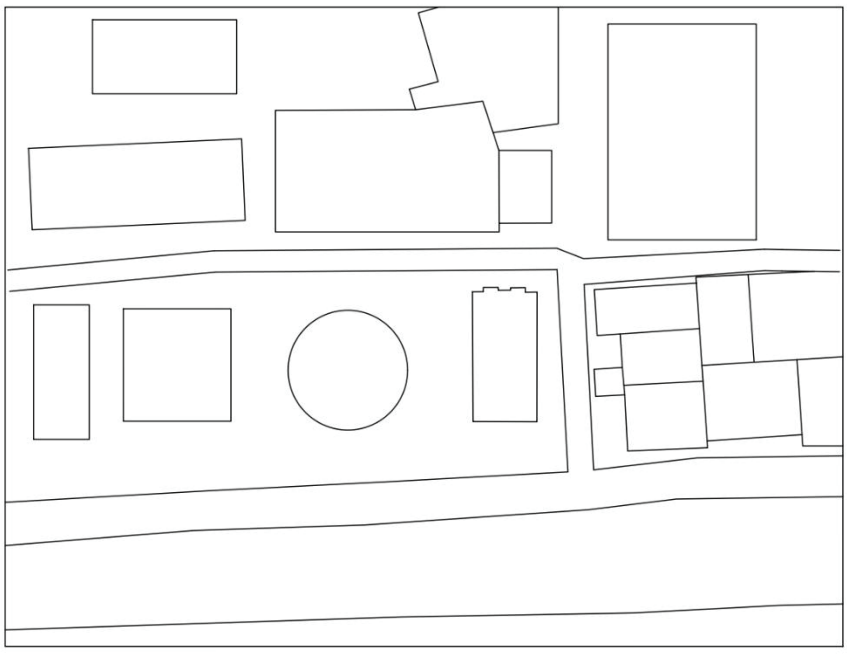

Figure 3.9. The simplified plan of the typical apartment in Bornova

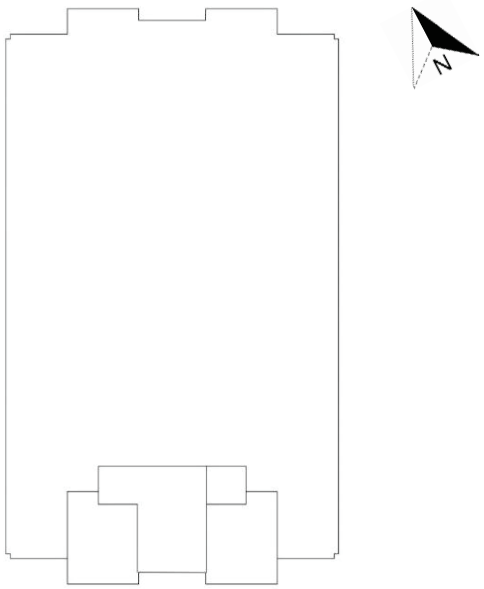

Figure 3.10. The simplified plan of the typical apartment floor in Bornova

Table 3.4. Properties of site materials in the model

	Material (as indicated in DesignBuilder)	**Maximum transmittance**	**Transmittance schedule**
Case building	Brickwork outer	0	On 24/7
Sidewalks	Concrete paviour	0	On 24/7
Roads	Concrete	0	On 24/7
Buildings (excluding case building)	Plaster (dense)	0	On 24/7
Trees	Oak (Radial)	0.5	Summer (Northern Hemisphere)
Subway track	Gravel	0	On 24/7

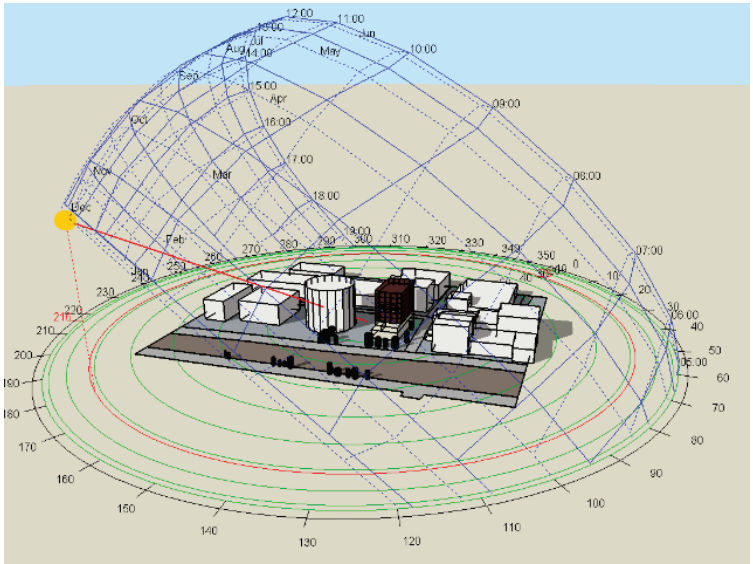

Figure 3.11. The model of case building and surroundings

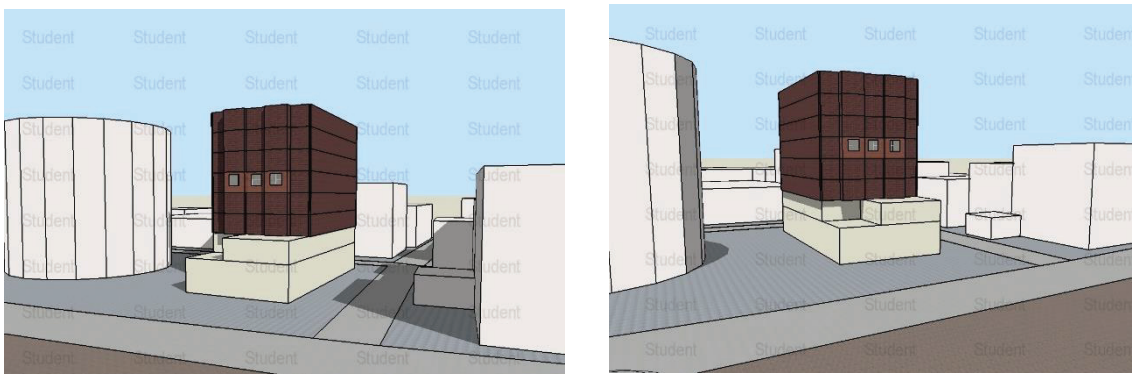

Figure 3.12. Rendered views of case building (left: from southeast, right: from southwest)

3.4.1. Structural Components

The apartment block, built in 2019, was constructed with a reinforced concrete structural system. Information about the materials and their technical properties was obtained from the architect of the building. 19 cm pumice concrete blocks (BIMS) of the 'Okyap' brand were used as the wall infill material. The number and thickness of layers and thermal properties of building components such as conductivity, specific heat, and density are given in detail in Table 3.5. U values of the building components are calculated by DesinBuilder according to the layer information. Since the apartment is a newly built residential block, the air infiltration level (0.4 ac/h) is assumed to be low.

Table 3.5. Specification of building materials

	Position	**Layer Name**	**Conductivity**	**Specific Heat**	**Density**	**Thickness**	**U Value**
Unit			**W/m.K**	**j/kg.K**	**kg/ m³**	**m**	**W/m². K**
External Wall	Inner most	Gypsum plaster	0.51	960	1120	0.013	
		Cement plaster	0.72	840	1760	0.01	
		Pumice concrete block	0.127	1000	715	0.19	
		Cement plaster	0.72	840	1760	0.02	
		Adhesive mortar	0.88	896	2800	0.008	
	Outer most	Brick cladding[1]	0.476	1000	1660	0.015	
							0.564
Internal Wall	Inner most	Gypsum plaster	0.51	960	1120	0.013	

[1] Thermal properties for the brick cladding of Işıklar brand on the outer surface of external walls are accepted as the properties of pressed brick material of the same brand.

Table 3.5. (cont.)

		Cement plaster	**0.72**	**840**	**1760**	**0.01**	
		Horizontal perforated brick	0.17	1000	800	0.085	
		Cement plaster	0.72	840	1760	0.01	
	Outer most	Gypsum plaster	0.51	960	1120	0.013	
							1.182
Internal Floor	Outer most	Timber Flooring	0.14	1200	650	0.015	
		Adhesive mortar	0.88	896	2800	0.005	
		Levelling mortar	0.88	896	2800	0.015	
		Reinforced concrete	1.13	1000	2000	0.12	
	Inner most	Gypsum Plaster	0.51	960	1120	0.02	
							1.946
Window Frame		Polyvinylchloride (PVC)	0.17	900	1390	0.024	
							3.214
Glazing	Outer most	Generic Clear 4 mm	0.9			0.004	
		Argon 13 mm				0.013	
	Inner most	Generic Clear 4 mm	0.9			0.004	
							2.54
Doors		Pine				0.025	
							2.86

3.4.2. Schedules

To make the simulation results as close to reality as possible, it is essential to upload the input of occupancy pattern, heating, cooling and ventilation regime, and electrical device and shading element usage habits into the DesignBuilder model. Therefore, the schedule charts were prepared based on the information received from the female living in the flat.

First of all, activity templates were assigned to each zone of the flat by their functions, as indicated in Figure 3.13. The study room is the room where the measurement campaign was conducted (see Chapter 3). Since it was not used during the monitoring period and heating-cooling system was not operated, no activity was assigned to this room for the model calibration. Yet the occupancy schedules and HVAC settings were activated for each room including the study room in the process of energy and thermal comfort simulation. Artificial lighting was assumed to be off for all zones throughout the year.

Occupancy schedules for the living room and kitchen and bedroom are shown in Table 3.6. Occupancy density is calculated by dividing the number of people to square

meters. Since one person lives in this house, the '1' number is divided into the square meters of the rooms. Table 3.7 shows the time periods active for natural ventilation hours per each room. Since the door between the living room and kitchen and the bedroom is always open, it is also defined as open in the model.

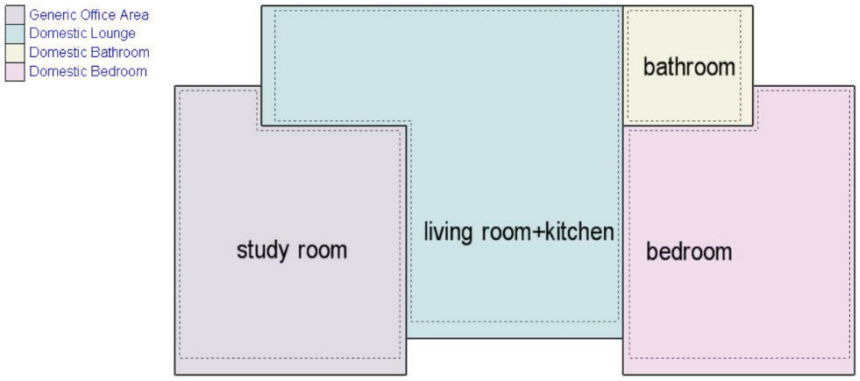

Figure 3.13. The schematic plan of the case housing

Table 3.8 shows the type, schedule, and positions of the window shading element selected for each room. An open weave drape was adjusted in the study room at the beginning of the measurement and remained that way throughout the measurement. The user stated that she always actively uses close-weave drapes because her bedroom receives a lot of light. A schedule has been assigned for the open weave drape used in the living room and kitchen. This schedule is set to be active when this space is occupied.

Table 3.6. The occupancy schedule

Occupancy	**Occupancy Density (people/m^2)**	**Period: Day**	**Occupied hours**
Living room and kitchen	0.0625	Weekdays	10:00- 17:00 20:00 - 24:00
		Weekends	10:00 - 13:00 20:00 - 24:00
Bedroom	0.095	Weekdays	24:00 - 09:00
		Weekends	24:00 - 10:00

Table 3.7. The schedule of natural ventilation

Natural ventilation…	**Period: Day**	**Period: Hours**
Living room and kitchen	Weekdays	10:00 - 11:00 17:00 – 19:00
	Weekends	10:00 - 14:00 19:00 – 20:00
Bedroom	Weekdays	10:00 - 11:00
	Weekends	10:00 - 12:00

Table 3.8. The type, schedule, and position of the window shading elements

Shding	**Window shading type**	**Position**	**Schedule**	
Study room	Drapes-open weave light	Inside	Always on	
Living room and kitchen	Drapes-open weave light	Inside	Weekdays	10:00- 17:00 20:00 - 24:00
			Weekends	10:00 - 13:00 20:00 - 24:00
Bedroom	Drapes-close weave medium	Inside	Always on	

3.4.3 HVAC Settings

The case flat is heated by central heating and cooled by air conditioning. Heating set point and set back temperatures are 19-21 °C for the living room and kitchen and study room, and 18-20 °C for the bedroom. Cooling set point and set back temperatures are 24-26 °C for the living room and kitchen and study room, and 26-28 °C for the bedroom (Table 3.9). There is no mechanical ventilation in the building. Heating set points specified were determined according to TS 2164 (TS 2164 1983). Cooling set points were determined according to ASHRAE Guideline 13 (ASHRAE Guideline 13 2005).

The 'air to water heat pump hybrid with gas boiler, nat vent' option was selected as the template library of HVAC settings section in DesignBuilder,. The HVAC template was adapted according to the flat's realtime conditions:

- Natural gas and electricity were chosen as the source of heating and cooling, respectively.

- The cooling system is activated from the beginning of May to the end of October. The heating is activated from the beginning of November to the end of April.
- The coefficient of performance (CoP) of the cooling system was defined as 3.5, while the efficiency of the heating system was selected as 0.9.

During the calibration process, the resident chose to use the heating and cooling systems only in the living room and kitchen, thus HVAC was enabled only in the living room and kitchen. However, it is assumed that heating and cooling are used in all rooms during the simulation and optimization process. Therefore, the HVAC systems for all three zone was enabled to calculate energy consumption.

Table 3.9. Heating / cooling set point and set back temperatures for the living room and kitchen, study room, and bedroom

	Living room and kitchen	Study room	Bedroom
Heating set point (°C)	21	21	20
Heating set back (°C)	19	19	18
Cooling set point (°C)	24	24	26
Cooling set back (°C)	26	26	28

3.4.4. Calibration of Model

A calibration process was applied to analyze the deviation and uncertainty that may occur in the output of the model, adtjust the model and obtain results closest to reality. The model was calibrated according to two statistical error indicators specified in ASHRAE Guideline 14: root mean squared error (RMSE) (Eq. 3.1) and mean bias error (MBE) (Eq. 3.2) (ASHRAE Guideline 14 2002). According to ASHRAE Guideline 14, if the calibration process is performed using hourly data, MBE should be less than ±10%, and RMSE should be less than ±30%. In this study, the calibration process was carried out based on hourly indoor air temperature by monitoring carried out between 5 May 00:00 2023 and 1 January 00:00 2024.

$$\mathrm{RMSE}\ (\%) = (100/\mathrm{T_{ma}}) * \ [1/\mathrm{N} * (\mathrm{S}(\mathrm{T_s} - \mathrm{T_m})^2)]^{1/2} \quad (3.1)$$

$$\mathrm{MBE}\ (\%) = \ (100/\mathrm{T_{ma}}) * [\mathrm{S}(\mathrm{T_s} \ - \mathrm{T_m})]/\mathrm{N} \quad (3.2)$$

The calibration process was completed in six steps. Each step is in addition to the previous step. In the first step, a simulation was made using the information and schedules in section 3.5. In this simulation, it was determined that the temperatures were higher than the monitoring results, especially in the summer months. To reduce this difference, in the second step of calibration, the cooling set point temperatures for the living room and kitchen were reduced from 24-26 °C to 22-24 °C. In this case, it has been analyzed that the simulation temperature values are generally higher than the monitoring temperature values. In the third step, the infiltration was increased from 0.4 ac/h to 0.8 ac/h. In the fourth step, since curtains were used in the living room and kitchen and studied throughout the monitoring period, the 'drapes-open weave light' type of curtains was added to both rooms. While the usage schedule for the curtain in the study room is defined as always active, the curtain in the living room and kitchen is set to be active during the hours used by the resident. In addition, it was determined that the error rates were high for August, and therefore, August was examined in detail. It was determined that the door of the room where the measurement was taken between 20-28 August may have been open, and this was recorded in the schedule of the door. In the results of the fourth step, it was analyzed that the temperatures decreased compared to the monitoring temperatures, especially in the winter months. Therefore, the infiltration was updated to 0.65 ac/h for the fifth step of the calibration. According to the error data obtained in the fifth step, especially the months of November and December, which were analyzed in more detail, and since the cooling for the living room and kitchen was active in March-October, it was concluded that the simulation values in October were quite low compared to the monitoring data. For the last step, cooling has been updated by enabling it for March-September. As a result of all these calibration steps, RMSE and MBE lower than the limit error rates specified in ASHRAE Guideline-14 were achieved.

3.5. Problem Formulation

While defining the problem for the thesis study, user opinions and simulation results stated in Section 4.3 were considered. Problem definition is a process in which objective functions and design variables are determined. In Section 3.6.1, it is explained how the objective functions are calculated and under what conditions they are determined, and in Section 3.6.2, the design variables and the lower and upper limits of these variables are specified.

3.5.1. Definition of Objective Functions

Energy consumption and thermal discomfort hours are high due to the high window-to-wall ratio on the south side of this flat, located in the Mediterranean region according to the Köppen climate classification (Köppen 2011, 351-360). When interviewed with the resident, it was determined that there was an overheating problem, especially in the summer months. For this reason, the objective functions in this thesis study were determined as annual energy consumption (total site energy) and thermal discomfort hours (Discomfort ASHRAE 55 (all clo)).

Thermal comfort, according to Fanger's definition, is a state of mind that expresses satisfaction with the thermal environment. Povl Ola Fanger, the pioneer of studies on thermal comfort, developed a comfort model to express the thermal comfort level for artificially heated-cooled spaces (Fanger 1986). In this comfort model, a seven-point scale is presented to evaluate the thermal comfort of many people (Table 3.10). As a result of the experiments conducted using this scale, it was predicted that these votes could be predicted, and the index of PMV (Predicted Mean Vote) was introduced in line with six variables affecting thermal comfort. These variables: are metabolic rate due to activity (M), the resistance of clothing (R_c), air temperature (T_a), mean radiant temperature (T_{mr}), air velocity (v), and air relative humidity (RH). The numerical calculation of the PMV index can be seen in Equation 1.2. The index of PPD (Percentage of Dissatisfied People), which is related to PWM, also indicates the percentage of dissatisfied people (1.3). PPD index is accepted as a minimum of 5% for each building, shown in the graphs. In this thermal comfort model, it is accepted that even if the PMV is neutral, there are always at least 5% of dissatisfied people.

Table 3.10. Fanger seven-point scale

-3	Cold
-2	Cool
-1	Slightly Cool
0	Neutral
1	Slightly Warm
2	Warm
3	Hot

$$PMV=(0.303(e)^{0.303}+0.028)\ \{(M-W)-3.05[5.73-0.007(M-W)-p_a]-0.42[(M-W)-58.15]-0.0173M(5.87-p_a)-0.00014M(34-t_a)-3.96x10^{-8}f_{cl}[(t_{cl}+273)^4-(t_{mr}+273)^4]-f_{cl}h_c\,(t_{cl}-t_a)\}$$

Where:

$$t_{cl}=35.7-0.0275(M-W-I_{cl}\{(M-W)-3.05[5.73-0.007(M-W)-p_a]-0.42[(M-W)-58.15]-0.0173M(5.87-p_a)-0.0014M(34-t_a)\}$$

(M: metabolic heat rate[W/m^2], W: activity level [W/m^2], t_{cl}: the temperature at clothes level [°C], p_a: water vapor pressure[Pa], t_a: air temperature [°C], I_{cl}: thermal insulation of clothes [Clo], f_{cl}: clothing factor [-], t_{mr}: mean radiant temperature [°C], h_c: convective heat transfer [W/m^2°C]) (1.2)

$$PPD = 100-95exp\ [-(0.03353(PMV)^4+0.2179(PMV)^2)] \quad (1.3)$$

In the context of these definitions of thermal comfort, there are ASHRAE standards determined in 2004 for indoor thermal comfort situations (ASHRAE 55 2004). Calculations are made according to these standards when calculating thermal discomfort hours in the DesignBuilder software.

Table 3.11. Acceptable thermal environment for general comfort (Source: ASHRAE 55 2004)

PPD	PMV
<10	-0.5 < PMV < +0.5

The basis of the calculations is the PMV and PPD indexes specified in Table 3.11. A PPD index of 10% or less corresponds to the range between -0.5 and +0.5 for PMV on

the Fanger scale, and these values mean acceptable thermal comfort conditions according to ASHRAE 55.

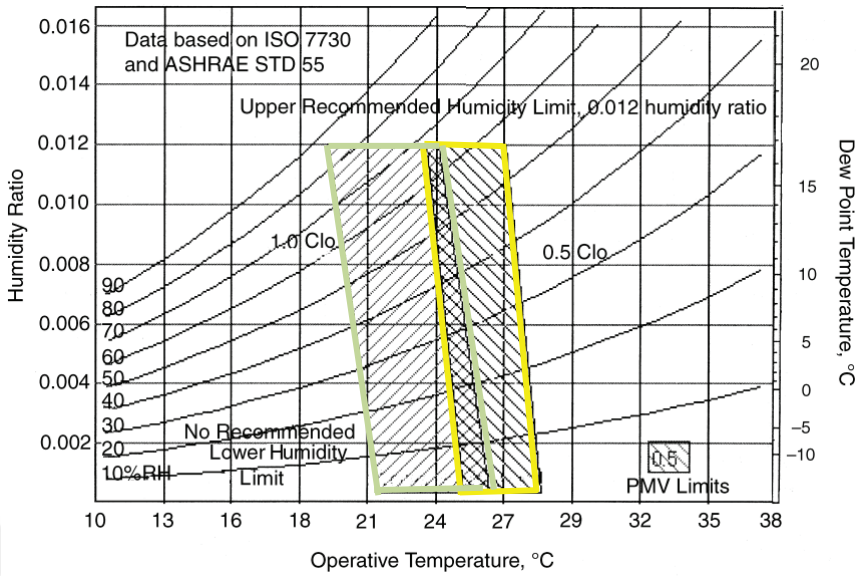

Figure 3.14. The acceptable range of operative temperature and humidity for typical indoor environments (Source: ASHRAE 55 2004)

The comfort zone specified in the psychometric chart in Figure 3.14 is defined by the combination of air temperature, mean radiant temperature, air speed, clothing insulation, humidity, and metabolic rate for these lower and upper limits of PMV. In Figure 3.14, comfort zones are defined as two separate areas: 0.5 clo clothing insulation (yellow rectangle) when the outdoor environment is hot and 1.0 clo clothing insulation (green rectangle) when the outdoor environment is cold. The regions indicated by these green and yellow rectangles indicate comfort conditions for environments where the airspeed is not more than 0.2 m/s. Additionally, for this chart, it is assumed that users perform activities with a metabolic rate between 1.0 met and 1.3 met. 1.0 met represents the metabolic rate of an individual sitting quietly, and 1.2 met represents the metabolic rate of an individual standing. If the analyzed situation falls outside the specified comfort zone, it is defined as a thermal discomfort hour. In addition, the calculation of thermal discomfort hours is made for the hours included in the occupancy schedule defined in DesignBuilder.

While calculations are made for each zone, thermal discomfort hours can also be calculated for the building level in the DesignBuilder software. The software calculates this data using the floor area-weighted average of all regions (DesignBuilder 2024).

The 'Total site energy' output was selected in the DesignBuilder software to calculate the annual energy consumption of the flat. In this output, the total gross energy consumed in the building is calculated. The unit is given in 'kWh'.

The 'Cooling load' output gives the heat energy required to keep an environment at a specified temperature. Its unit is 'kWh'.

3.5.2. Determination of Design Variables

After determining the objective functions according to user comments and simulation results, the next stage is to determine the design variables. Design variables were selected in line with the variable results studied in the literature review in Chapter 2. Table 3.12 contains the general list of design variables, distribution categories, distribution curves, and information about target objects. The lower and upper values of the design variables were decided by considering the literature.

Table 3.12. List of design variables

Variable type	Distribution category	Distribution curve	Min value	Max value	Options list	Target objects
Window to wall ratio (%) for bedroom	Continuous	Uniform (Continuous)	20	80	-	Bedroom
Window-to-wall ratio (%) for living room and kitchen	Continuous	Uniform (Continuous)	20	80	-	Living room and kitchen
Window-to-wall ratio (%) for study room	Continuous	Uniform (Continuous)	20	80	-	Study room
Glazing t type	Discrete	Uniform (Discrete)	-	-	16 options	Bedroom, living room and kitchen, study room
External wall construction	Discrete	Uniform (Discrete)	-	-	35 options	Bedroom, living room and kitchen, study room
Infiltration (ac/h)	Continuous	Uniform (Continuous)	0.3	1	-	Building
Window frame	Discrete	Uniform (Discrete)	-	-	8 options	Building
Partition Construction	Discrete	Uniform (Discrete)	-	-	12 options	Bedroom, living room and kitchen, study room
Shading type	Discrete	Uniform (Discrete)	-	-	13 options	Building
Natural ventilation max. temp. difference	Continuous	Uniform (Continuous)	-100	2	-	Building

(cont. on the next page)

Table 3.12. (cont.)

Heating system seasonal CoP	Continuous	Uniform (Continuous)	0.9	6.29	-	Building
Cooling system seasonal CoP	Continuous	Uniform (Continuous)	2.2	6.0	-	Building
Heating set-point temperature (°C)	Continuous	Uniform (Continuous)	19	23	-	Building
Cooling set-point temperature(°C)	Continuous	Uniform (Continuous)	24	28	-	Building
Heating system schedule	Discrete	Uniform (Discrete)	-	-	3 options	Building
Cooling system schedule	Discrete	Uniform (Discrete)	-	-	3 options	Building

The window-to-wall ratio is considered as a separate variable for each zone, with a minimum of 20 and a maximum of 80. There are studies in the literature that reference these lower and upper values for window wall ratio (Long et al. 2023; Gou et al. 2018).

Natural ventilation maximum temperature difference is a variable that determines the operating schedule of natural ventilation. A schedule of natural ventilation is defined for each zone in the model. Three values and states are defined in the DesignBuilder software for the maximum temperature difference (Scheduled natural ventilation data 2024). If this value is defined as 0, natural ventilation will be activated when the outside temperature is lower than the indoor temperature. When this variable is entered as -100, natural ventilation will always be active during the specified schedule. If the maximum temperature difference is 2, natural ventilation will only be activated when the outside temperature is at least two degrees lower than the indoor temperature.

Air infiltration rate ranges are discussed at different values in the literature. Yıldız et al. (2012; 2011) determined the range of air infiltration rate as a minimum of 0.5 ach and a maximum of 2 ach. While Albatayneh (2021) evaluated the air infiltration rate range as a minimum of 0.2 $ac.h^{-1}$ and maximum of 1.5 $ac.h^{-1}$, Escandon et al. (2019) evaluated it as a minimum 0.3 $ac.h^{-1}$ and a maximum 1 $ac.h^{-1}$. In another study, the basic air infiltration rate was assumed to be 0.6 ach and the design variables were considered as discrete variables at 25%, 50%, and 75% less than this value (Abdou et al. 2021). Carpino et al. (2022) kept the range narrow and referenced minimum 0.24 and maximum 0.33 values. Rasouli et al. (2013) took values between 0.4 ach and 0.72 ach. In this study, infiltration is stated as a continuous variable, with a minimum of 0.3 $ac.h^{-1}$ and a maximum of 1 $ac.h^{-1}$.

The material of the louver blades, which are positioned as seen in Figure 3.15, is designed as steel, with a thickness of 0.002 m. There will be 6 blades, the depth of the blades is 0.2 m and there is 0.30 m between each blade. Options for the shading element are defined in the range of 0-60, with angle degrees increasing by five degrees. 13 different options for the shading element were considered by changing the angle values.

16 different glass types were considered as discrete variables. Different situations were created, with the inner and outer glass thicknesses being 3 or 6 mm, and the thickness of the gas in between being 6- or 12 mm. Argon or air was chosen for the gas of the gap. Glass types are diversified including transparent glass and low-emissivity glass. Table 3.13 gives the options list of glass types and the U and SHGC values of these options. These values were calculated in the DesignBuilder software by entering each material layer.

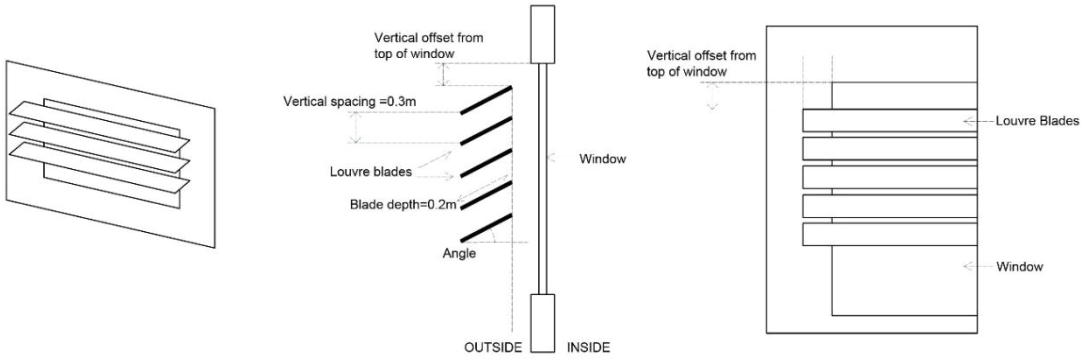

Figure 3.15. Perspective, side elevation, and front elevation of the louvre

Table 3.13. Glazing type option list

Glazing type option list	U value (W/m^{2}K)	Total Solar Transmission (SHGC)
Base Case (clear4, argon 12, clear4)	2.554	0.742
Glazing type-1 (clear4, air6, clear4)	3.146	0.74
Glazing type-2 (clear4, air12, clear4)	2.725	0.742
Glazing type-3 (clear6, air6, clear6)	3.107	0.713
Glazing type-4 (clear6, air12, clear6)	2.695	0.715
Glazing type-5 (clear4, argon6, clear4)	2.873	0.741
Glazing type-6 (clear6, argon6, clear6)	2.84	0.714
Glazing type-7 (clear6, argon12, clear6)	2.526	0.716
Glazing type-8 (lowe4, air6, lowe4)	1.81	0.512
Glazing type-9 (lowe 4, air12, lowe 4)	1.375	0.527
Glazing type-10 (lowe 6, air6, lowe 6)	1.792	0.471
Glazing type-11 (lowe 6, air12, lowe 6)	1.364	0.482

(cont. on the next page)

Table 3.13. (cont.)

Glazing type-12 (lowe 4, argon6, lowe 4)	1.534	0.521
Glazing type-13 (lowe 4, argon12, lowe 4)	1.172	0.534
Glazing type-14 (lowe 6, argon6, lowe 6)	1.521	0.477
Glazing type-15 (lowe 6, argon12, lowe 6)	1.164	0.487

The existing layers for the external wall and the material properties of the layers are shown in Table 3.14. Table 3.15 gives the thermal properties of aerated concrete, pumice concrete block, and horizontal perforated brick materials used as materials in the scenarios. For insulation and building materials, different wall types and U values were designed with different thicknesses of aerated concrete, pumice concrete block, and horizontal perforated brick in different cases where insulation is provided without insulation, with rock wool and EPS are given in Table 3.16.

Table 3.14. Layers of external wall

	Position	Layer	Conductivity (W/mK)	Specific Heat (J/kgK)	Density (kg/m^3)	Thickness (m)
External wall	Innermost	Gypsum plaster	0.51	960	1120	0.013
		Cement plaster	0.72	840	1760	0.01
		Material				
		Insulation Material				
		Cement plaster	0.72	840	1760	0.02
		Adhesive mortar	0.88	896	2800	0.008
	Outermost	Brick cladding	0.476	1000	1660	0.015

Table 3.15. Thermal properties of external wall materials

	Conductivity (W/mK)	Specific Heat (J/kgK)	Density (kg/m^3)
Aerated Concrete (Ytong)	0.11	1000	400
Pumice Concrete Blocks (BIMS)	0.127	1000	715
Horizontal Perforated Brick	0.17	1000	800

Table 3.16. External wall option list

External Wall Option List	Insulation Material	Material	U value (W/m^{2}K)
External wall-1	Without insulation	Aerated concrete (20cm)	0.477
External wall-2		Aerated concrete (25cm)	0.392
External wall-3		Aerated concrete (30cm)	0.333
Base Case		BIMS (19cm)	0.564

(cont. on the next page)

Table 3.16. (cont.)

External wall-4		BIMS (25cm)	0.445
External wall-5		BIMS (30cm)	0.379
External wall-6		Horizontal Perforated Brick(19cm)	0.717
External wall-7	Stone wool (3cm)	Aerated concrete (20cm)	0.347
External wall-8		Aerated concrete (25cm)	0.299
External wall-9		Aerated concrete (30cm)	0.264
External wall-10		BIMS (19cm)	0.39
External wall-11		BIMS (25cm)	0.329
External wall-12		BIMS (30cm)	0.292
External wall-13		Horizontal Perforated Brick(19cm)	0.458
External wall-14	Stone wool (5cm)	Aerated concrete (20cm)	0.293
External wall-15		Aerated concrete (25cm)	0.259
External wall-16		Aerated concrete (30cm)	0.231
External wall-17		BIMS (19cm)	0.324
External wall-18		BIMS (25cm)	0.281
External wall-19		BIMS (30cm)	0.253
External wall-20		Horizontal Perforated Brick(19cm)	0.369
External wall-21	EPS (3cm)	Aerated concrete (20cm)	0.351
External wall-22		Aerated concrete (25cm)	0.303
External wall-23		Aerated concrete (30cm)	0.266
External wall-24		BIMS (19cm)	0.396
External wall-25		BIMS (25cm)	0.334
External wall-26		BIMS (30cm)	0.295
External wall-27		Horizontal Perforated Brick(19cm)	0.466
External wall-28	EPS (5cm)	Aerated concrete (20cm)	0.299
External wall-29		Aerated concrete (25cm)	0.263
External wall-30		Aerated concrete (30cm)	0.235
External wall-31		BIMS (19cm)	0.331
External wall-32		BIMS (25cm)	0.286
External wall-33		BIMS (30cm)	0.257
External wall-34		Horizontal Perforated Brick(19cm)	0.378

While the thermal properties of the layers for the internal wall are given in Table 3.17, the wall U values for scenarios are given in Table 3.18. For the internal walls, scenarios were used with different thicknesses of the materials used in the exterior walls (aerated concrete, pumice concrete block, and horizontal perforated brick).

Table 3.17. Layers of internal wall

	Position	Layer	Conductivity (W/mK)	Specific Heat (J/kgK)	Density (kg/m^3)	Thickness (m)
Internal wall	Innermost	Gypsum plaster	0.51	960	1120	0.013
		Cement plaster	0.72	840	1760	0.01
		Material				
		Cement plaster	0.72	840	1760	0.01
	Outermost	Gypsum plaster	0.51	960	1120	0.013

Table 3.18. Internal wall option list

Internal wall option list	Material	Thickness (cm)	U value
Partition wall-1	Aerated Concrete (Ytong)	8	0.938
Partition wall-2		10	0.801

(cont. on the next page)

Table 3.18. (cont.)

Partition wall-3		**13.5**	0.639
Partition wall-4		15	0.587
Partition wall-5	Pumice Concrete Block (BIMS)	8	1.032
Partition wall-6		9	0.955
Partition wall-7		10	0.888
Partition wall-8		13	0.734
Partition wall-9		15	0.658
Base Case	Horizontal Perforated brick	8.5	1.192
Partition wall-10		10	1.079
Partition wall-11		13.5	0.883

The list of base conditions and options for the window frame can be seen in Table 3.19. U values of the window frame vary between 1.554 and 5.869 $W.m^{-2}. K^{-1}$. These values were calculated in the DesignBuilder software by entering the material and thickness.

Table 3.19. Window frame option list

Window frame option list	Thickness (m)	Conductivity(W/mK)	Specific Heat(J/kgK)	Density (kg/m3)	U value
Base Case (PVC)	0.024	0.1700	900	1390	3.214
Polyvinylchloride(PVC)	0.03	0.1700	900	1390	2.886
Polyvinylchloride(PVC)	0.044	0.1700	900	1390	2.332
Polyvinylchloride(PVC)	0.052	0.1700	900	1390	2.101
Aluminium	0.06	160	880	2800	5.869
Oak	0.068	0.19	2390	700	1.894
Oak	0.078	0.19	2390	700	1.723
Oak	0.09	0.19	2390	700	1.554

Various ranges are discussed in the literature for heating and cooling setpoints, as well as air infiltration rates. Some studies reference the ranges of 23.5-28 °C, 24-28 °C, 25-27 °C, 24-28 °C, 25-28 °C, 20-26 °C, 24-26 °C for the cooling setpoint (Carpino et al. 2022; Chen et al. 2022; Long et al. 2023; Mostafazadeh et al. 2023; Saryazdi et al. 2022; Si et al. 2019; Yıldız and Arsan 2011). The cooling setpoint range for this study was determined to be 24-28 °C. The heating set point temperature range was determined by Chen et al. (2022) as 18-22.5 °C, Carpino et al. (2022) as 18-22 °C, Si et al. (2019) as 18-23 °C, Mostafazadeh et al. (2023) as 20-23 °C, and Yıldız and Arsan (2011) as 19-23 °C. In this study, the minimum temperature for the heating set point was determined as 19 °C, and the maximum temperature was determined as 23 °C.

The lowest coefficient of performance of the heating system was 0.9, while the highest was 6.29 (Buderus 2024; City Multi 2014). The coefficient of performance range

for the cooling system is determined between 2.2 and 6 (Mitsubishi Klima 2020; City Multi 2014).

Schedules for heating and cooling systems were also considered as a design variable. Three different operating schedules have been created for both heating and cooling systems. The operating schedule for heating is varied, including always active, active only in the winter months (December, January, February), and active for seven months (October, November, December, January, February, March, April). The heating system is activated depending on the set point during the activated months. Similarly, three options have been defined for the cooling system: always active, active only during the summer months (June, July, August), and active for seven months (April, May, June, July, August, September, October).

3.6. Uncertainty and Sensitivity Analysis of Existing Building

Sensitivity analysis of the case flat was performed in DesignBuilder software. In sensitivity analysis, the aim is to analyze the sensitivity of design variables on the output.

To run UA/SA in DesignBuilder software, it is first necessary to take a simulation from the model. After the simulation is taken, the analysis type, outputs, and design variables are adjusted from the settings option specified in Figure 3.16. For this stage of the thesis study, the analysis type was selected as 'Uncertainty/Sensitivity Analysis' and the level was selected as simple. The 'simple' option at the level provides access to only the most frequently used variable distributions for design variables, and this level is sufficient for this thesis study.

After determining the analysis type and level, analysis outputs are defined in the 'Outputs' option. Analysis outputs are collected under headings such as comfort, cost, daylight, energy and loads, environmental impact, and heat gains, as seen in Figure 3.17. 'Discomfort ASHRAE 55(all clo)' and 'total site energy' were selected for this study.

In the next step, design variables need to be defined (Fig. 3.18). For design variables, the distribution category, distribution curve, and the building zone targeted by the input must be entered in the DesignBuilder software. The distribution category is a probability distribution type, and there are two options for this property: Discrete and continuous. Discrete probability distribution type is defined for list type or numerical variables. Continuous probability distribution type is used for variables with min and max numerical values. The distribution curve is a statistical function that describes the

probabilities of possible values for the design variable (DesignBuilder 2024). There are various functions such as uniform, normal, lognormal, exponential, triangular, and binomial. Uniform distribution is used for variables where all situations between the specified lower and upper variable values have an equal probability of occurring and there is no probabilistic advantage. The normal distribution has a symmetrical pattern and shows that data close to the mean occurs more frequently than data far from the mean. The probability of any value occurring in a normal distribution is determined by calculating the mean and standard deviation of the data. Target objects indicate the building zone that is desired to be evaluated for input. With this option, it can be chosen just one room, two rooms, or the entire building.

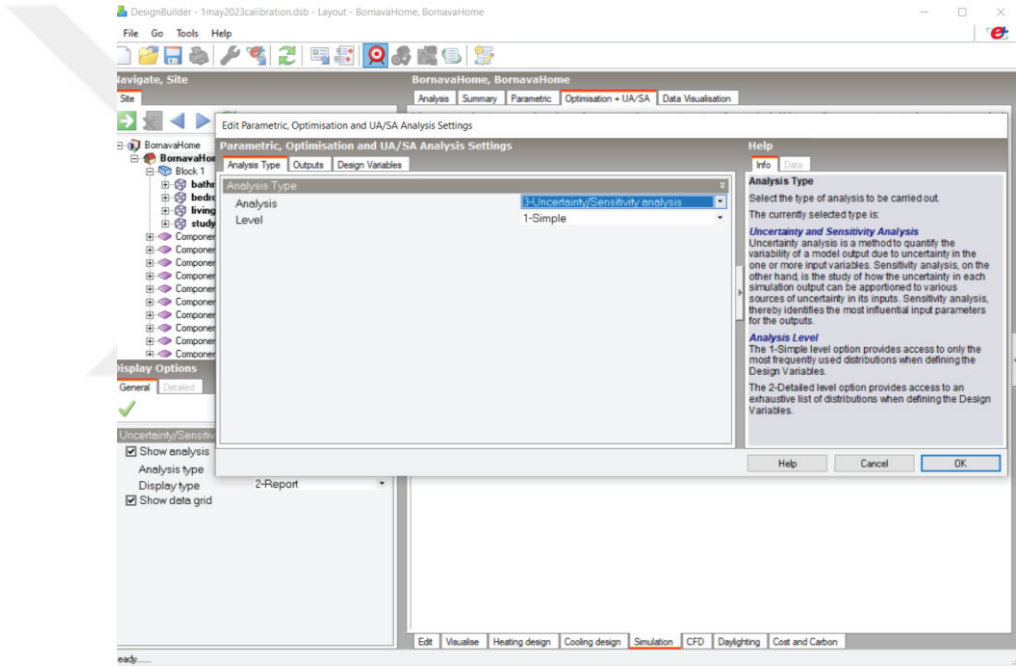

Figure 3.16. 'Edit Parametric, Optimization, and UA/SA Analysis Settings' in DesignBuilder

After design variables and outputs settings are made, calculation settings related to the analysis must be made in the UA/SA calculation options box. First, the sampling method to be used in the uncertainty and insensitivity analysis process should be determined. Determining the sampling method is an important decision for creating the input matrix and examining the input-output distributions accordingly. DesignBuilder software has five different method options for this process: random, random walk, Latin hypercube sampling, Sobol, and Halton (Figure 3.19).

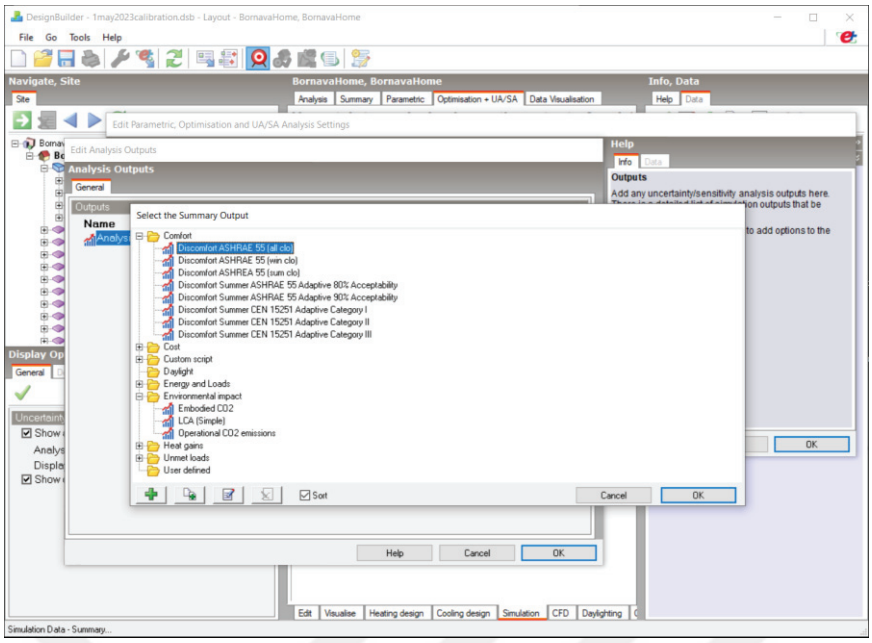

Figure 3.17. Defining the outputs for UA/SA in DesignBuilder

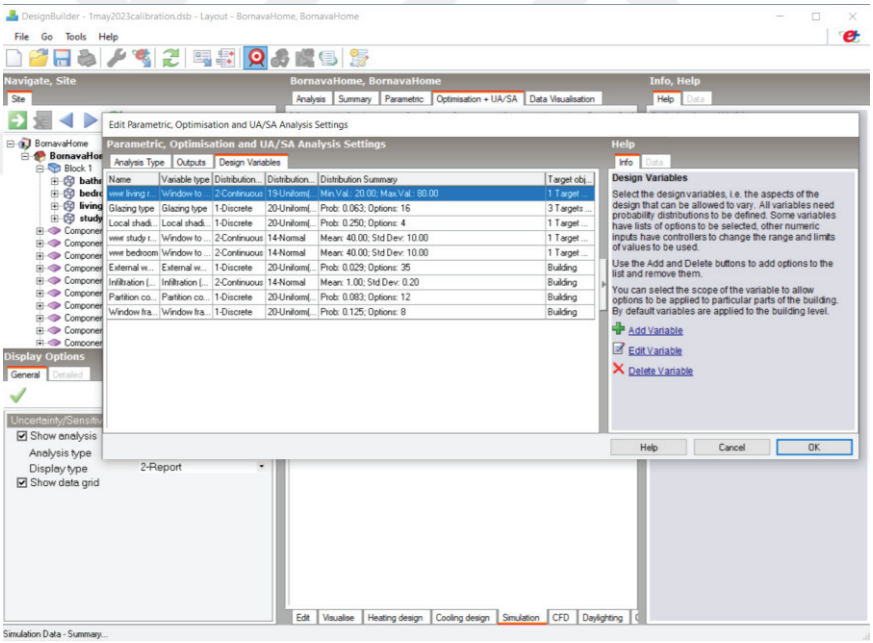

Figure 3.18. Defining design variables and properties for UA/SA in DesignBuilder

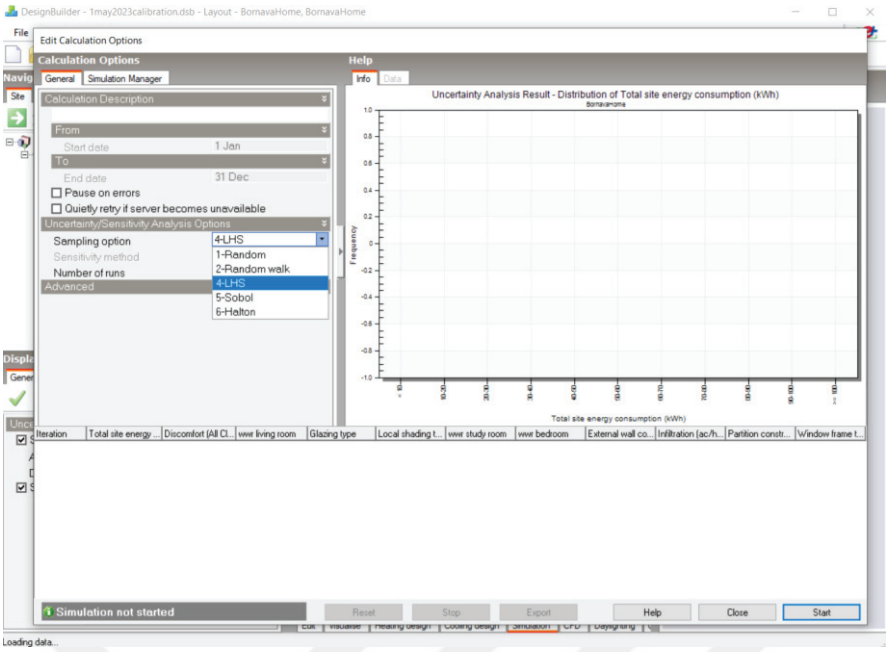

Figure 3.19. Editing calculation options for UA/SA in DesignBuilder

In this thesis study, Latin hypercube sampling (LHS) was chosen as the sampling method. LHS provides effective stratification by dividing the inputs into layers and is a widely used method in uncertainty and sensitivity analysis as it makes it possible to evaluate with a relatively small number of samples compared to other methods (Helton et al. 2006). After defining input-output and sampling selection, the desired number of samples should be entered in the last stage. Loeppky et al. (2009, 366-376) recommended the sampling number as 10*n (n is the number of input) for regression methods such as sensitivity analysis. To obtain the most accurate data in this study, the sample size was determined as 2000.

3.7. Multi-objective Optimization of Existing Building

In DesignBuilder software, multi-objective optimization is done using the non-dominated sorting genetic algorithm (NSGA-II) developed by Deb et al. (2002). NSGA-II algorithm gives non-dominant results, also known as Pareto optimal results, as a result of multi-objective optimization.

In NSGA-II, a random initial population is first created. The designer decides how many individuals will be in this initial population and this is called generation population size. The solutions obtained from the initial population are ranked according to their superiority over the Pareto solution. The fast dominant sorting method is used in this

sorting. In the fast dominant sorting method, the objective function values of each individual are examined, and the dominance of the individuals is calculated by comparing them with other results. In this way, the fitness of each solution is assigned equal to its non-suppression level (Aksoy 2016). In the next step, binary tournament selection, crossover, and mutation functions based on the crowding distance approach are applied to the initial population. NSGA-II uses the crowding distance approach to ensure that the distribution of the Pareto optimal solution set is equal and balanced (Kocatürk and Altunkaynak 2019). In addition, crossover and mutation functions are applied to ensure diversity in the algorithm and to prevent repetition. The rates of these functions are entered by the designer as mutation rate and crossover rate. In the last step, the selection process is performed, and the best non-suppressed solutions (Pareto-front solution set) are stated.

In this thesis, multi-objective optimization is divided into three scenarios and progressed with the variables determined to be sensitive. In the first and fourth scenario, variables related to the building envelope, in the second and fifth scenario, variables related to the heating and cooling system, and in the third and sixth scenario, all variables are considered together (Table 3.20).

Table 3.20. Scenarios for multi-objective optimization

Scenario-1 & 4 (Building envelope)				
Design Variables	**Distribution category**	**Min value**	**Max value**	**Option list**
Window to wall ratio (%) for bedroom	Continuous	20	80	-
Window-to-wall ratio (%) for living room and kitchen	Continuous	20	80	-
Window-to-wall ratio (%) for study room	Continuous	20	80	-
Glazing type	Discrete	-	-	16 options
External wall construction	Discrete	-	-	35 options
Infiltration (ac/h)	Continuous	0.3	1	-
Shading type	Discrete	-	-	13 options
Natural vent. schedule				
Scenario-2 & 5 (HVAC settings)				
Heating set-point temperature	Continuous	19	23	-
Cooling set-point temperature	Continuous	24	28	-
Cooling operation schedule	Discrete	-	-	3 options
Scenario-3 & 6 (Building envelope and HVAC settings)				

To apply these steps in the DesignBuilder software, it is first necessary to run an hourly, monthly, or annual simulation without running the optimization. Afterward, in order to start the optimization, objective functions, additional outputs, constraints, and design variables are entered from the 'Edit Parametric, Optimization, and UA/SA Analysis Settings' settings (Figure 3.20). No constraints were identified for this study. As an additional output, energy consumption for cooling is defined to analyze the overheating problem. Objective functions are defined as thermal discomfort hours and energy consumption as stated in Section 3.6.1, and design variables are defined as stated in Section 3.6.2.

After defining the objective functions and design variables and selecting the analysis type as 'optimization', maximum generations, generations for convergence, mutation rate, crossover rate, and initial population size data should be entered in the optimization calculation options section. These data vary depending on the type of problem, its size, and the number of targets. Ascione et al. (2019) stated that the most important parameters for the reliability of multi-objective optimization are the maximum number of generations and generation population size.

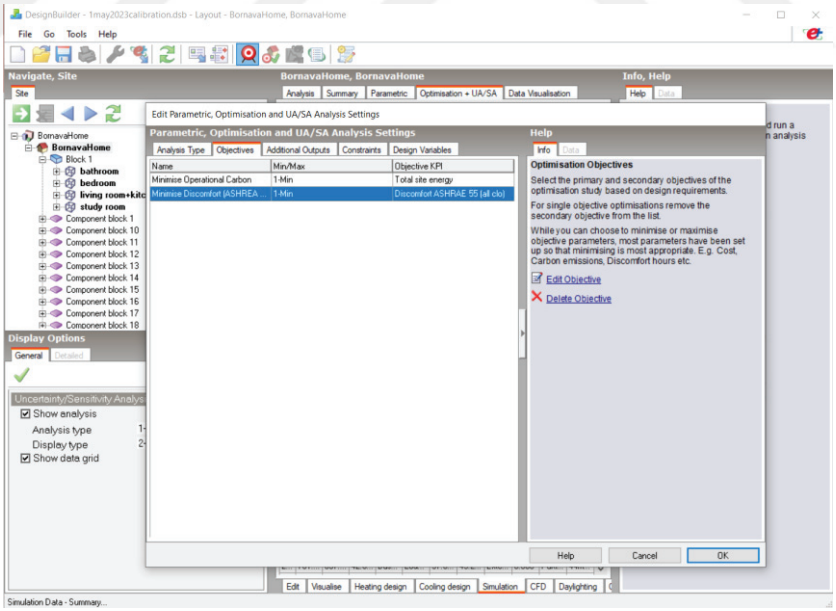

Figure 3.20. Editing objective functions, additional outputs, constraints, and design variables

Generation population size indicates how many individuals will be in the first randomly selected population. The larger the population size, the more different solutions

there are in the same generation. In some studies, it has been stated that it is appropriate to determine the population size to be between 2 and 6 times the number of design variables (Ascione et al. 2016; Mukkavaara and Shadram 2021; Ascione et al. 2019; Mostafazadeh et al. 2023; Rosso et al. 2020; Ascione et al. 2017; D'Agostino et al. 2023). Table 3.21 shows the number of variables and population sizes considered in the scenarios in this study.

Table 3.21. Parameters of genetic algorithm for each scenario

	Scenario 1 & 4	Scenario 2 & 5	Scenario 3 & 6
Number of design variables	8	3	11
Generation population size	35	30	30
Maximum generations	100	100	100
Generation for convergence	20	20	20
Mutation rate	0.1	0.2	0.1
Crossover rate	0.9	0.9	0.9

The maximum number of generations indicates how many populations will be created. The maximum number of generations varies because the problem size of each scenario is different. In similar studies in the literature, it is seen that this parameter takes values between 25 and 200 (Abdou et al. 2021; Acar et al. 2021; Ascione et al. 2015; Bagheri-Esfeh and Dehghan 2022; Baghoolizadeh et al. 2023; Bre and Fachinotti 2017; Bre et al. 2016; Chaantrelle et al. 2011; D'Agostino et al. 2023; Gao et al. 2023; Magnier and Haghighat 2010; Mostafazadeh et al. 2023; Mukkavaara and Shadram 2021; Yigit 2021). Considering the problem size and number of variables, the maximum number of generations was determined as 100.

Generations for convergence are used to decide when to stop optimization simulations. As the number of generations progresses in the optimization process, the number of optimum solutions found decreases. If an optimum solution cannot be found for that number of generations with the value specified in the generations option for convergence, the optimization process will end. In this study, generations for convergence were determined as 20.

In addition to these data, crossover rate and mutation rate values can also be changed in the advanced section of the DesignBuilder calculation options. The mutation function allows to increase the diversity in the population and the discovery ability of the

genetic algorithm. A high mutation rate may cause the algorithm to behave randomly and may extend the optimization time. The mutation rate for this study was determined by examining similar studies in the literature. In similar studies, it has been analyzed that it is generally considered as 0.02, 0.05, 0.1 or 0.2 (Abdou et al. 2021; Ascione et al. 2015; Bagheri-Esfeh and Dehghan 2022; Baghoolizadeh et al. 2023; Bre and Fachinotti 2017; Bre et al. 2016; Gao et al. 2023; Khani et al. 2022; Magnier and Haghighat 2010; Rosso et al. 2020; Yigit 2021; Yu et al. 2015). In this study, the mutation rate was taken as 0.1 for scenarios, while in the second and fifth scenario, it was taken as 0.2 due to the small number of design variables. Another parameter is the crossover rate. The crossover function enables the production of new individuals. Through the crossover function, diversity increases, and new solution candidates are produced. When similar studies were examined, it was analyzed that the crossover rate generally took a value between 0.7 and 1, and the most common value was 0.9 (Abdou et al. 2021; Bagheri-Eshef and Dehghan 2022; Baghoolizadeh et al. 2023; Bre and Fachinotti 2017; Bre et al. 2016; D'Agostino et al. 2023; Gao et al. 2023; Gou et al. 2018; Khani et al. 2022; Magnier and Haghighat 2010; Mukkavaara and Shadram 2021; Yigit 2021; Yu et al. 2015). In this study, the crossover rate for each scenario was considered as 0.9.

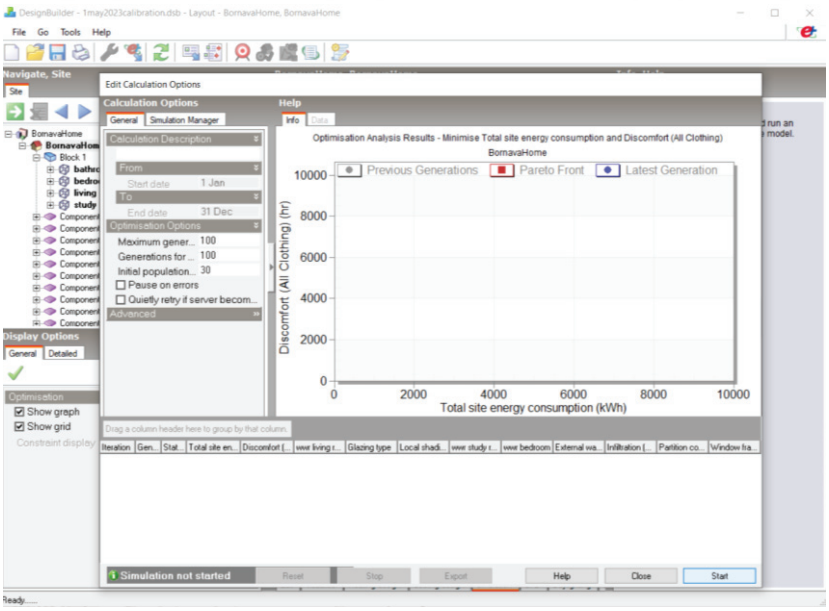

Figure 3.21. Editing calculation options for optimization

After the parameters of the NSGA-II genetic algorithm are determined, these values are entered in the section shown in Figure 3.21. The algorithm starts looking for optimum values. There is a limitation in DesignBuilder software for multi-objective

optimization, and this limitation is that more than one optimization result cannot be stored at the same time.

CHAPTER 4

RESULTS AND DISCUSSION

4.1. Measurement Results

In line with the objectives of the thesis, monitoring results for indoor and outdoor conditions were collected and evaluated between 05.05.2023 00:00 and 01.01.2024 00:00. While outdoor weather data were obtained from the Bornova Zeytincilik Research Station of the General Directorate of Meteorology, indoor weather data were obtained from the HOBO device placed in the case room.

4.1.1. Indoor measurement results

The temperature and relative humidity values of the case room were monitored between May 5, 2023, and January 1, 2024. Temperature, relative humidity, and light intensity values observed for eight months are shown in Figures 4.1, 4.2, and 4.3.

Minimum, maximum, and average monthly values are evaluated in Table 4.1. The highest average temperature is seen in July with 34.5 °C. The difference between minimum and maximum temperatures is higher for November and December, while it is between 7-8 °C for the other months. The lowest average temperature is seen in November with 27.1 °C.

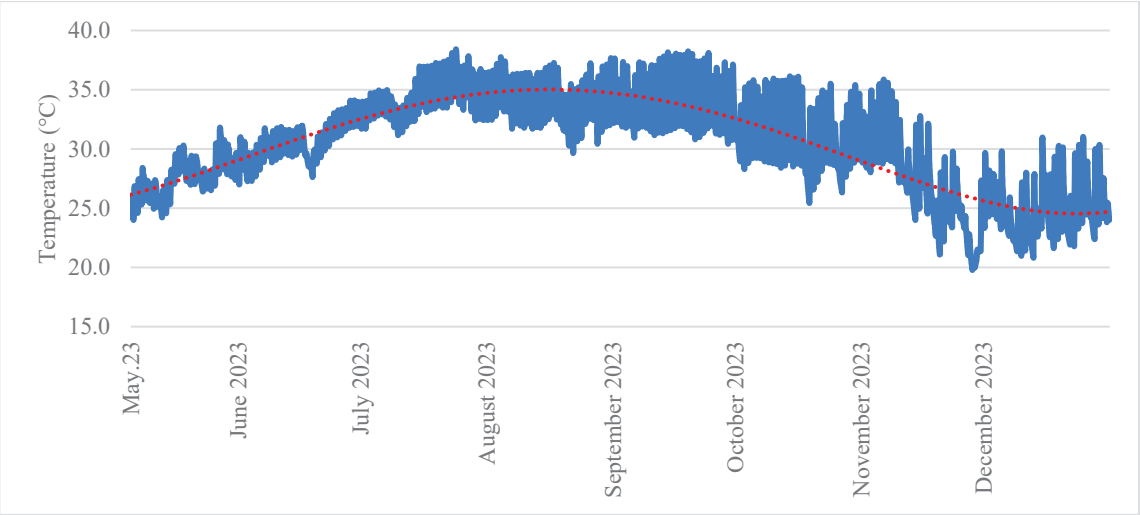

Figure 4.1. Temperature values of indoor for May 2023 - December 2023

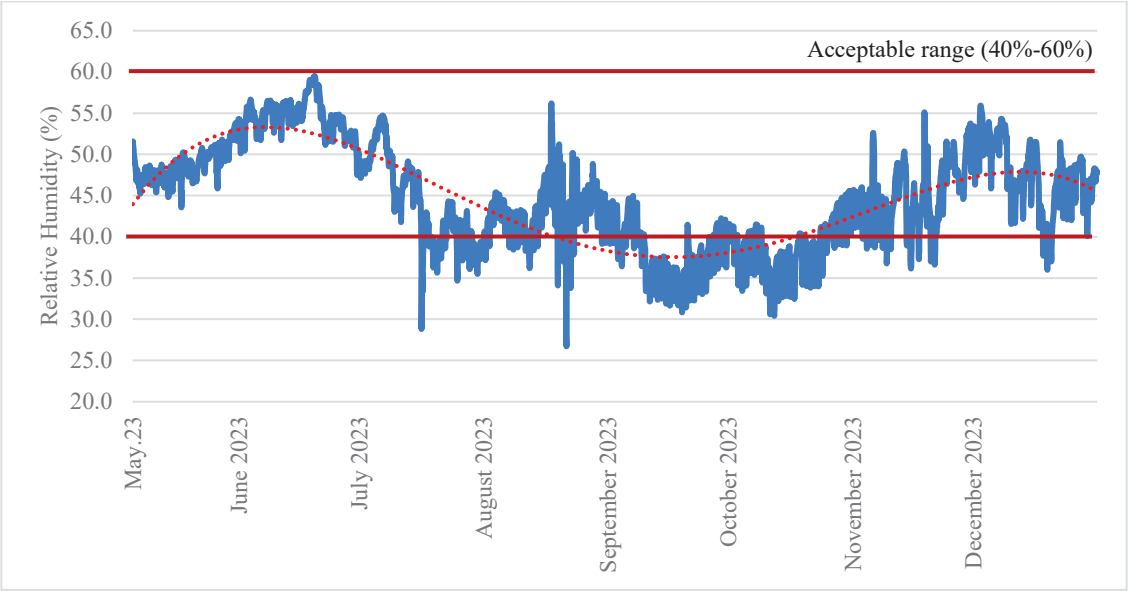

Figure 4.2. Relative humidity values of indoor for May 2023 - December 2023

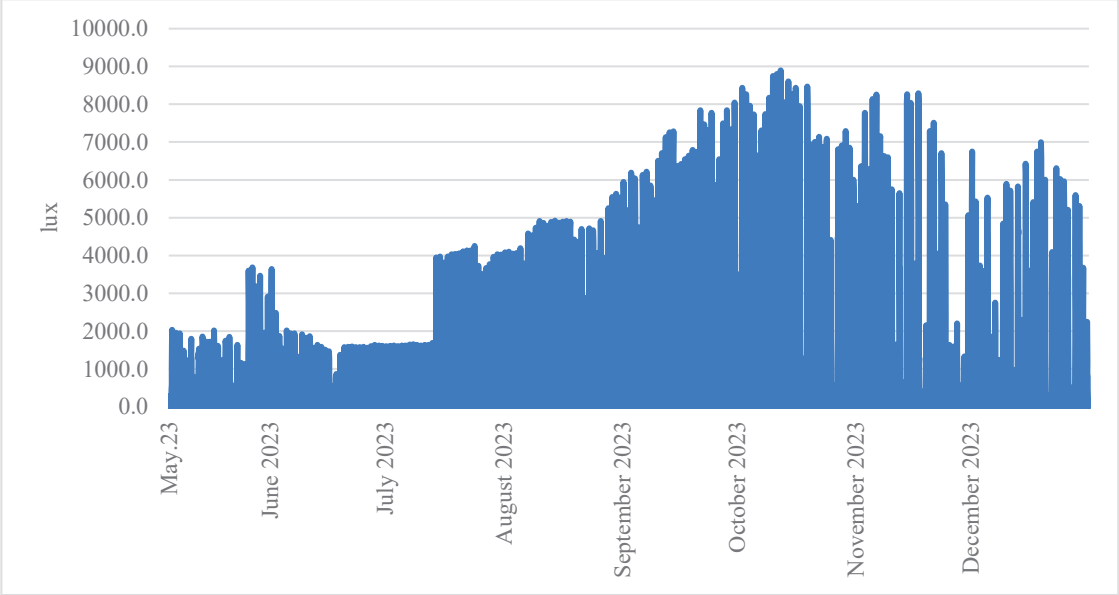

Figure 4.3. Light intensity values of indoor for May 2023 - December 2023

Research emphasizes that relative humidity values, in addition to temperature, are important for indoor air quality, individual health and comfort, and the optimum relative humidity value is recommended between 40% and 60% (Wolkoff et al. 2021). It is seen that the average relative humidity values are outside the specified range in September and October.

Table 4.1. Maximum, minimum and average of indoor's T and RH values in a monthly

2023	Minimum			Maximum			Average		
	Temperature (°C)	Relative Humidity (%)	Light intensity (lux)	Temperature (°C)	Relative Humidity (%)	Light intensity (lux)	Temperature (°C)	Relative Humidity (%)	Light intensity (lux)
May	24.0	43.6	3.9	31.8	54.3	3687.0	27.6	48.8	442.3
June	27	47.5	3.9	34.1	59.5	3646.3	30.7	54.6	434.4
July	31.1	28.8	3.9	38.4	54.7	4254.6	34.5	44.1	757.9
Aug	29.7	26.7	3.9	37.8	56.2	5634.3	34.0	43.0	1110.9
Sep	30.4	30.8	3.9	38.2	44.9	8045.4	34.0	37.9	1425.1
Oct	25.4	30.4	6.5	36.1	45.6	8896.8	31.1	38.6	1400.9
Nov	19.8	36.2	11.8	35.9	55.1	8288.5	27.1	45.3	892.3
Dec	20.8	36	3.9	31.0	55.9	6998.2	24.9	47.7	765.9

Thermal discomfort hours were calculated in the 'Climate Consultant' software for the temperature and relative humidity data obtained from the 8-month monitoring period (Climate Consultant 2024). In Figure 4.4, it is stated that 94% of the total 4416 hours between May and October were discomfort hours. Blue rectangles indicate the frame that meets thermal comfort standards. Red dots show monitoring data. The monitoring data shows that the temperature and relative humidity values are higher than thermal comfort standards. In Figure 4.5, calculations are made for the months of May and December. For this period, 80% of 5880 hours were evaluated as discomfort hours.

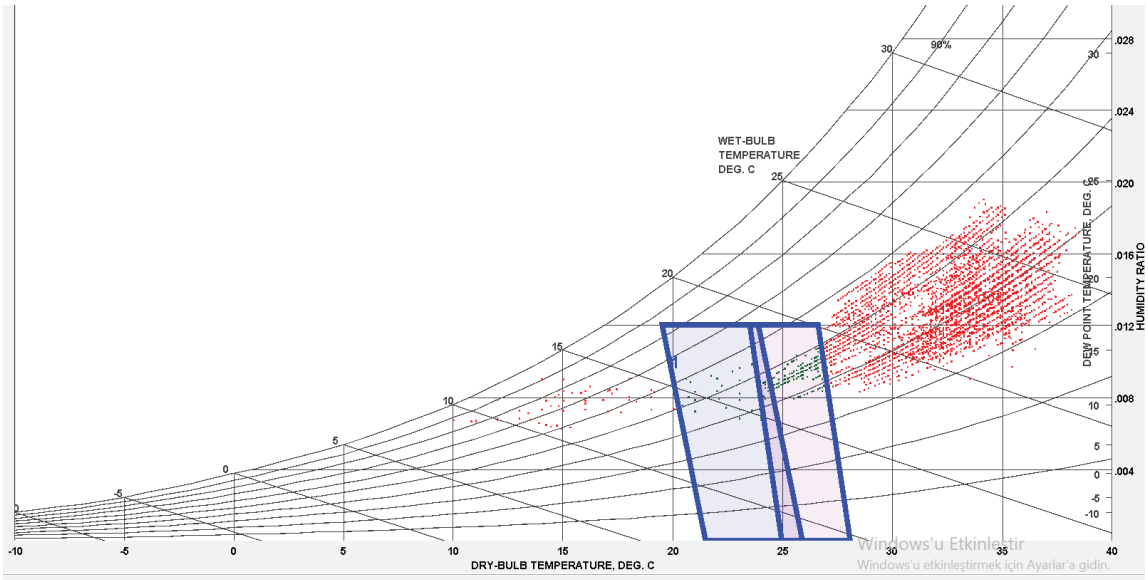

Figure 4.4. Psychrometric chart according to monitoring data for May-October

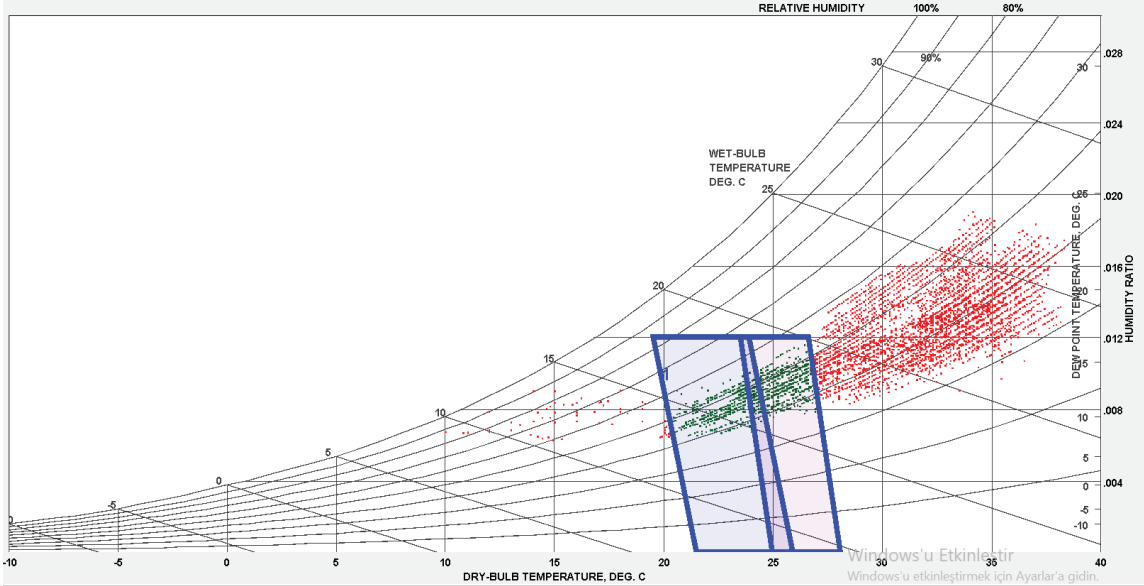

Figure 4.5. Psychrometric chart according to monitoring data for May-December

Thermal discomfort hours calculated according to monitoring data and calculated in the DesignBuilder software for each month are shown in Table 4.2. To calculate all hours, the study room is defined as occupied 24/7 in DesignBuilder. From the table, it can be seen that all hours are thermally uncomfortable in the summer months (June, July, August). It is noteworthy that especially in September and October, high hours of thermal discomfort are observed.

Table 4.2. Comparison between monitoring data and model for discomfort hours

Discomfort hours	May	June	July	August	September	October	November	December
Monitoring data	523	720	744	744	720	722	401	144
DB model	732	720	744	744	720	744	530	340

Heating-cooling energy consumption of the case flat: The electricity and natural gas energy consumptions of the case flat obtained from the invoices are given in Table 4.3. The blank spaces in the table are months for which invoices cannot be accessed. Electricity consumption includes not only cooling but also lighting and appliance use. Based on these data, the energy consumption of the case flat for heating and cooling can be evaluated approximately.

Table 4.3. Heating-cooling energy consumption of the case flat

	Electricity (kWh)	Heating (natural gas) (kWh)
February 2023		62
March 2023		102
April 2023		45
May 2023	61.983	3
June 2023	51.466	0
July 2023	90.674	0
August 2023	150.452	0
September 2023	215.746	0
Octorber 2023	77.89	0
November 2023	83.012	10
December 2023	59	79

4.1.2. Outdoor measurement results

Temperature, relative humidity, global solar radiation, wind speed, and pressure values recorded every ten minutes for the Bornova Zeytincilik Research Station were received from the General Directorate of Meteorology. These data, recorded every ten minutes, were converted into hourly averages to prepare the outdoor climate data file. With this hourly data, graphs were created between January 2023 and December 2023.

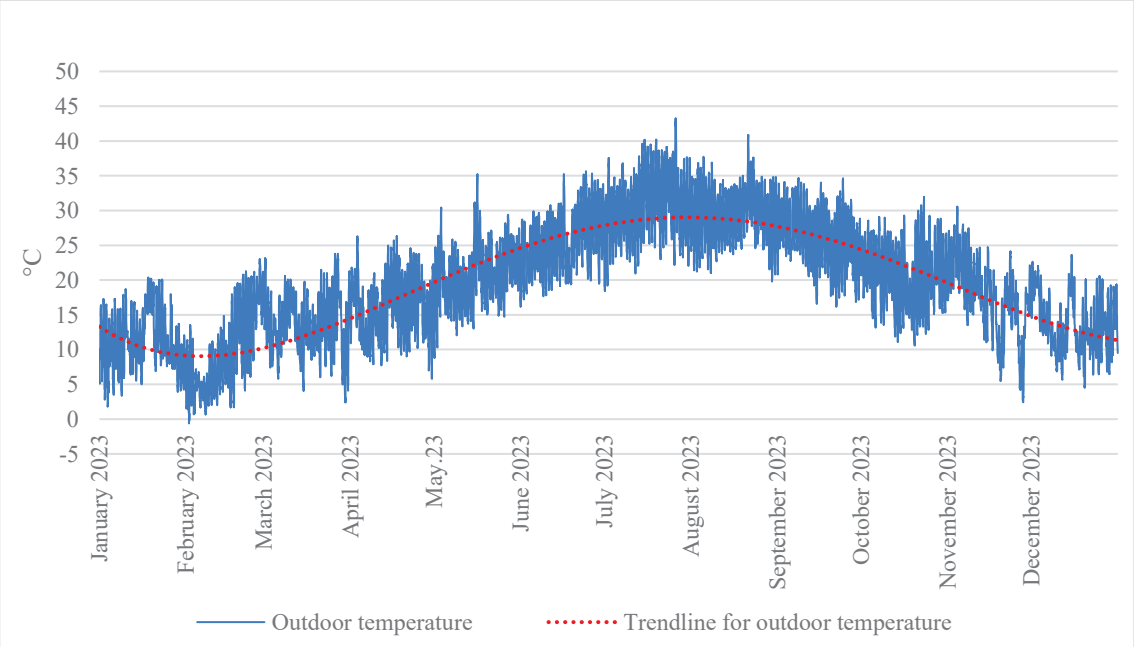

Figure 4.6. Temperature values of outdoor for January 2023 - December 2023

Figure 4.6 shows hourly temperature data. Table 4.4 shows the monthly minimum, maximum, and average temperature and relative humidity values. According to this table, the month with the highest average temperature is July, with 30.7 °C. July is followed by August, September, and June. The month with the highest minimum and maximum temperature difference is November. The average lowest temperatures are seen in November and December.

Figure 4.7 shows that relative humidity values are recorded to be relatively high, especially in November and December. Average outdoor relative humidity values vary between 19% and 100%. It was determined that the month with the highest average relative humidity value was December. The lowest average relative humidity is in July.

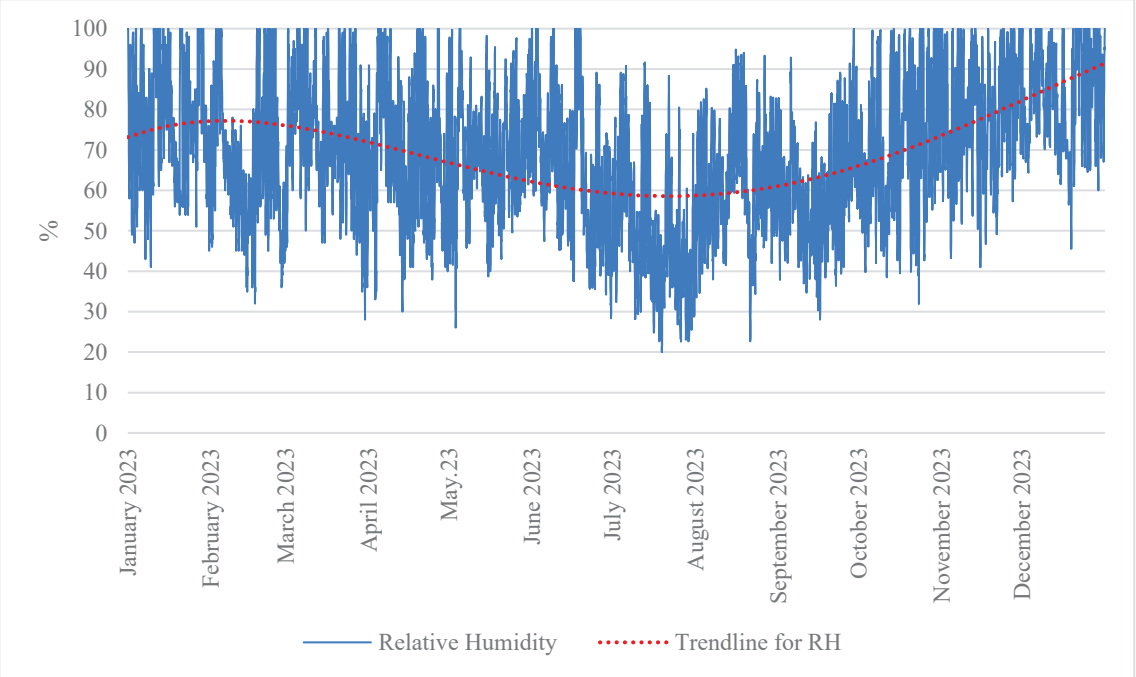

Figure 4.7. Relative humidity values of outdoor for January 2023 - December 2023

Data recorded between May and December are available for global solar radiation. Figure 4.8 shows that global solar radiation is higher in May, June, July, and August than in September, October, November, and December. It was determined that the monthly average of global solar radiation was highest in July with 322.2 W/m^2 and lowest in December with 66.75 W/m^2 (Table 4.4).

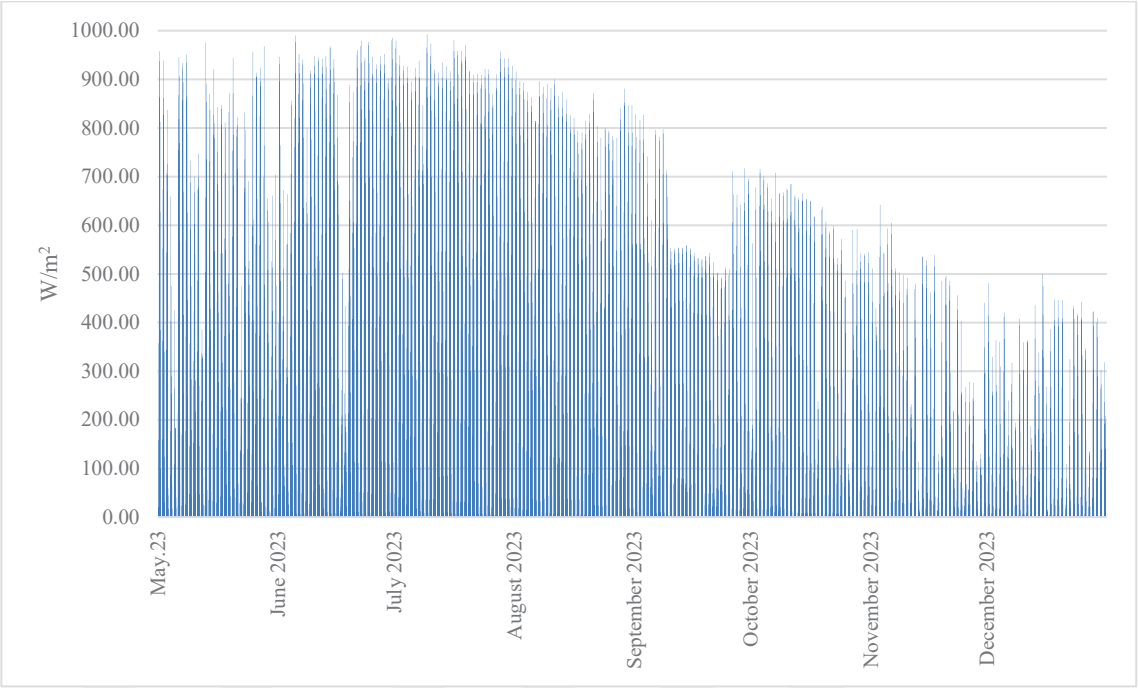

Figure 4.8. Global solar radiation for May 2023 - December 2023

Table 4.5 shows the minimum, maximum, and average values of monthly wind speed. The average wind speed was highest in September with 2.58 m/sec, and lowest in December with 1.76 m/sec. It is seen that atmospheric air pressure is lower on some days compared to other days, especially in November and December, in its one-year values. Low pressure creates rising air, it starts to rain as it rises. At high pressure, descending air movements occur; in this case, the weather becomes frosty.

Table 4.4. Maximum, minimum and average of outdoor's temperature and relative humidity values in a monthly

2023	Minimum			Maximum			Average		
	Temperature (°C)	Relative Humidity (%)	Global solar radiation (W/m^2)	Temperature (°C)	Relative Humidity (%)	Global solar radiation (W/m^2)	Temperature (°C)	Relative Humidity (%)	Global solar radiation (W/m^2)
Jan	4.4	77.5		11.7	84.5		9.1	80.8	
Febr	1.8	70.5		4.9	100		3.7	89.6	
March	5.4	84.5		9.1	96.5		7.2	90.5	
April	1.8	70.5		15.3	100		8.1	90.8	
May	8.8	26	0	35.2	100	975.4	20.6	69.7	230.1
June	17.2	27	0	35.7	100	990.2	25.7	65.6	289.2

(cont. on the next page)

Table 4.4.(cont.)

July	18.5	20	0	43.2	93	993	30.8	49.2	322.2
Aug	19.8	21	0	40.9	97	915.6	29.5	61.8	266.6
Sept	16.2	27	0	34.7	100	828.5	26.0	59.9	177.7
Oct	10.6	29	0	32.0	100	716.2	20.4	73.2	147.6
Nov	2.4	39	0	30.6	100	642.1	17.3	79.9	87.5
Dec	4.5	44	0	23.6	100	499.2	13.3	84.9	66.75

Table 4.5. Maximum, minimum and average of outdoor's global solar radiation, wind speed and pressure values in a monthly

2023	Minimum			Maximum			Average		
	Wind Speed (m/sec)	Wind direction	Pressure (hPa)	Wind Speed (m/sec)	Wind direction	Pressure (hPa)	Wind Speed (m/sec)	Wind direction	Pressure (hPa)
Jan	0.1	0	1015.7	6.5	337.5	1024.9	2.1	114.7	1021.7
Febr	0.1	0	1012	11.7	337.5	1021.3	2.4	113.1	1015.9
March	0.1	0	1012.6	7.8	337.5	1016.8	2.2	138.8	1014.6
April	0.1	0	1001.95	11.7	337.5	1013.5	2.2	154.4	1005.8
May	0.27	21.3	1004.4	4.85	335.1	1020.6	2.19	142.7	1012
June	0.25	15.3	1002.1	5.13	322.1	1015.5	2.17	149.9	1009.5
July	0.35	19.5	1001.6	5.93	308	1016.2	2.51	144.45	1009.1
Aug	0.38	23.3	1003.2	5.97	280.3	1013.5	2.36	162.9	1007.5
Sept	0.33	28.8	1002.7	5.67	277.5	1016.6	2.58	128.06	1011.3
Oct	0.33	18.1	1009.1	7.38	295.8	1020.5	1.85	142.4	1015.7
Nov	0.32	24	985.6	7.67	298.1	1020.5	1.98	161.6	1012.9
Dec	0.28	34.3	999.9	5.70	301.6	1030.9	1.76	132.7	1017.0

4.2. Calibration Results

The temperature and relative humidity values collected by the data logger in the study room were calibrated according to the error indices specified in ASHRAE Guideline 14. These error indices are root mean squared error (RMSE) and mean bias error (MBE). These error indices are acceptable among simulated and monitored hourly temperature data according to ASHRAE standards when RMSE is below ±30%, and MBE is below ±10% (ASHRAE Guideline 14 2002).

Table 4.6. RMSE and MBE results for each simulation

	Calibration-1		Calibration-2		Calibration-3	
	RMSE (%)	MBE (%)	RMSE (%)	MBE (%)	RMSE (%)	MBE (%)
May	15.25	14.45	12.25	11.25	8.76	7.44
June	14.32	13.79	11.49	10.84	8.91	8.02
July	11.07	10.75	8.48	8.08	6.77	6.23
August	16.29	15.59	13.69	12.86	11.36	10.33
September	8.12	6.79	6.07	4.12	4.67	1.37
October	7.64	1.03	7.78	-1.81	8.81	-5.25
November	11.29	3.85	11.33	3.31	10.26	-1.27
December	13.87	10	13.87	10	9.62	3.31
	Calibration-4		Calibration-5		***Calibration-6***	
	RMSE (%)	MBE (%)	RMSE (%)	MBE (%)	***RMSE (%)***	***MBE (%)***
May	5.51	2.96	6.24	4.08	***6.24***	***4.08***
June	5.46	3.54	6	4.34	***6***	***4.34***
July	3.57	1.85	3.81	2.3	***3.81***	***2.3***
August	7.02	5.13	7.45	5.7	***7.45***	***5.7***
September	5.27	-3.26	4.8	-2.4	***4.83***	***-2.48***
October	11.19	-9.25	10.4	-8.2	***6.47***	***-0.07***
November	10.77	-5.23	10.2	-3.4	***9.4***	***-2.03***
December	8.75	-2.62	8.48	-0.14	***8.48***	***-0.14***

The calibration process was carried out for eight-months period between 5 May 00:00 2023 and 1 January 00:00 2024. Calibration steps proceeded in line with the steps specified in Section 3.5.4. Figure 4.9 shows the graph of temperature data from the simulation and monitoring temperature data. Table 4.6 gives the RMSE and MBE error rates calculated for each calibration step.

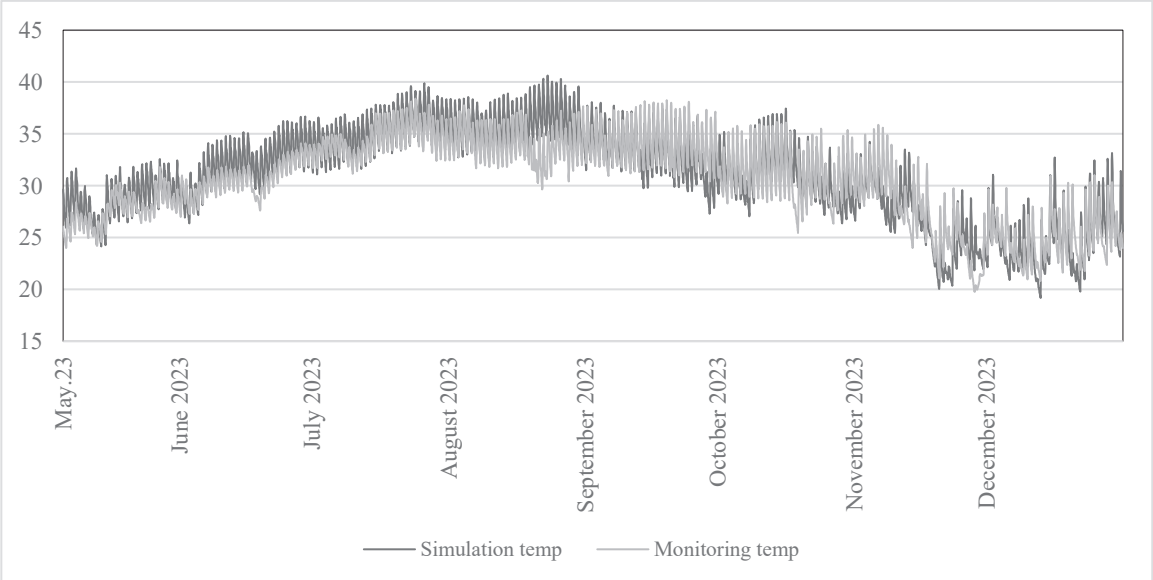

Figure 4.9. Graph of simulation and monitoring data

4.3. Simulation Results

4.3.1. Simulation Results with HVAC

Heating and cooling systems were activated in each of the bedroom, study room, and living room and kitchen while the simulation results were being obtained. Since the study room was never used during the calibration process, occupancy was not defined, but when the simulation results were obtained, it was assumed that one person lived in the house and each room was used. In this context, an occupancy schedule has been assigned to the study room (Table 4.7).

Table 4.7. The occupancy schedule of living room and kitchen and bedroom

Occupancy of…	**Occ. Density (people/m^2)**	**Period: Day**	**Occupied hours**
Study Room	0.095	Weekdays	13:00-15:30 17:00-20:00
		Weekends	13:00-15:30 17:00-20:00

In Table 4.8, the results obtained from the simulation are stated monthly and annually. Annual thermal discomfort hours are 402.83 hours, and especially in July and August, thermal discomfort hours are higher than other months. The energy consumption for cooling is 1507.98 kWh annually, and the energy consumption for heating is 437.42 kWh annually. Annual carbon emissions are 995.88 kgCO_2e'dir. The area of the heated and cooled zone is 39 m^2. Energy consumption per square meter is 49.8 kWh/m^2.

Table 4.8. Results of simulation

	Cooling energy(kWh)	Heating energy(kWh)	CO_2 emission (kgCO_2e)	Discomfort hours (hrs)
January	0.86	283.87	53.76	122.46
February	21.32	42.06	20.8	12.14
March	11	64.65	18.79	18.9
April	25.55	29.89	21.09	8.09
May	125.28	0	75.92	8.63
June	226.85	0	137.47	29.38
July	314.39	0	190.52	54.53
August	346.6	0	210.04	68.29

(cont. on the next page)

Table 4.8. (cont.)

September	240.06	0	145.47	25.08
October	114.46	0	69.36	22.67
November	49.38	6.07	31.06	28.83
December	32.18	10.85	21.54	3.76
Annual	**1507.98**	**437.42**	**995.88**	**402.83**

4.3.2. Simulation Results without HVAC

It will be more apparent to detect an overheating problem when the heating and cooling systems are passive. This part aims to analyze the thermal comfort situation of the case flat without using the heating-cooling system. All other model data remained the same. Only the HVAC system was turned off for this section. In this case, annual thermal discomfort hours are calculated as 2222.55 hours. One-year graphs created with hourly PMV and PPD values are shown in Figures 4.10 and 4.11.

Figure 4.10 shows high temperatures in spring, summer and autumn, causing thermal discomfort hours. Similarly, in Figure 4.11, PPD values are always 100% in summer and autumn. When heating-cooling systems are passive, the high number of hours of thermal discomfort throughout the year, especially in the summer and autumn months, is noteworthy.

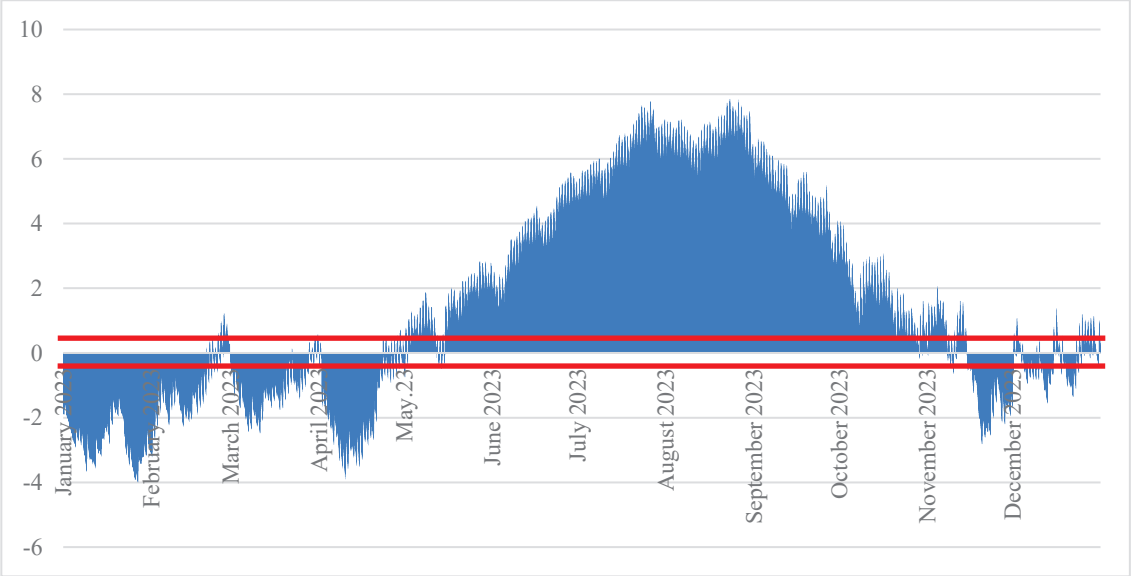

Figure 4.10. PMV graph for simulation without HVAC (red lines for acceptable range)

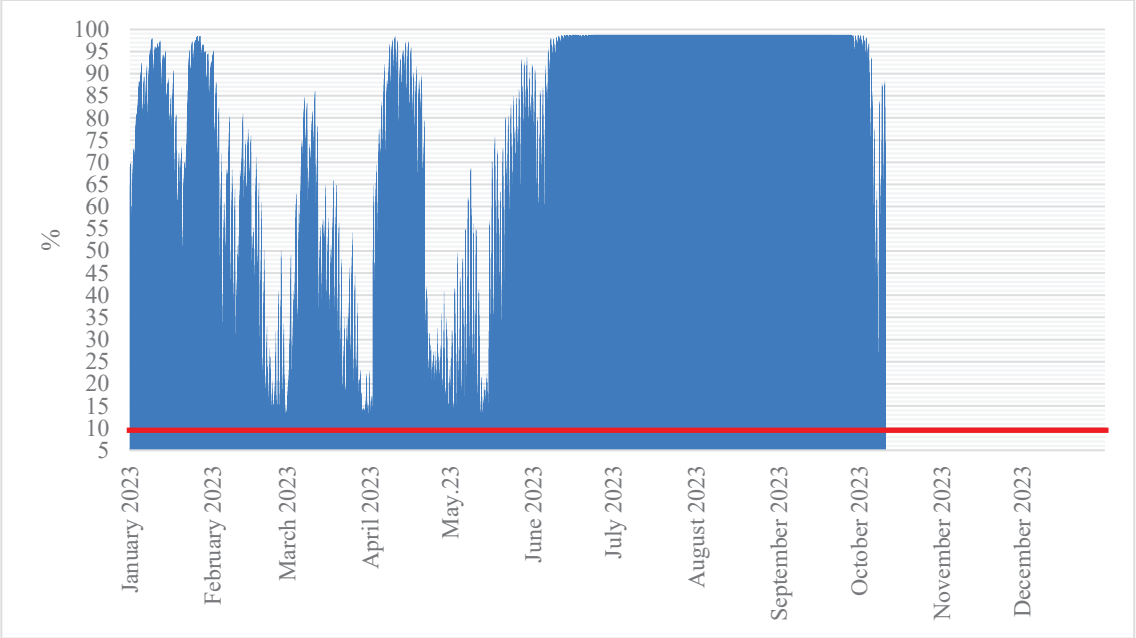

Figure 4.11. PPD graph for simulation without HVAC

4.4. Uncertainty and Sensitivity Analysis Results

4.4.1. Uncertainty Analysis Results

Uncertainty analysis shows the values that the outputs can take according to the upper and lower values determined for the design variables. The values of the design variables and value ranges specified in Section 3.6.2 and the thermal discomfort hours and annual energy consumption outputs for 2000 samples are shown in Figures 4.12 and 4.13.

The average of the outputs calculated for the thermal discomfort hours output is 1301.3 hours. The minimum decreased to 184.2 hours, the maximum increased to 2605.6 hours, and the median value was 1373.3 hours (Table 4.9). The standard deviation of the outputs taken for thermal discomfort hours is 613.8. Since the standard deviation is not close to the mean value, it is understood that the diversity of the variables is high.

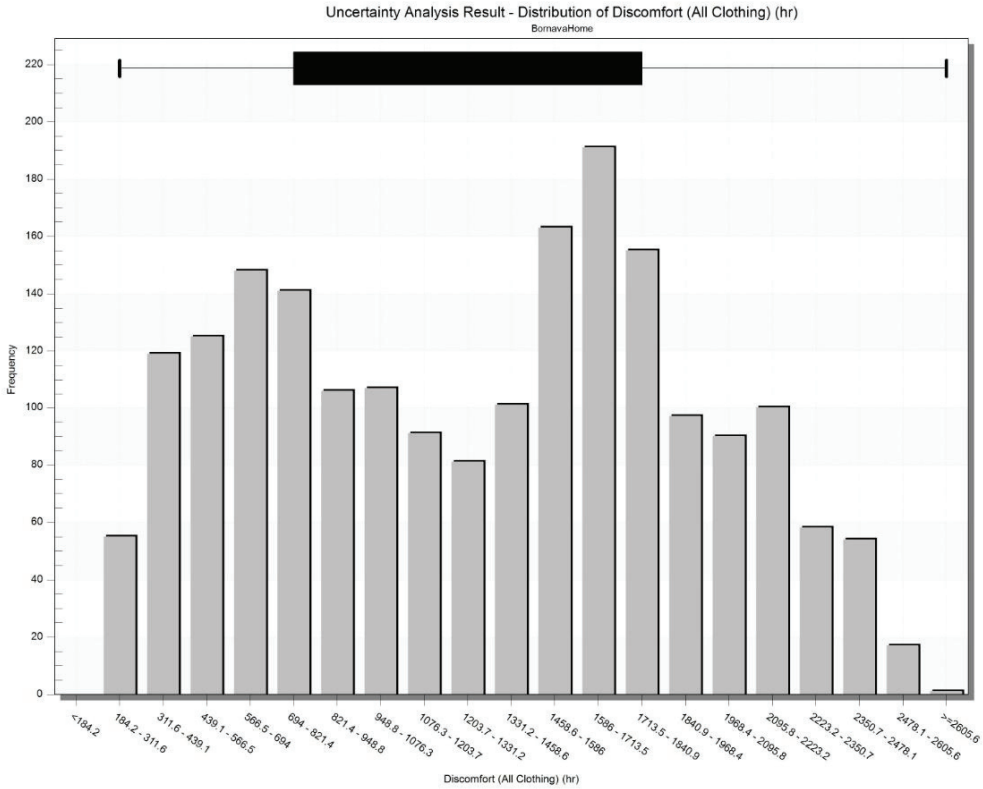

Figure 4.12. Uncertainty analysis graph for discomfort hours

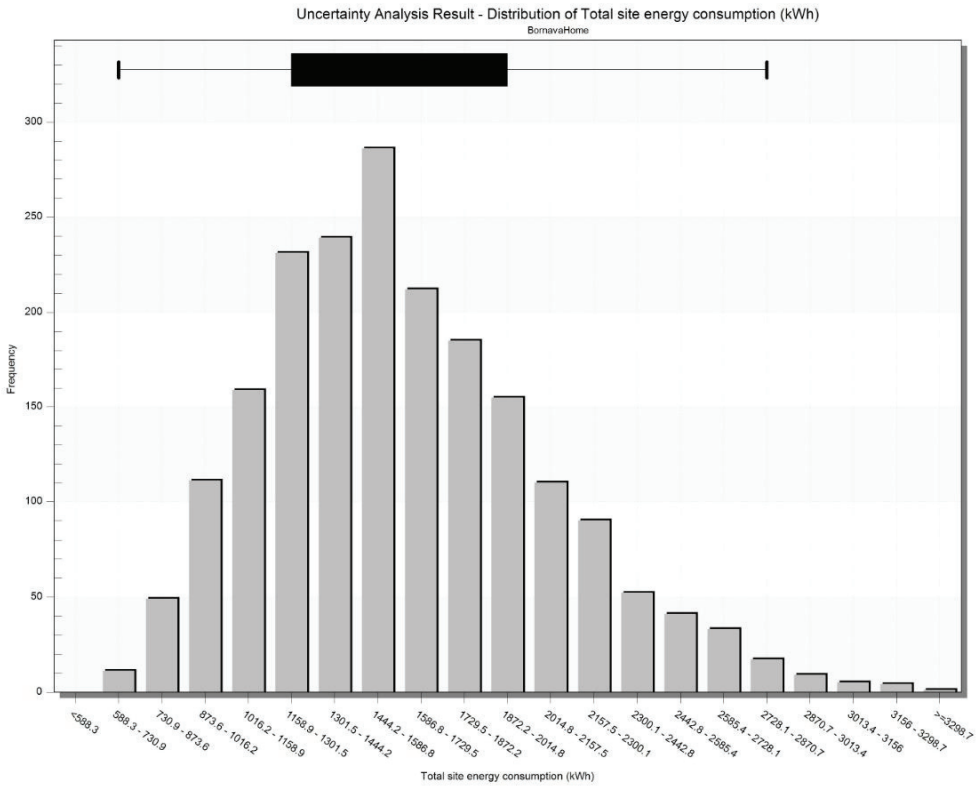

Figure 4.13. Uncertainty analysis graph for energy consumption

The lowest value in annual energy consumption output is 588.3 kWh, the highest value is 3298.7 kWh, and the median value is 1544.1 kWh. While the average of energy consumption outputs is 1603.9 kWh, the standard deviation is 462.9. Since this standard deviation value is not close to the mean value, it can be interpreted that the diversity is high for these variables.

Table 4.9. Summary statistics of uncertainty analysis

	For discomfort hours	For energy consumption
Mean	1301.3	1603.9
Standard deviation	613.8	462.9
Min	184.2	588.3
Median	1373.3	1544.1
Max	2605.6	3298.7

4.4.2. Sensitivity Analysis Results

The sensitivity analysis discussed in the study is a regression analysis that examines the relationships between design variables and objective functions. In this analysis, the dependent variables are thermal discomfort hours and total energy consumption, while the independent variables are the design variables specified in Section 3.6.2. Since there is more than one design variable, the regression analysis is multiple regression analysis.

In multiple regression analyses, analysis can be interpreted according to the coefficient of determination (R^2) and p-value obtained as a result of the analysis. The coefficient of determination (R^2) gives the rate at which the changes in the dependent variable are explained by the independent variables (Yüzük 2019, 51). It has been stated that since there is more than one independent variable in multiple regression analyses, using the coefficient of determination is not efficient, and instead, using the adjusted coefficient of determination will give more accurate results (Koutsoyıannis 1989, 101). The closer the R^2 coefficient is to 1, the more meaningful the model is, and it is concluded that the relationship between input and output can be fully fitted into the regression curve (Ulukavak Harputlugil 2009). The model is assumed to be acceptable when the adjusted R^2 coefficient is 0.7 and above. The ‘p’ value or probability value is used to tell whether the model is statistically meaningful or not. The fact that the p-value is less than 0.05 indicates a significant difference in the result of the dependent variables when the independent variables take different values.

In sensitivity analysis, a type of multiple regression analysis, the sensitivity indicator must also be determined to make a sensitivity assessment. There are sensitivity indicators such as Partial Correlation Coefficient (PCC), Partial Rank Correlation Coefficient (PRCC), Standardized Rank Regression Coefficient (SRRC), and Standardized Regression Coefficient (SRC). SRC sensitivity indicator is widely used in building energy analysis studies (Tian 2013). For this study, the SRC sensitivity indicator, which is also used in the DesignBuilder software, is used. The SA results show the SRC for each variable, which are ranked in order of sensitivity. The magnitude of each SRC value signifies the relative influence of the input on the output, and the sign indicates whether there is a direct or inverse relationship. If the SRC value of the design variable is less than 0.05, it is considered to have low sensitivity, if it is between 0.05 and 0.2, it is considered to have medium sensitivity, and if it is greater than 0.2, it is considered to have high sensitivity.

When there are very dominant design variables in the sensitivity analysis, conclusions may be drawn that the other variables are not sensitive compared to the dominant variables. However, they may be sensitive (DesignBuilder Case Study). In this case, the p values of these variables will also be high, and this analysis needs to be improved.

In this thesis study, sensitivity analyses for thermal discomfort hours and energy consumption are given under subheadings. Since some design variables remained dominant in the first step of the sensitivity analysis for both objective functions, the dominant variables were removed, and the second sensitivity analysis was performed. In the second sensitivity analysis, it is seen that there is a retrofit in the p values of the variables.

Sensitivity Analysis for Discomfort Hours: Design variables of high sensitive for thermal discomfort hours are heating and cooling set points (Fig. 4.14). These variables are directly related to the thermal discomfort hours output. The cooling setpoint has a positive sensitivity coefficient, while the heating setpoint has a negative SRC coefficient. This shows that as the cooling set point increases, the hours of thermal discomfort will increase, and as the heating set point increases, the hours of thermal discomfort will decrease. As seen from the graph in Figure 4.14 and the SRC values given in Table 4.10, heating and cooling set points remained quite dominant compared to other variables and the p values of some variables were high. For this situation, the heating and

cooling set point variables that were too dominant were removed, and the sensitivity analysis was repeated with 2000 samples.

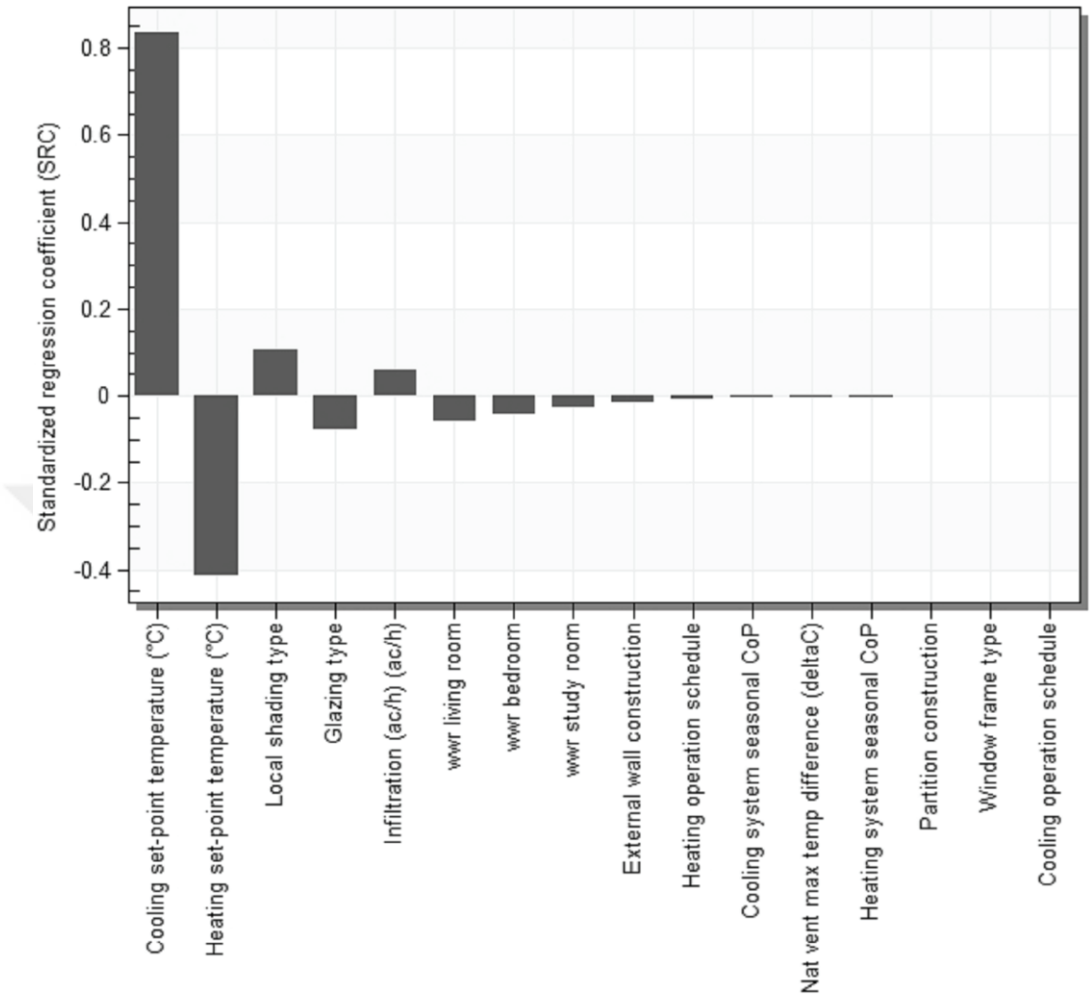

Figure 4.14. Sensitivity analysis graph for discomfort hours (SA-1)

Table 4.10. Adjusted R Squared, SRC and p values for discomfort hours (SA-1)

	For Discomfort Hours	
Adjusted R squared value	0.8818	
Variable	Standardized Regression Coefficient (SRC)	p value
Cooling set-point temperature (°C)	0.8342	0.0000
Heating set-point temperature (°C)	-0.4113	0.0000
Shading type (No Units)	0.1046	0.0000
Glazing type (No Units)	-0.0770	0.0000
Infiltration (ac/h)	0.0610	0.0000
WWR living room and kitchen (No Units)	-0.0595	0.0000
WWR bedroom (No Units)	-0.0404	0.0000
WWR study room (No Units)	-0.0273	0.0004
External wall construction (No Units)	-0.0149	0.0537

(cont. on the next page)

Table 4.10.(cont.)

Heating operation schedule (No Units)	-0.0083	0.2823
Cooling system seasonal CoP (No Units)	-0.0043	0.5795
Nat vent max temp difference (deltaC)	-0.0035	0.6459
Heating system seasonal CoP (No Units)	-0.0019	0.8050
Partition construction (No Units)	0.0015	0.8422
Window frame type (No Units)	0.0013	0.8627
Cooling operation schedule (No Units)	0.0005	0.9532

In the second sensitivity analysis, the most sensitive variable was the shading type, with an SRC value of 0.5855 (Fig. 4.15). The second most sensitive design variable was the window-to-wall ratio of the living room and kitchen. It is inferred that as the window-to-wall ratio decreases, the number of hours of discomfort increases. The infiltration rate is the third most sensitive variable; its SRC value is 0.3590. Since the SRC value is positive, thermal discomfort hours will increase as the infiltration rate increases. The infiltration rate is followed by the window-to-wall ratio of the bedroom and study room. These five design variables are highly sensitive to the output of thermal discomfort hours. Glazing type, cooling operating schedule, and natural ventilation activity schedule are moderately sensitive variables for discomfort hours. Heating system operating schedule, external and internal wall type are design variables with low sensitivity, and their SRC values are low (Table 4.11). p values for performance coefficients of heating-cooling systems and frame type were higher than the accepted range. The reason for this is that these variables have almost no effect on thermal discomfort hours.

As a result, from these two sensitivity analyses, it is concluded that the sensitive variables for the thermal discomfort hours output are heating setpoint, cooling setpoint, shading type, window-to-wall ratios for each room, and infiltration rate. Variables with low sensitivity for thermal discomfort hours are heating system operating schedule, external and partition wall type, heating-cooling system performance coefficients, and frame type.

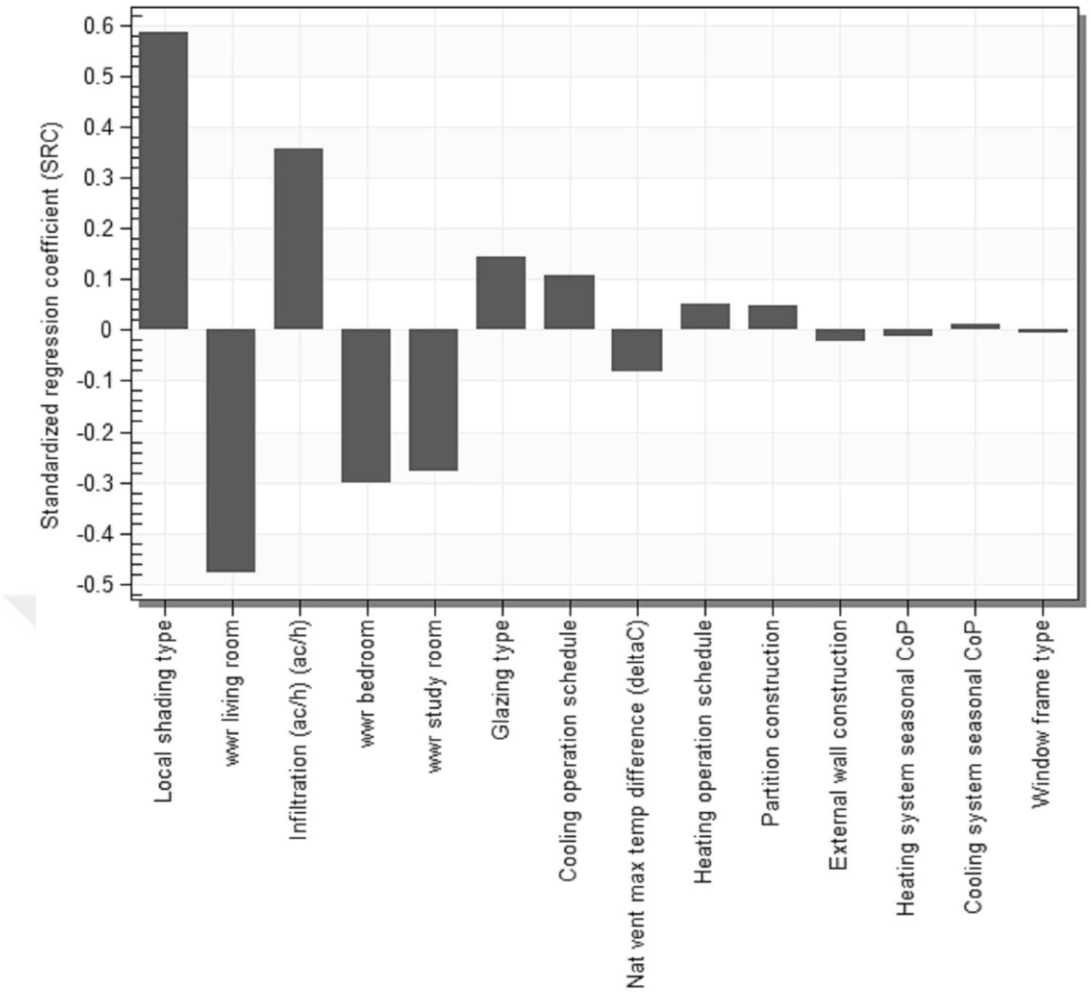

Figure 4.15. Sensitivity analysis graph for discomfort hours (SA-2)

Table 4.11. Adjusted R Squared, SRC and p values for discomfort hours (SA-2)

	For Discomfort Hours	
Adjusted R squared value	0.8962	
Variable	Standardized Regression Coefficient (SRC)	p value
Shading type (No Units)	0.5855	0.0000
Glazing type (No Units)	0.1453	0.0000
Infiltration (ac/h)	0.3590	0.0000
WWR living room and kitchen (No Units)	-0.4763	0.0000
WWR bedroom (No Units)	-0.3014	0.0000
WWR study room (No Units)	-0.2767	0.0000
External wall construction (No Units)	-0.0222	0.0022
Heating operation schedule (No Units)	0.0503	0.0000
Cooling system seasonal CoP (No Units)	0.0120	0.0971
Nat vent max temp difference (deltaC)	-0.0815	0.0000
Heating system seasonal CoP (No Units)	-0.0127	0.0785

(cont. on the next page)

Table 4.11.(cont.)

Partition construction (No Units)	0.0466	0.0000
Window frame type (No Units)	-0.0063	0.3854
Cooling operation schedule (No Units)	0.1079	0.0000

Sensitivity Analysis for Energy Consumption: The most sensitive variable for energy consumption was the infiltration rate, with a sensitivity coefficient of 0.6201 (Table 4.12). As the infiltration rate increases, energy consumption also increases. The second most sensitive variable is the heating set point, with a sensitivity coefficient of 0.4799 (Fig. 4.16). Heating set point is followed by glazing type (sensitivity coefficient is -0.4241), cooling set point temperature (sensitivity coefficient is -0.2571), and shading type (sensitivity coefficient is 0.1957). These five design variables appear to remain dominant as sensitive variables. The second sensitivity analysis for energy consumption was conducted by removing these five variables.

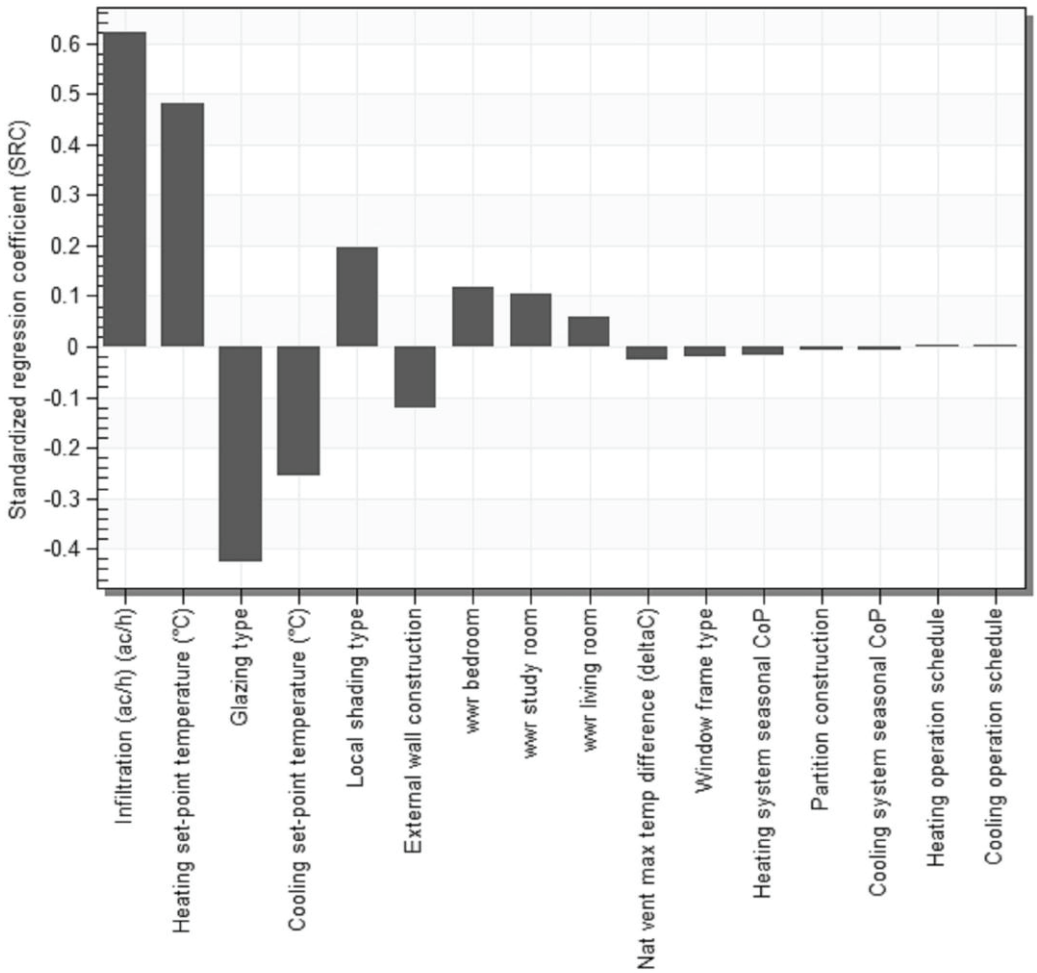

Figure 4.16. Sensitivity analysis graph for energy consumption (SA-1)

Table 4.12. Adjusted R Squared, SRC and p values for energy consumption (SA-1)

	For Energy Consumption	
Adjusted R squared value	0.95	
Variable	Standardized Regression Coefficient (SRC)	p value
Infiltration	0.6201	0.0000
Heating set-point temperature	0.4799	0.0000
Glazing type	-0.4241	0.0000
Cooling set-point temperature	-0.2571	0.0000
Shading type	0.1957	0.0000
External wall construction	-0.1210	0.0000
wwr bedroom	0.1169	0.0000
wwr study room	0.1031	0.0000
wwr living room and kitchen	0.0579	0.0000
Nat vent max temp difference	-0.0254	0.0000
Window frame type	-0.0203	0.0001
Heating system seasonal CoP	-0.0159	0.0015
Partition construction	-0.0083	0.0991
Cooling system seasonal CoP	-0.0074	0.1383
Heating operation schedule	0.0046	0.3580
Cooling operation schedule	0.0042	0.4076

In the second sensitivity analysis, it is seen that the window-to-wall ratios of the rooms are sensitive variables for energy consumption (Figure 4.17). As the window-to-wall ratios increase, the energy consumption of the case flat also increases. External wall type is a moderately sensitive design variable for energy consumption. The sensitivity coefficient is -0.1140. Heating and cooling systems operating schedule and performance coefficients, natural ventilation schedule, frame type, and partition wall type are design variables with low sensitivity coefficients for energy consumption (Table 4.13).

Table 4.13. Adjusted R Squared, SRC and p values for energy consumption (SA-2)

	For Energy Consumption	
Adjusted R squared value	0.9851	
Variable	Standardized Regression Coefficient (SRC)	p value
wwr study room	0.6125	0.0000
wwr bedroom	0.6049	0.0000
wwr living room and kitchen	0.5144	0.0000
External wall construction	-0.1140	0.0000
Cooling system seasonal CoP	-0.0373	0.0000
Nat vent max temp difference	-0.0351	0.0000
Cooling operation schedule	-0.0106	0.0001
Heating system seasonal CoP	-0.0084	0.0023
Window frame type	-0.0061	0.0262
Partition construction	0.0042	0.1228
Heating operation schedule	-0.0009	0.7439

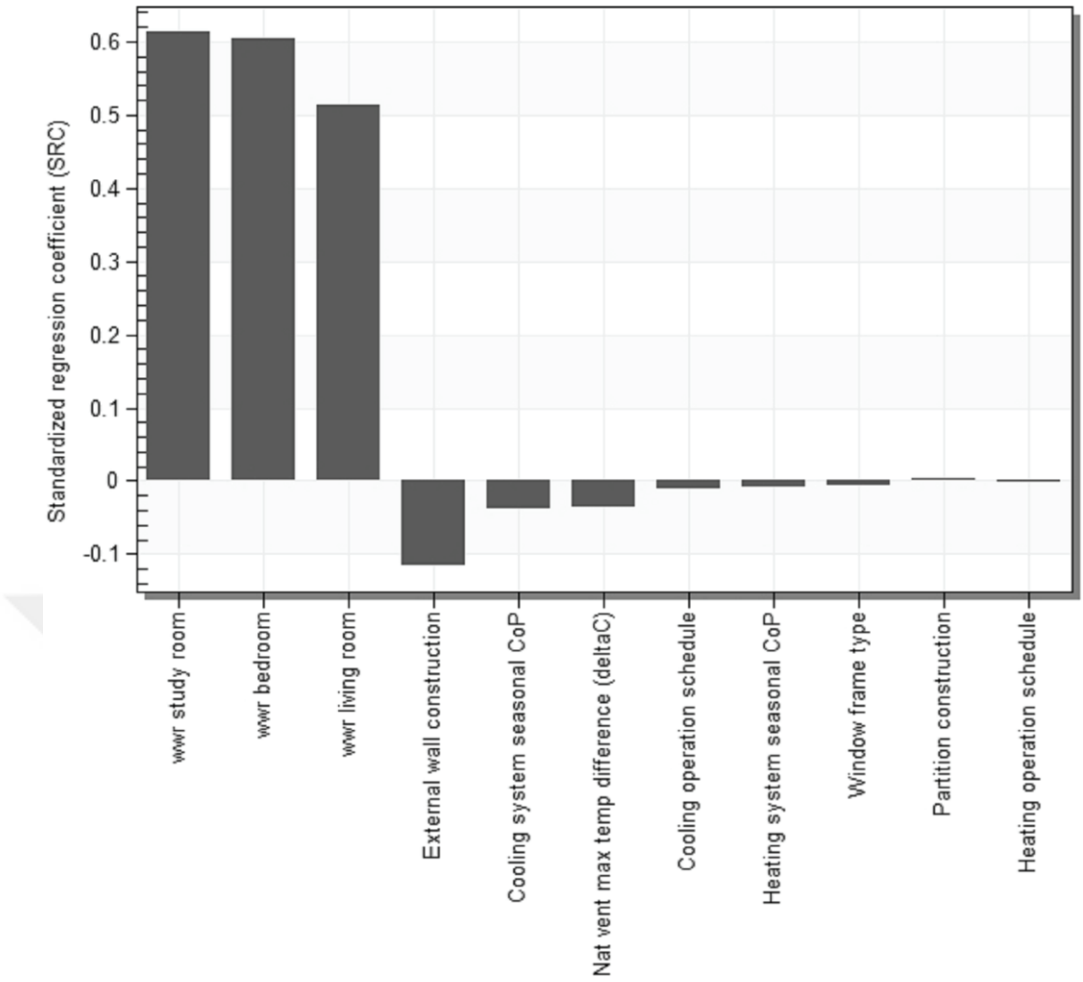

Figure 4.17. Sensitivity analysis graph for energy consumption (SA-2)

Sensitivity Analysis for both Objective Functions: It is necessary to evaluate the two outputs together to decide which design variables to consider in the multi-objective optimization process. Table 4.14 shows the sensitivity levels of design variables for energy consumption and thermal discomfort hours. Cooling set point, heating set point, shading type, glass type, infiltration rate, window-to-wall ratio for each room, external wall type, natural ventilation schedule, and cooling system operating schedule are sensitive design variables. It is seen that the heating system operating schedule, performance coefficients of heating and cooling systems, frame type, and partition wall type are design variables with low sensitivity for both variables. Therefore, these five design variables will not be considered for multi-objective optimization. In multi-objective optimization, faster and more efficient results were obtained with fewer design variables.

Table 4.14. Sensitivity degrees of design variables for thermal discomfort hours and energy consumption (White lines for discomfort hours)

	High sensitive	Medium sensitive	Low sensitive
Cooling set-point temperature	X		
	X		
Heating set-point temperature	X		
	X		
Shading type	X		
	X		
Glazing type		X	
	X		
Infiltration (ac/h)	X		
	X		
wwr living room and kitchen	X		
	X		
wwr bedroom	X		
	X		
wwr study room	X		
	X		
External wall construction			X
		X	
Heating operation schedule			X
			X
Cooling system seasonal CoP			X
			X
Natural ventilation		X	
			X
Heating system seasonal CoP			X
			X
Partition construction			X
			X
Window frame type			X
			X
Cooling operation schedule		X	
			X

4.5. Multi-objective Optimization Results

In this study, multi-objective optimization results were examined under three scenarios. In the first scenario, the building envelope and its features are discussed, and in the second scenario, the heating-cooling system and its features are discussed. In the third scenario, both the building envelope and its features and the heating-cooling system and its features are considered design variables. Five optimal variables for each scenario were examined in detail. Among these optimal results, the results with the least thermal discomfort hours, the least energy consumption, and those at the midpoint of the optimal results were selected to be analyzed. The other two optimal results considered are the lower and upper middle values according to the middle optimal result. The results for each scenario are given in the subheadings.

Multi-objective optimization results for scenario 1: For the first scenario, building envelope materials and properties were considered as design variables and the maximum number of generations is 100 and population size is 30. The heating and cooling system is set to be active 24/7. The heating set point is 18-20 °C, and the cooling set point is 26-28 °C for the bedroom. The heating set point is 19-21 °C, and the cooling set point is 24-26 °C for the living room and kitchen and study room.

In the first scenario, where building envelope materials and properties were discussed, 52 optimal results were found. Figure 4.18 shows the distribution of optimal results and other results. In all optimal results, energy consumption decreased while thermal discomfort hours increased. This is likely due to the type of shading where the base case is not added as an option. For all other design variables, the base case has also been added as an option.

In the optimal result 1.1, where the annual energy consumption is minimum, it is seen that the energy consumption is 619.2475 kWh, the discomfort hours are 703.47 hours, and the energy consumption for cooling is 493.773 kWh (Table 4.15). In this case, the window-to-wall ratios were determined as 21% for the living room and kitchen, 23% for the study room, and 29% for the bedroom. The glass type with a U value of 1.172 $W.m^{-2}.K$ and the external wall type with a U value of 0.235 $W.m^{-2}.K$ were selected. The angle of the shading element was determined as 20 degrees, and the infiltration rate was determined as 0.3 ac/h. Natural ventilation is activated at specified schedule when the outside temperature is lower than the indoor temperature.

The optimal result between the median optimal value and the optimal value at which energy consumption is minimum is evaluated in optimal results 1.2. In this sampling, the window-to-wall ratio was determined as 40% for the living room and kitchen, 24% for the study room, and 48% for the bedroom. The infiltration rate is 0.3 ac/h, and natural ventilation is active when the indoor temperature is higher than the outside temperature. The shading type is the case where the angle is zero and the glass type is the 15th option where the U value is 1.164 $W.m^{-2}.K$. This is the case where a 30-centimeter pumice block is used as the external wall type, and insulation is provided with 5 centimeter stone wool. With these design variables, annual energy consumption was calculated as 700.2 kWh, annual cooling consumption was calculated as 618.9 kWh, and thermal discomfort hours were calculated as 550.87h.

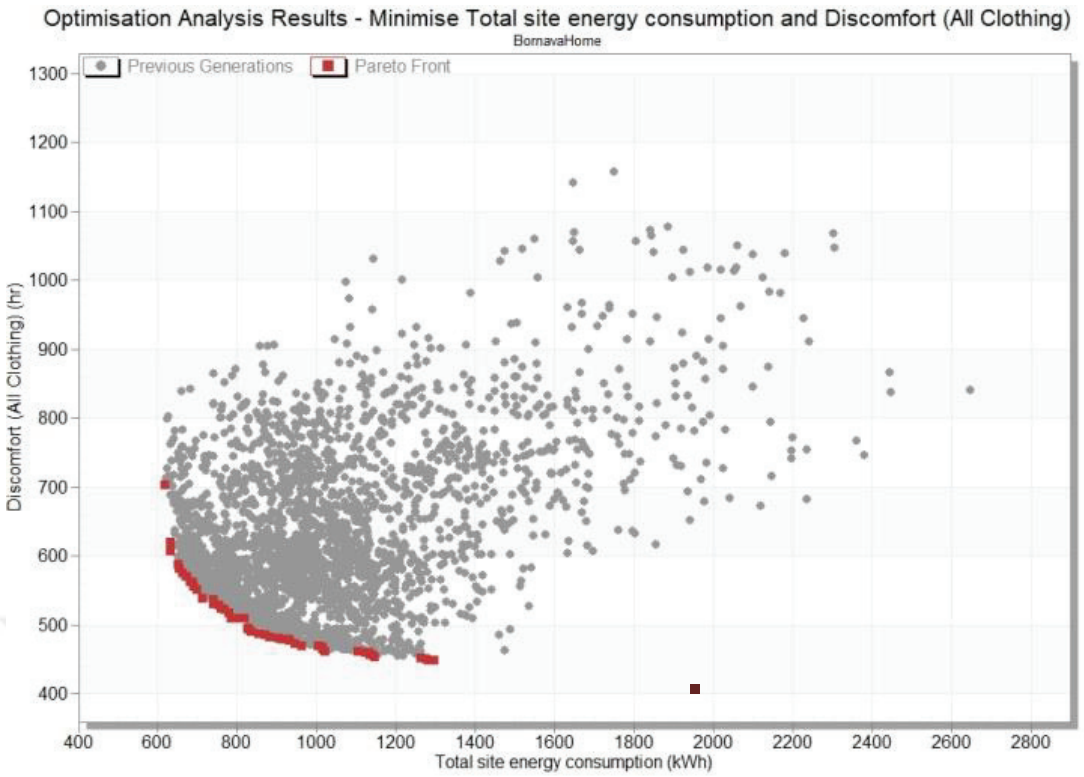

Figure 4.18. Multi-objective optimization result graph for scenario-1 (Purple dot: base case)

The result at the midpoint of the optimal results is optimal result 1.3. For this situation, energy consumption was calculated as 819.12 kWh, thermal discomfort hours as 508.91 hours, and consumption for cooling as 756.31 kWh. In this case, the window-to-wall ratios are designed as 50% for the living room and kitchen, 23% for the study room, and 67% for the bedroom. It was calculated to select the 13th glass type with a U value of 1.172 $W.m^{-2}.K$ and a SHGC value of 0.534. For glass type-13, 4 mm low-emissivity glass and 12 mm argon gas are used. The shading type was chosen when the angle of the blades was 0 degrees. The external wall type was 30 centimeters of aerated concrete with 5 cm stone wool insulation and a U value of 0.231 $W.m^{-2}.K$. Infiltration rate is considered as 0.3 ac/h. Natural ventilation will be activated when the outside temperature is lower than the indoor temperature within the specified schedule.

The optimal result is the solution between 1.4, the median optimal value, and the optimum result with minimum thermal discomfort hours. In this sampling, the angle of the shading element is 0 degrees, the glass type is 4cm low-emission glass, and there is 12mm argon gas between it. Insulation on the external wall was provided with 5 centimeters of EPS and 30 centimeters of aerated concrete was used as the material. Window-to-wall ratios is 76% for the living room, 24% for the study room, and 76% for

the bedroom. Natural ventilation is active according to schedule. With these values of the design variables, the annual energy consumption of the case flat is 1006.1 kWh, the energy consumption for cooling is 949.86 kWh, and the discomfort hours are 469.38h.

Table 4.15. Objective functions and design variables for optimal results in scenario-1

	Optimal result 1.1 (min energy)	Optimal result 1.2	Optimal result 1.3	Optimal result 1.4	Optimal result 1.5(min discomfort)
Iteration	2885	2732	3061	2991	1343
Generation	94	89	99	97	44
Energy Consumption (kWh)	619.25	700.2	819.12	1006.1	1295.65
Discomfort hours (h)	703.47	550.87	508.91	469.38	448.08
Cooling (kWh)	493.77	618.9	756.31	949.86	1248.51
WWR living room (%)	21	40	50	76	80
Glazing type	Glazing type-13	Glazing type-15	Glazing type-13	Glazing type-13	Glazing type-13
Shading type	Angle:20	Angle:0	Angle:0	Angle:0	Angle:0
WWR study room (%)	23	24	23	24	53
WWR bedroom (%)	29	48	67	76	79
External wall type	External wall-30	External wall-19	External wall-16	External wall-30	External wall-30
Infiltration (ac/h)	0.3	0.3	0.3	0.3	0.3
Nat. Vent.	Natural ventilation only operates when *OutdoorTemp < IndoorTemp*	Natural ventilation only operates when *OutdoorTemp < IndoorTemp*	Natural ventilation only operates when *OutdoorTemp < IndoorTemp*	Active according to schedule	Active according to schedule

In the optimal result 1.5, where the annual thermal discomfort hours are lowest, the thermal discomfort hours were reduced to 448.08 hours. While annual energy consumption is 1295.65 kWh, energy consumption for cooling is 1248.51 kWh. In this case, the shading type is the option with an angle of 0 degrees. Window-to-wall ratios are determined as 80% for the living room, 53% for the study room, and 79% for the

bedroom. The glass type is the type in which 4 cm low-emission glasses are used, and a 12 mm gap is left in between with argon gas. External wall type is the 30th option, using 5 cm EPS insulation and 30 centimeters of aerated concrete. The infiltration rate is 0.3 ac/h, and natural ventilation is active according to schedule.

Multi-objective optimization results for scenario 2: There are a total of 242 samples for scenario-2 design variables, so multi-objective optimization was completed before reaching the number of generations. There are 39 optimal results in the Pareto-front solution set in Figure 4.19. Compared to the base case, thermal discomfort hours increased in samples where energy consumption decreased, and energy consumption increased in samples where thermal discomfort hours decreased. There is no sample where both objective functions decrease compared to the base case.

In the optimal result where energy consumption is minimum, annual energy consumption is reduced to 990.47 kWh and energy consumption for cooling is reduced to 682.95 kWh (Table 4.16). Thermal discomfort hours increased to 2174.62 hours. For these outputs, the heating setpoint is set at 19 °C, and the cooling setpoint is set at 28 °C. The cooling system will be active during the summer months (June, July, August).

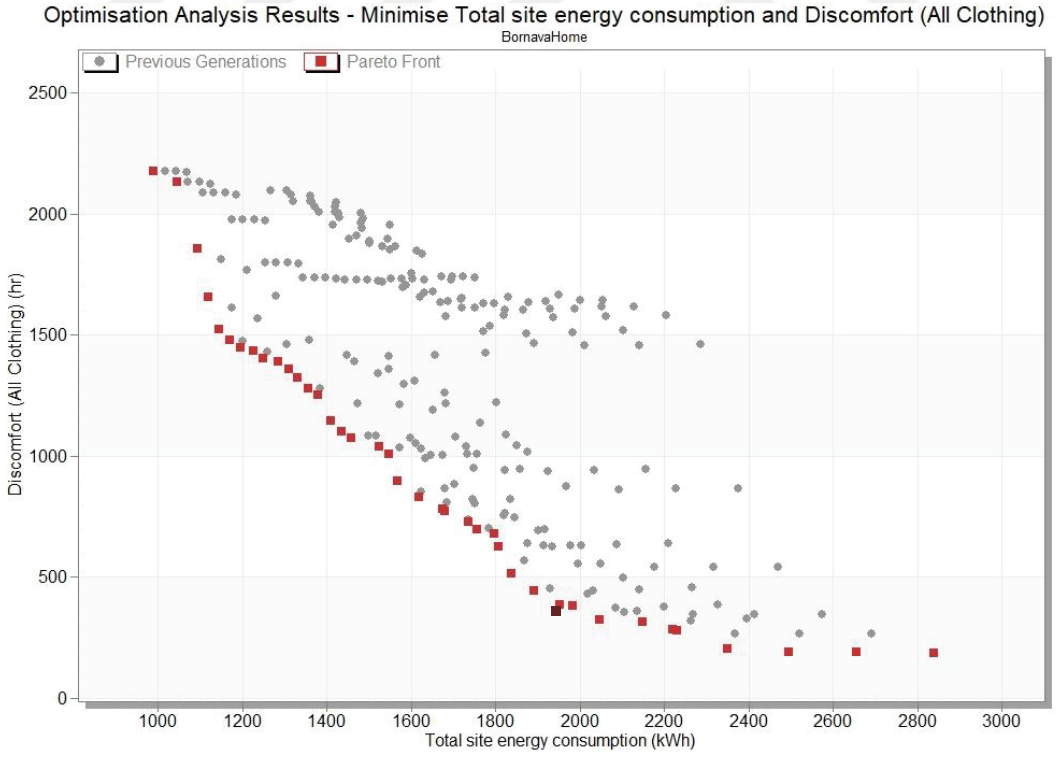

Figure 4.19. Multi-objective optimization result graph for scenario-2 (Purple dot: base case)

For the second optimal result, the heating set point was set at 20.5 °C, and the cooling set point was set at 25 °C. The cooling system is active during the summer months. With these variables, annual energy consumption was calculated as 1330.22 kWh, and energy consumption for cooling was calculated as 837.95 kWh. Thermal discomfort hours are 1322.22 hours.

In the third optimal result, the cooling system is active from April to October, and the set point is 28 °C. The heating set point is 20.5 °C. In this case, annual energy consumption is 1619.53 kWh, energy consumption for cooling is 1310.34 kWh, and discomfort hours are 829.46 hours.

Table 4.16. Objective functions and design variables for optimal results in scenario-2

	Optimal result 2.1 (min energy)	Optimal result 2.2	Optimal result 2.3	Optimal result 2.4	Optimal result 2.5(min discomfort)
Iteration	116	28	147	22	159
Generation	5	1	8	0	9
Energy Consumption (kWh)	990.47	1330.22	1619.53	1982.97	2837.91
Discomfort hours (h)	2174.62	1322.22	829.46	379.05	186.63
Cooling (kWh)	682.95	837.95	1310.34	1313.69	1578.144
Heating set-point temp. (°C)	19	20.5	19	21.5	23
Cooling set-point temp. (°C)	28	25	24.5	24.5	24
Cooling operation schedule	June-August	June-August	April-October	April-October	On 7/24

For the fourth optimal result, the heating set point was determined as 21.5 °C, and the cooling set point was determined as 24.5 °C. The cooling system is active between April and October. Annual energy consumption is 1982.97 kWh, energy consumption for cooling is 1313.69 kWh and discomfort hours are 379.05 hours.

In the fifth optimal result, where the discomfort hours were minimum, the discomfort hours were reduced to 186.63 hours. Annual energy consumption is 2837.91 kWh, and energy consumption for cooling is 1578.14 kWh. The heating set point is 23 °C, and the cooling set point is 24 °C. The cooling system is active throughout the year.

Multi-objective optimization results for scenario 3: In the multi-objective optimization, where the building envelope and its features and the heating-cooling system and its features were considered as design variables, the maximum generations is 100,

and the population size is 30. Ninety-nine optimal results were found. Figure 4.20 shows the Pareto-front and other simulation results. In 34 of the 99 optimal results, both thermal discomfort hours, energy consumption for cooling, and total annual energy consumption decreased.

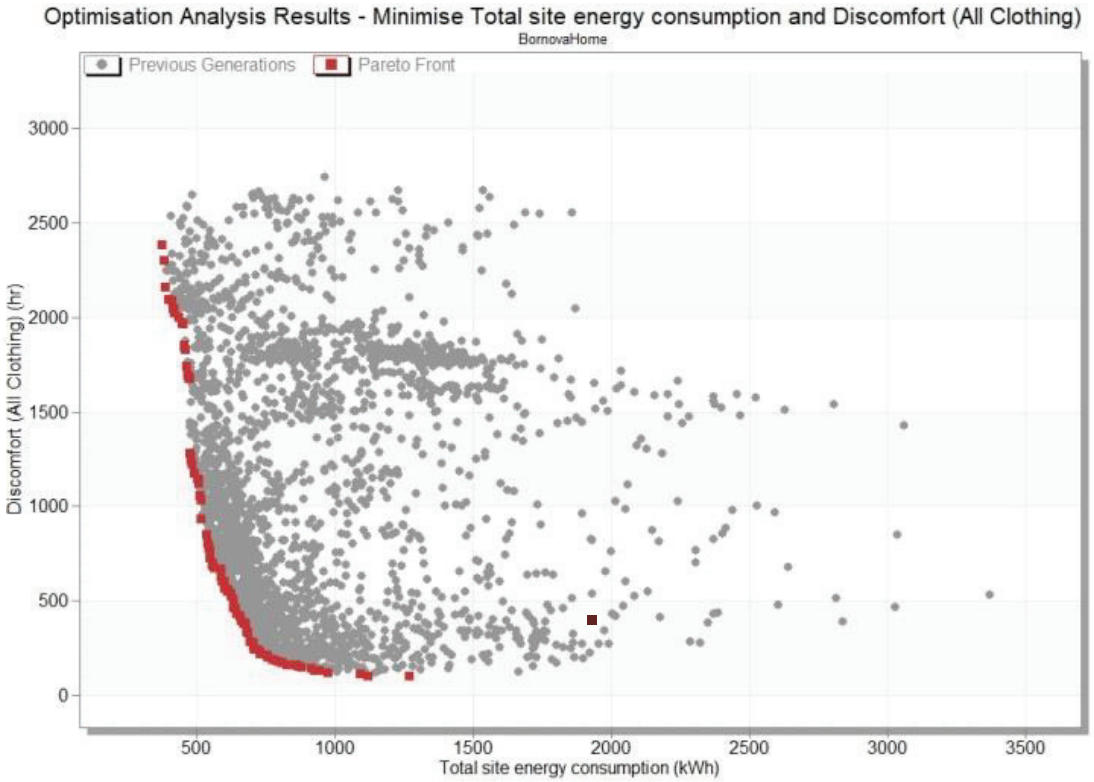

Figure 4.20. Multi-objective optimization result graph for scenario-3 (Purple dot: base case)

In the optimal result 3.1, where the annual energy consumption is minimum, it is seen that the energy consumption is 375.56 kWh, the discomfort hours are 2381.54 hours, and the energy consumption for cooling is 321.12 kWh (Table 4.17). In this case, the window-to-wall ratios were determined as 29% for the living room, 27% for the study room, and 37% for the bedroom. The glass type with a U value of 1.164 $W.m^{-2}.K$ and the external wall type with a U value of 0.257 $W.m^{-2}.K$ were selected. The angle of the shading element was determined as 15 degrees, and the infiltration rate was determined as 0.3 ac/h. The heating set point is 19 °C, and the cooling set point is 28 °C. The cooling system is active between April and October. Additionally, natural ventilation will be active for the period specified in the schedule.

The optimal result between the median optimal value and the optimal value at which energy consumption is minimum is evaluated in optimal results 3.2. In this

sampling, the window-to-wall ratio was determined as 37% for the living room, 26% for the study room, and 34% for the bedroom. The infiltration rate is 0.3 ac/h, and natural ventilation is active according to schedule. The shading type is the case where the angle is ten degrees, and the glass type is the 13th option where the U value is 1.172 $W.m^{-2}.K$. This is where 25-centimeter aerated concrete is used as the external wall type, and insulation is provided with 5-centimeter stone wool. The heating setpoint temperature is 19 °C while the cooling setpoint is 26 °C, and the cooling system is active during the summer months (June, July, August). With these design variables, annual energy consumption was calculated as 700.2 kWh, annual cooling consumption as 618.9 kWh, and thermal discomfort hours as 550.87h.ive for the period specified in the schedule.

Table 4.17. Objective functions and design variables for optimal results in scenario-3

	Optimal result 3.1 (min energy)	Optimal result 3.2	Optimal result 3.3	Optimal result 3.4	Optimal result 3.5(min discomfort)
Iteration	1791	2592	2347	2547	2454
Generation	67	95	86	93	90
Energy Consumption (kWh)	375.56	504.26	611.21	706.26	1270.17
Discomfort hours (h)	2381.54	1144.67	558.8	250.16	97.96
Cooling (kWh)	321.12	466.82	572.66	597.13	1216.6
WWR living room (%)	29	37	33	30	78
Glazing type	Glazing type-15	Glazing type-13	Glazing type-13	Glazing type-13	Glazing type-13
Shading type	Angle: 15	Angle: 10	Angle: 10	Angle: 5	Angle: 0
WWR study room (%)	27	26	26	26	62
WWR bedroom (%)	37	34	35	37	78
External wall type	External wall-33	External wall-15	External wall-15	External wall-15	External wall-34
Infiltration (ac/h)	0.3	0.3	0.3	0.3	0.3
Heating set-point temp. (°C)	19	19	19	21	21
Cooling set-point temp. (°C)	28	26	24	24	24
Nat. Vent.	Active according to schedule	Active according to schedule	Active according to schedule	Active according to schedule	Active according to schedule
Cooling operation schedule	April-October	June-August	April-October	On 7/24	On 7/24

The result at the midpoint of the optimal results is optimal result 3.3. For this situation, energy consumption was calculated as 611.21 kWh, thermal discomfort hours as 558.8 hours, and consumption for cooling as 572.66 kWh. In this case, the window-to-wall ratios are designed as 33% for the living room, 26% for the study room, and 35% for the bedroom. It was calculated to select the 13th glass type with a U value of 1.172 $W.m^{-2}.K$ and a SHGC value of 0.534. For glass type-13, 4 mm low-emissivity glass and 12 mm argon gas are used. The shading type was chosen when the angle of the blades was 10 degrees. The external wall type was 25 centimeters of aerated concrete with 5 cm stone wool insulation and a U value of 0.259 $W.m^{-2}.K$. The infiltration rate is 0.3 ac/h. Natural ventilation will be activated according to schedule. The heating set point is 19 °C, and the cooling set point is 24 °C. The cooling system is active between April and October.

The optimal result is the solution between 3.4, the median optimal value, and the optimum result with minimum thermal discomfort hours. In this sampling, the angle of the shading element is 5 degrees, the glass type is 4cm low-emission glass, and there is 12mm argon gas between it. Insulation on the external wall was provided with 5 centimeters of stone wool and 25 centimeters of aerated concrete was used as the material. Window-to-wall ratios are 30% for the living room, 26% for the study room and 37% for the bedroom. Natural ventilation is active according to schedule. The heating set point is 19 °C, and the cooling set point is 24 °C. The cooling system is active between April and October. With these values of the design variables, the annual energy consumption of the case flat is 1006.1 kWh, the energy consumption for cooling is 949.86 kWh, and the discomfort hours are 469.38h.

In the optimal result 3.5, where the annual thermal discomfort hours are lowest, the thermal discomfort hours were reduced to 97.96 hours. While annual energy consumption is 1270.17 kWh, energy consumption for cooling is 1216.6 kWh. In this case, the shading type is the option with an angle of 0 degrees. Window-to-wall ratios are 78% for the living room, 62% for the study room, and 78% for the bedroom. The glass type is the type in which 4 cm low-emission glasses are used, and a 12 mm gap is left in between with argon gas. External wall type is the 34th option, using 5 cm EPS insulation and 19 centimeters of horizontal perforated brick. The infiltration rate is 0.3 ac/h and natural ventilation is active according to schedule. The cooling set point is 24 °C, and the cooling system is active all year. The heating set point is 21 °C.

Multi-objective optimization results for scenario 4: For the fourth scenario, building envelope materials and properties were considered as design variables. It is

aimed to minimize the cooling load and thermal discomfort hours. The number of maximum generations is 100 and population size is 30. The heating and cooling system is set to be active 24/7. The heating set point is 18-20 °C, and the cooling set point is 26-28 °C for the bedroom. The heating set point is 19-21 °C, and the cooling set point is 24-26 °C for the living room and study room.

In this scenario, 87 optimal results were found. Figure 4.21 shows the distribution of optimal results and other results. In all optimal results, energy load decreased while thermal discomfort hours increased. This is likely due to the type of shading where the base case is not added as an option. For all other design variables, the base case has also been added as an option.

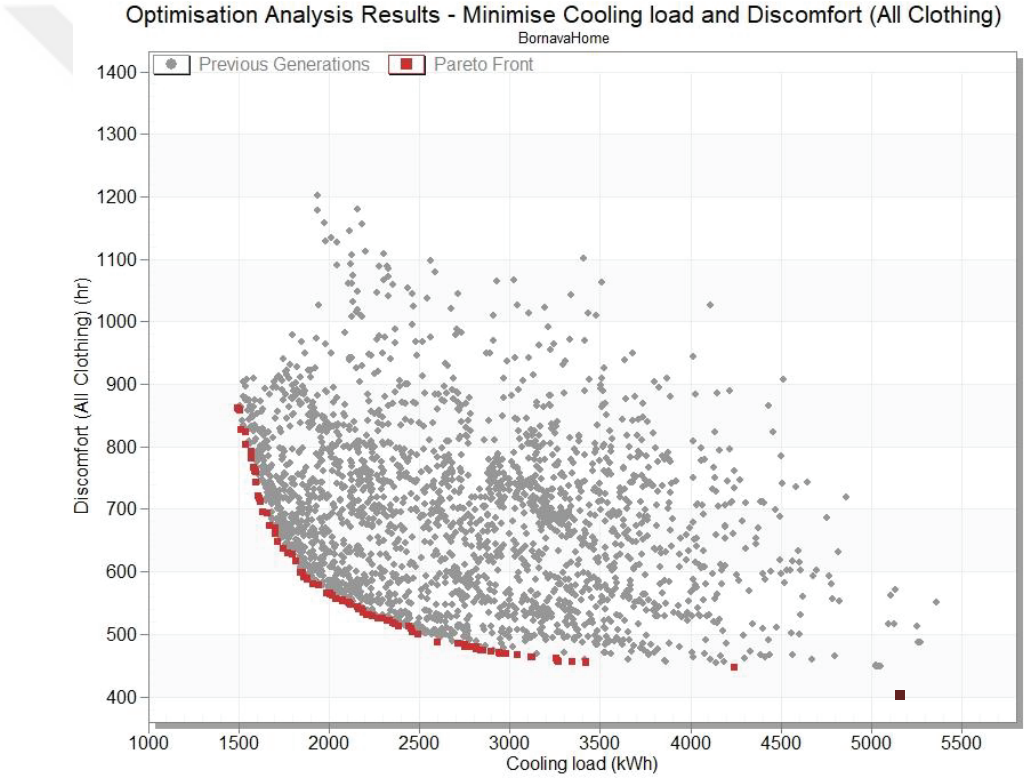

Figure 4.21. Multi-objective optimization result graph for scenario-4 (Purple dot: base case)

In the optimal result 4.1, where the cooling load is minimum, it is seen that the cooling load is 1498.35 kWh, the discomfort hours are 861.72 hours, and the energy consumption for cooling is 428.1 kWh (Table 4.18). In this case, the window-to-wall ratios were 30% for the living room, 20% for the study room and 28% for the bedroom. The glass type with a U value of 1.521 $W.m^{-2}.K$ and the external wall type with a U value of 0.253 $W.m^{-2}.K$ were selected. The angle of the shading element was determined to be

60 degrees, and the infiltration rate was determined to be 0.3 ac/h. Natural ventilation is activated at specified schedule when the outside temperature is lower than the indoor temperature.

The optimal result between the median optimal value and the optimal value at which the cooling load is minimum is evaluated in optimal results 4.2. In this sampling, the window-to-wall ratios were 33% for the living room, 20% for the study room and 26% for the bedroom. The infiltration rate is 0.3 ac/h, and natural ventilation is active when the outside temperature is lower than the indoor temperature. Shading type is the case where the angle is five degrees and the glass type is the 11th option where the U value is 1.364 $W.m^{-2}.K$. This is where 30-centimeter aerated concrete is used as the external wall type, and insulation is provided with 5-centimeter EPS. With these design variables, the cooling load was calculated as 1705.73 kWh, annual cooling consumption was calculated as 487.35 kWh, and thermal discomfort hours were calculated as 660.41h.

The result at the midpoint of the optimal results is optimal result 4.3. For this situation, the cooling load was calculated as 2119.79 kWh, thermal discomfort hours as 548.21 hours, and consumption for cooling as 605.65 kWh. In this case, the window-to-wall ratios were 41% for the living room, 21% for the study room, and 36% for the bedroom. It was calculated to select the 13th glass type with a U value of 1.172 $W.m^{-2}.K$ and a SHGC value of 0.534. For glass type-13, 4 mm low-emissivity glass and 12 mm argon gas are used. The shading type was chosen when the angle of the blades was 0 degrees. The external wall type was 30 centimeters of aerated concrete with 5 cm EPS insulation and a U value of 0.235 $W.m^{-2}.K$. Infiltration rate is considered as 0.3 ac/h. Natural ventilation will be activated when the outside temperature is lower than the indoor temperature.

The optimal result is the solution between 4.4, the median optimal value, and the optimum result with minimum thermal discomfort hours. In this sampling, the angle of the shading element is 0 degrees, the glass type is 6cm low-emission glass, and there is 12mm argon gas between it. Insulation on the external wall was provided with 5 centimeters of EPS, and 30 centimeters of aerated concrete was used as the material. Window-to-wall ratios were 45% for the living room, 24% for the study room, and 75% for the bedroom. Natural ventilation is active when the outside temperature is lower than the indoor temperature. With these values of the design variables, the cooling load of the case flat is 2602.69 kWh, the energy consumption for cooling is 743.62 kWh, and the discomfort hours are 487.06h.

Table 4.18. Objective functions and design variables for optimal results in scenario-4

	Optimal result 4.1 (min cooling load)	Optimal result 4.2	Optimal result 4.3	Optimal result 4.4	Optimal result 4.5(min discomfort)
Iteration	2449	2400	1482	1737	1695
Generation	97	95	59	69	68
Cooling load (kWh)	1498.35	1705.73	2119.79	2602.69	4245.45
Discomfort hours (h)	861.72	660.41	548.21	487.06	446.07
Cooling (kWh)	428.1	487.35	605.65	743.62	1212.98
WWR living room (%)	30	33	41	45	78
Glazing type	Glazing type-14	Glazing type-11	Glazing type-13	Glazing type-15	Glazing type-13
Shading type	Angle:60	Angle:5	Angle:0	Angle:0	Angle:0
WWR study room (%)	20	20	21	24	52
WWR bedroom (%)	28	26	36	75	79
External wall type	External wall-19	External wall-30	External wall-30	External wall-30	External wall-25
Infiltration (ac/h)	0.3	0.3	0.3	0.3	0.3
Nat. Vent.	Natural ventilation only operates when *OutdoorTemp* < *IndoorTemp*	Natural ventilation only operates when *OutdoorTemp* < *IndoorTemp*	Natural ventilation only operates when *OutdoorTemp* < *IndoorTemp*	Natural ventilation only operates when *OutdoorTemp* < *IndoorTemp*	Natural ventilation only operates when *OutdoorTemp* < *IndoorTemp*

In the optimal result 4.5, where the annual thermal discomfort hours are lowest, the thermal discomfort hours were reduced to 446.07 hours. While the cooling load is 4245.45 kWh, energy consumption for cooling is 1212.98 kWh. In this case, the shading type is the option with an angle of 0 degrees. Window-to-wall ratios were 78% for the living room, 52% for the study room, and 79% for the bedroom. The glass type is the type in which 4 cm low-emission glasses are used, and a 12 mm gap is left in between with argon gas. External wall type is the 25th option, using 3 cm EPS insulation and 25

centimeters of BIMS. The infiltration rate is 0.3 ac/h, and natural ventilation is active when the outside temperature is lower than the indoor temperature.

Multi-objective optimization results for scenario 5: There are 242 samples for scenario-5 design variables, so multi-objective optimization was completed before reaching the number of generations. There are 36 optimal results in the Pareto-front solution set in Figure 4.22. Compared to the base case, thermal discomfort hours increased in samples where the cooling load decreased, and cooling load increased in samples where thermal discomfort hours decreased. There is no sample where both objective functions decrease compared to the base case.

In the optimal result where the cooling load is minimum, the cooling load is reduced to 2733.6 kWh and energy consumption for cooling is reduced to 781.03 kWh (Table 4.19). Thermal discomfort hours increased to 5158.25 hours. For these outputs, the heating setpoint is set at 21.5 °C, and the cooling setpoint is set at 28 °C. The cooling system will be active during the summer months (June, July, August).

For the second optimal result, the heating set point was set at 21 °C, and the cooling set point was set at 26 °C. The cooling system is active between April and October. With these variables, cooling load was calculated as 4788.56 kWh, and energy consumption for cooling was calculated as 1368.16 kWh. Thermal discomfort hours are 3002.57 hours.

In the third optimal result, the cooling system is active from April to October, and the set point is 25 °C. The heating set point is 21 °C. In this case, the cooling load is 5168.66 kWh, energy consumption for cooling is 1476.76 kWh and discomfort hours are 1463.67 hours.

For the fourth optimal result, the heating set point was determined as 23 °C, and the cooling set point was determined as 25 °C. The cooling system is active during the year. The cooling load is 5819.76 kWh, energy consumption for cooling is 1662.79 kWh and discomfort hours are 850.27 hours.

In the fifth optimal result, where the discomfort hours were minimum, the discomfort hours are reduced to 422.88 hours. The cooling load is 6528.75 kWh, the energy consumption for cooling is 1865.35 kWh. The heating set point is 23 °C, and the cooling set point is 24 °C. The cooling system is active throughout the year.

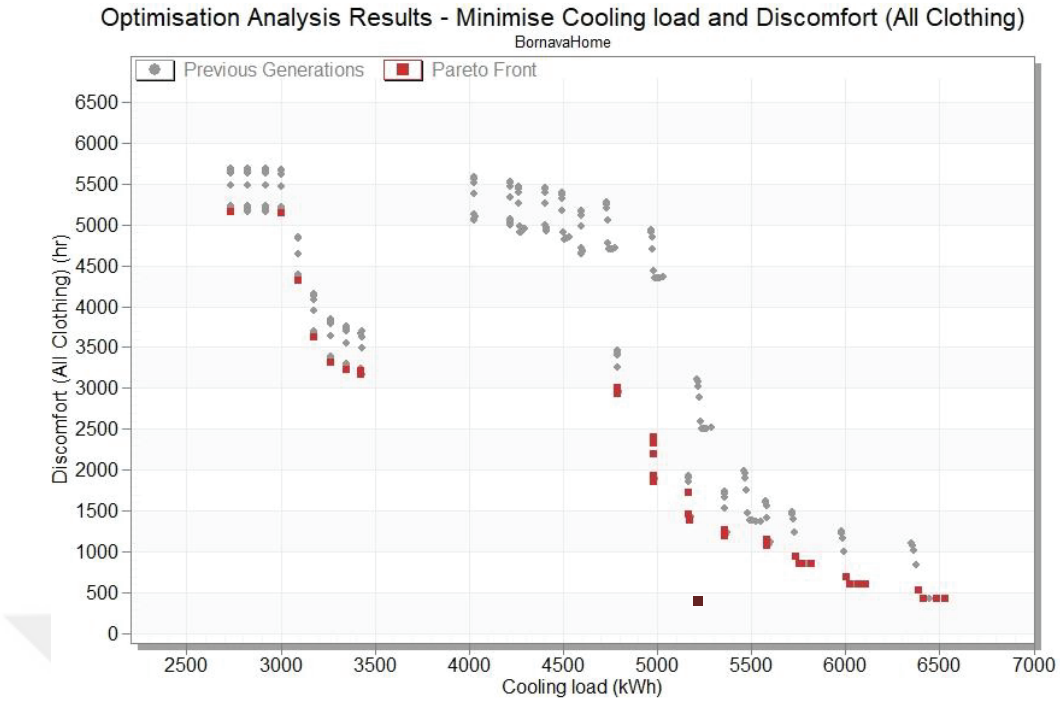

Figure 4.22. Multi-objective optimization result graph for scenario-5 (Purple dot: base case)

Table 4.19. Objective functions and design variables for optimal results in scenario-5

	Optimal result 5.1 (min cooling load)	Optimal result 5.2	Optimal result 5.3	Optimal result 5.4	Optimal result 5.5(min discomfort)
Iteration	134	201	102	139	98
Generation	7	18	5	7	4
Cooling load (kWh)	2733.61	4788.56	5168.66	5819.76	6528.75
Discomfort hours (h)	5158.25	3002.57	1463.67	850.27	422.88
Cooling (kWh)	781.03	1368.16	1476.76	1662.79	1865.35
Heating set-point temp. (°C)	21.5	21	21	23	23
Cooling set-point temp. (°C)	28	26	25	25	24
Cooling operation schedule	June- August	April-October	April-October	On 24/7	On 24/7

Multi-objective optimization results for scenario 6: In the multi-objective optimization, where the building envelope and its features and the heating-cooling system and its features were considered as design variables, the number of maximum generations is 100 and population size is 30. One hundred fifteen optimal results were found. Figure 4.23 shows the Pareto-front and other simulation results. In 45 of the 115 optimal results,

both thermal discomfort hours, energy consumption for cooling and cooling load decreased.

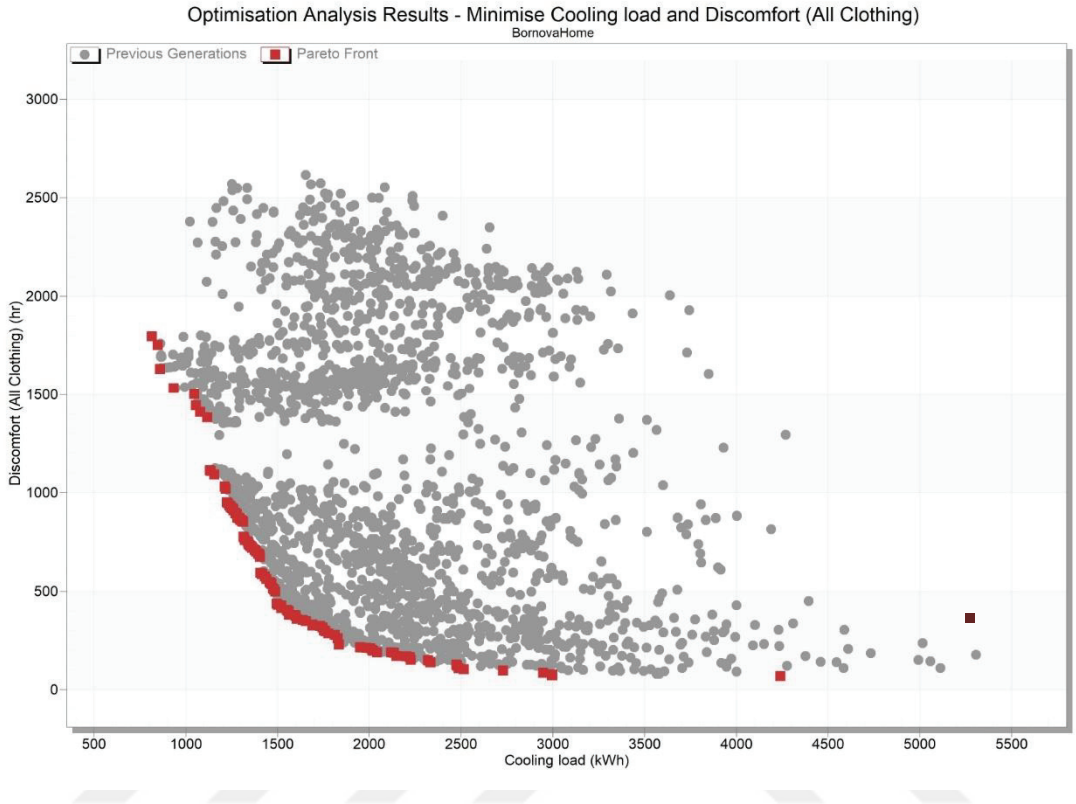

Figure 4.23. Multi-objective optimization results for scenario-6 (Purple dot: base case)

In the optimal result 6.1, where the cooling load is minimum, it is seen that the cooling load is 814.37 kWh, the discomfort hours are 1796.28 hours, and the energy consumption for cooling is 232.67 kWh (Table 4.20). In this case, the window-to-wall ratios were 27% for the living room, 29% for the study room, and 25% for the bedroom. The glass type with a U value of 1.521 $W.m^{-2}.K$ and the external wall type with a U value of 0.264 $W.m^{-2}.K$ were selected. The angle of the shading element was determined as 50 degrees, and the infiltration rate was determined as 0.3 ac/h. The heating set point is 21 °C, and the cooling set point is 28 °C. The cooling system is active throughout the year. Additionally, natural ventilation will be active when the outside temperature is lower than the indoor temperature.

The optimal result between the median optimal value and the optimal value at which energy consumption is minimum is evaluated in optimal results 6.2. In this sampling, the window-to-wall ratios were 31% for the living room, 29% for the study room, and 29% for the bedroom. The infiltration rate is 0.3 ac/h, and natural ventilation

is active when the outside temperature is lower than the indoor temperature. Shading type is the case where the angle is 50 degrees, and glass type is the 12th option where the U value is 1.534 $W.m^{-2}.K$. This is where 25-centimeter BIMS is used as the external wall type, and insulation is provided with 5-centimeter EPS. The heating setpoint temperature is 21.5 °C while the cooling setpoint is 25.5 °C, and the cooling system is active during the year. With these design variables, the cooling load was calculated as 1301.6 kWh, annual cooling consumption was calculated as 371.88 kWh, and thermal discomfort hours were calculated as 861.61h.

The result at the midpoint of the optimal results is optimal result 6.3. For this situation, the cooling load was calculated as 1430.37 kWh, thermal discomfort hours as 575.85 hours, and consumption for cooling as 408.67 kWh. In this case, the window-to-wall ratios were 31% for the living room, 27% for the study room, and 30% for the bedroom. It was calculated to select the 14th glass type with a U value of 1.521 $W.m^{-2}.K$ and a SHGC value of 0.477. For glass type-14, 6 mm low-emissivity glass and 12 mm argon gas are used. The shading type was chosen when the angle of the blades was 50 degrees. The external wall type was 25 centimeters of BIMS with 5 cm EPS insulation and a U value of 0.286 $W.m^{-2}.K$. Infiltration rate is considered as 0.3 ac/h. Natural ventilation will be activated when the outside temperature is lower than the indoor temperature. The heating set point is 22 °C, and the cooling set point is 24.5 °C. The cooling system is active between April and October.

The optimal result is between 6.4, the median optimal value, and the optimum result with minimum thermal discomfort hours. In this sampling, the angle of the shading element is 25 degrees, the glass type is 6-cm low-emission glass and there is 12mm air between it. Insulation on the external wall was provided with 3 centimeters of stone wool and 30 centimeters of BIMS was used as the material. Window-to-wall ratios were 49% for the living room, 33% for the study room, and 31% for the bedroom. Natural ventilation is active when the outside temperature is lower than the indoor temperature. With these values of the design variables, the cooling load of the case flat is 1828.64 kWh, the energy consumption for cooling is 522.46 kWh, and the discomfort hours are 261.65h.

In the optimal result 6.5, where the annual thermal discomfort hours are lowest, the thermal discomfort hours were reduced to 59.09 hours. While the cooling load is 4240.58 kWh, energy consumption for cooling is 1211.59 kWh. In this case, the shading type is the option with an angle of 0 degrees. Window-to-wall ratios were 65% for the living room, 69% for the study room, and 61% for the bedroom. The glass type is the type

in which 4 cm clear glasses are used, and a 12 mm gap is left in between with air. External wall type is the 17th option, using 5 cm stone wool insulation and 19 centimeters of BIMS. The infiltration rate is 0.3 ac/h and natural ventilation is active when the outside temperature is lower than the indoor temperature.

Table 4.20. Objective functions and design variables for optimal results in scenario-6

	Optimal result 6.1 (min cooling load)	Optimal result 6.2	Optimal result 6.3	Optimal result 6.4	Optimal result 6.5(min discomfort)
Iteration	2010	2108	1895	2125	2263
Generation	86	90	82	91	97
Cooling load (kWh)	814.37	1301.6	1430.37	1828.64	4240.58
Discomfort hours (h)	1796.28	861.61	575.85	261.65	69.09
Cooling (kWh)	232.67	371.88	408.67	522.46	1211.59
WWR living room (%)	27	31	31	49	65
Glazing type	Glazing type-14	Glazing type-12	Glazing type-14	Glazing type-11	Glazing type-2
Shading type	Angle:50	Angle:50	Angle:50	Angle:25	Angle:0
WWR study room (%)	29	29	27	33	69
WWR bedroom (%)	25	29	30	31	61
External wall type	External wall-9	External wall-32	External wall-32	External wall-12	External wall-17
Infiltration (ac/h)	0.3	0.3	0.3	0.3	0.3
Heating set-point temp. (°C)	21	21.5	22	21.5	22.5
Cooling set-point temp. (°C)	28	25.5	24.5	24	24

(cont. on the next page)

Table 4.20.(cont.)

Nat. Vent.	Natural ventilation only operates when *OutdoorTemp* < *IndoorTemp*	Natural ventilation only operates when *OutdoorTemp* < *IndoorTemp*	Natural ventilation only operates when *OutdoorTemp* < *IndoorTemp*	Natural ventilation only operates when *OutdoorTemp* < *IndoorTemp*	Natural ventilation only operates when *OutdoorTemp* < *IndoorTemp*
Cooling operation schedule	On 24/7	On 24/7	April-October	On 24/7	April-October

4.6. Discussion

Energy consumption and thermal comfort outputs were analyzed in the uncertainty and sensitivity analysis for a residential building located in the Mediterranean climate region, where dry and hot summer climates are observed. For thermal comfort, the set point of the heating-cooling systems, shading type, infiltration and window to wall ratios were determined as sensitive variables. Similarly, another study that considered the thermal discomfort hours seen in the summer months as output, shading type, and night ventilation were evaluated as sensitive variables in the thermal comfort output for a residential building in the Mediterranean climate (Encinas and Herde 2013). In this thesis study, the set point of heating-cooling systems, shading type, glass type, infiltration, and window-to-wall ratios were determined as sensitive variables for energy consumption. When the two outputs were evaluated together, the frame type, partition wall type, heating operating schedule and performance coefficients of heating-cooling systems were not sensitive variables for both. SRC values for the design variables and two outputs are given in Table 4.21. Variables with low sensitivity in the last part of the table are not included in multi-objective optimization.

Table 4.21. SRC values of design variables

High Sensitive Variables	SRC for energy consumption	SRC for discomfort hours
Cooling set-point temperature	-0.2571	0.8342
Heating set-point temperature	0.4799	-0.4113
Shading type	0.1957	0.5855
Infiltration (ac/h)	0.6201	0.3590
wwr bedroom	0.6049	-0.3014
wwr living room	0.5144	-0.4763
wwr study room	0.6125	-0.2767

(cont. on the next page)

Table 4.21.(cont.)

Medium Sensitive Variables	SRC for energy consumption	SRC for discomfort hours
Glazing type	-0.4241	0.1453
External wall construction	-0.114	-0.022
Natural Ventilation	-0.0351	-0.0815
Cooling operation schedule	-0.0106	0.1079
Low Sensitive Variables	SRC for energy consumption	SRC for discomfort hours
Heating operation schedule	-0.0009	0.0503
Cooling system seasonal CoP	-0.0373	0.0120
Heating system seasonal CoP	-0.0084	-0.0127
Partition construction	0.0042	0.0466
Window frame type	-0.0061	-0.0063

Table 4.22 shows the energy consumption, thermal discomfort hours, cooling load and energy consumption for cooling for some optimum situations and the base case obtained by multi-objective optimization. These data are graphed in Figure 4.24 and 4.25. While the first three scenarios aim to minimize energy consumption and thermal discomfort hours, the other three scenarios aim to minimize the cooling load and thermal discomfort hours. In each scenario, the energy consumption for cooling was taken as an additional output.

In scenario one, where the building envelope materials and properties are evaluated as design variables, it is seen that the energy consumption values always decrease, while the discomfort hours do not decrease compared to the base case. Calculating the increase in each sample for discomfort hours, the reason why the base case conditions cannot be achieved is that the base case is not entered as an option in the shading type variable. In the base case, no shading element is used, but an option without a shading element is not defined in the optimization settings. In addition, considering the decrease in energy consumption for cooling, which is an additional output, it can be interpreted that the discomfort hours increase for the heated period. The multi-objective optimization results could not reduce both thermal discomfort hours and energy consumption, therefore it was inadequate. Although addressing the building envelope and its features is inadequate to reduce both outputs together, it has the potential to reduce energy consumption by 68.1%.

Table 4.22. Comparison of thermal discomfort hours, annual energy consumption, and energy consumption for cooling for scenarios

		Energy Consumption (kWh)	Increase or decrease	Discomfort hours (h)	Increase or decrease	Energy consumption for cooling (kWh)	Increase or decrease
	Base Case	1945.4		402.83		1507.98	
Building envelope	Optimal result 1.1	619.25	-68.1%	703.47	+74.4%	493.77	-67.28%
	Optimal result 1.2	700.2	-64%	550.87	+36.4%	618.9	-59%
	Optimal result 1.3	819.12	-57.8%	508.91	+26.3%	756.31	-49.8%
	Optimal result 1.4	1006.1	-48.2%	469.38	+16.3%	949.86	-37%
	Optimal result 1.5	1295.65	-18%	448.08	+11.1%	1248.51	-17.1%
HVAC system	Optimal result 2.1	990.47	-49.1%	2174.62	+439.7	682.95	-54.7%
	Optimal result 2.2	1330.22	-31.6%	1322.22	+228%	837.95	-44.4%
	Optimal result 2.3	1619.53	-16.7%	829.46	+105.7%	1310.34	-13%
	Optimal result 2.4	1982.97	+1.9%	379.05	-5.7%	1313.69	-12.8%
	Optimal result 2.5	2837.91	+45.8%	186.63	-53.7%	1578.144	+4.7%
Building envelope + HVAC system	Optimal result 3.1	375.56	-80.8%	2381.54	+491%	321.12	-78.6%
	Optimal result 3.2	504.26	-74%	1144.67	+183.8%	466.82	-69%
	Optimal result 3.3	611.21	-68.5%	558.8	+38.46	572.66	-62%
	Optimal result 3.4	706.26	-63.7%	250.16	-38%	597.13	-60.3%
	Optimal result 3.5	1270.17	-34.7%	97.96	-75.8%	1216.6	-19.3%
		Cooling load (kWh)	Increase or decrease	Discomfort hours (h)	Increase or decrease	Energy consumption for cooling (kWh)	Increase or decrease
	Base Case	5278		402.83		1507.98	
Building envelope	Optimal result 4.1	1498.35	-71.6%	861.72	+114.1%	428.1	-71.6%
	Optimal result 4.2	1705.73	-67.6%	660.41	+64.1%	487.35	-67.6%
	Optimal result 4.3	2119.79	-59.8%	548.21	+36.3%	605.65	-59.8%
	Optimal result 4.4	2602.69	-50.6%	487.06	+21.1%	743.624	-50.6%
	Optimal result 4.5	4245.45	-19.5%	446.07	+10.9%	1212.98	-19.6%

(cont. on the next page)

Table 4.22.(cont.)

HVAC system	Optimal result 5.1	2733.61	-48.2%	5158.25	+1179%	781.03	-48.1%
	Optimal result 5.2	4788.56	-9.2%	3002.57	+644.4%	1368.16	-9.2%
	Optimal result 5.3	5168.66	-2%	1463.67	+263.9%	1476.76	-2.1%
	Optimal result 5.4	5819.76	+10.2%	850.27	+111.4%	1662.79	+10.2%
	Optimal result 5.5	6528.75	+23.68%	422.88	+5.1%	1865.35	+23.7
Building envelope + HVAC system	Optimal result 6.1	814.37	-84.5%	1796.28	+346.5%	232.676	-84.6%
	Optimal result 6.2	1301.6	-75.3%	861.61	+114.1%	371.88	-75.3%
	Optimal result 6.3	1430.37	-72.9%	575.85	+43.2%	408.67	-72.9%
	Optimal result 6.4	1828.64	-65.3%	261.65	-34.8%	522.468	-65.3%
	Optimal result 6.5	4240.58	-19.6%	69.09	-82.8%	1211.59	-19.6%

In the second scenario, where the heating-cooling system and its features are discussed, there is no optimal situation in which annual energy consumption and thermal discomfort hours decrease together. If energy consumption decreased, discomfort hours increased, or if discomfort hours decreased, energy consumption increased. There are a limited number of variables that can be addressed when multi-objective optimization is made with only the heating-cooling system and its features without considering the building envelope. Heating-cooling system set points and cooling system operating schedule variables failed to achieve the goal of reducing both objective functions. When set point temperatures that provide acceptable thermal comfort are selected, energy consumption increases, and when set point temperatures that reduce energy consumption are selected, discomfort hours increase. However, considering the cases where the two outputs are minimum, there is a 49.1% reduction potential for energy consumption and a 53.7% reduction potential for discomfort hours.

In the third scenario, where all the variables discussed in the first two scenarios were evaluated together, more effective results were achieved compared to the other two scenarios. In 34 of the optimum results found, it was determined that both discomfort hours, energy consumption, and energy consumption for cooling were reduced. Considering both the heating-cooling system and its features, as well as the building envelope and its features, the retrofit scenario for a studio-type residential building in a Mediterranean climate, enabled more efficient results to be achieved. It has been

determined that there is a potential for approximately an 80% reduction in energy consumption and a 75.8% reduction in discomfort hours. For example, in the optimal result 3.4, it is predicted that energy consumption will decrease by 34.7%, hours of thermal discomfort will decrease by 38%, and energy consumption for cooling will decrease by 60.3%. In the other example optimal result 3.5, it is stated that energy consumption will decrease by 34.7%, energy consumption for cooling will decrease by 19.3%, and discomfort hours will decrease by 75.8%. With these optimum results, high energy consumption and discomfort hours caused by overheating problems will decrease. In addition, it has been analyzed that there is a potential to reduce energy consumption by 80.8% and reduce discomfort hours by 75.8% in this scenario with multi-objective optimization.

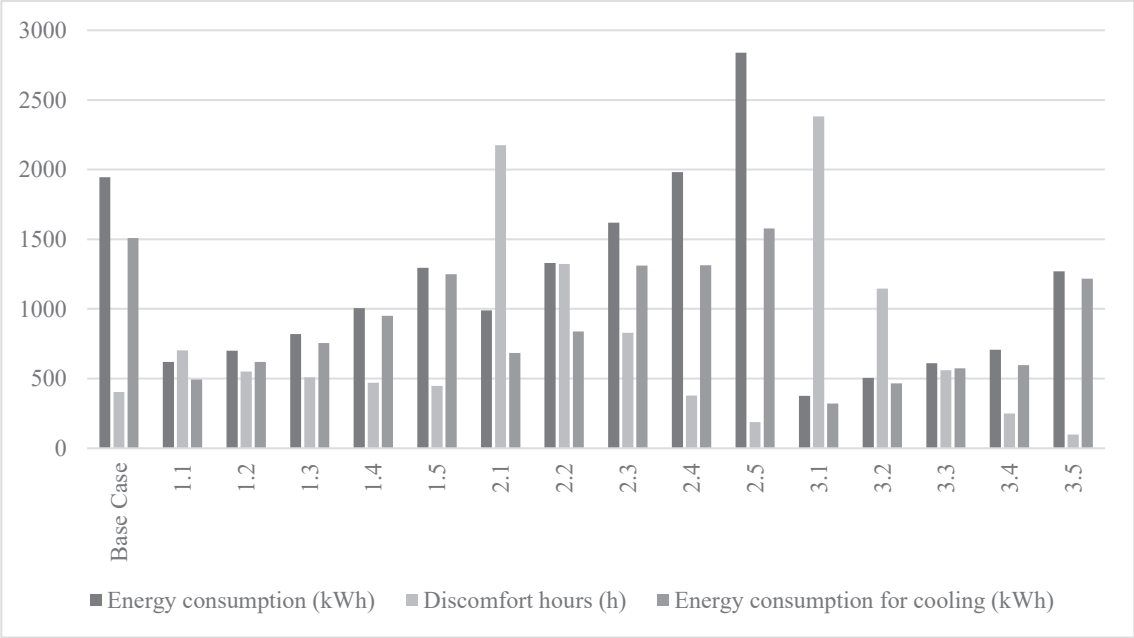

Figure 4.24. Comparison of thermal discomfort hours, annual energy consumption, and energy consumption for cooling for scenarios

In scenario four, where the building envelope materials and properties are evaluated as design variables, it is seen that the cooling load always decrease, while the discomfort hours do not decrease compared to the base case. Calculating the increase in each sample for discomfort hours, the reason why the base case conditions cannot be achieved is that the base case is not entered as an option in the shading type variable. In the base case, no shading element is used, but an option without a shading element is not defined in the optimization settings. In addition, considering the decrease in cooling load,

which is an additional output, it can be interpreted that the discomfort hours increase for the heated period. The multi-objective optimization results could not reduce both thermal discomfort hours and cooling load, therefore it was inadequate. Although it has the potential to reduce cooling load by 71.6%.

In the fifth scenario, where the heating-cooling system and its features are discussed, there is no optimal situation in which cooling load and thermal discomfort hours decrease together. There are a limited number of variables that can be addressed when multi-objective optimization is made with only the heating-cooling system and its features without considering the building envelope. Heating-cooling system set points and cooling system operating schedule variables failed to achieve the goal of reducing both objective functions. Although there are cases where the cooling load decreases, it is observed that discomfort hours increase. Considering the cases where the cooling load is reduced, a 48.2% reduction potential has been detected.

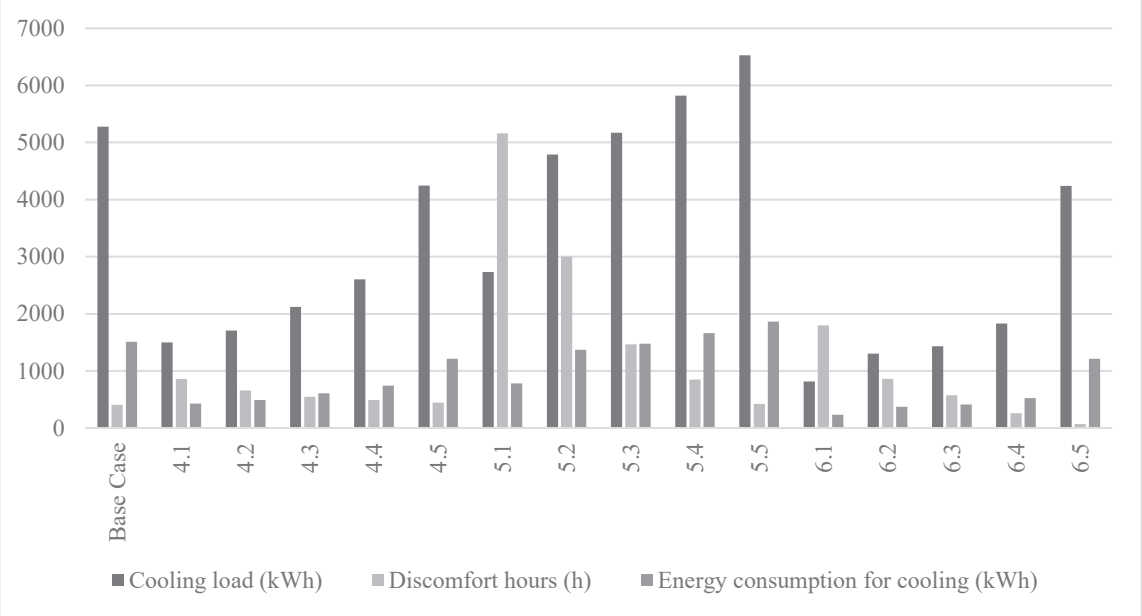

Figure 4.25. Comparison of thermal discomfort hours, cooling load, and energy consumption for cooling for scenarios

In the sixth scenario, where all the variables discussed in the first two scenarios were evaluated together, more effective results were achieved compared to the other two scenarios. In 45 of the optimum results found, it was determined that both discomfort hours, cooling load, and energy consumption for cooling were reduced. Considering both the heating-cooling system and its features, as well as the building envelope and its

features, the retrofit scenario for a studio-type residential building in a Mediterranean climate, enabled more efficient results to be achieved. It has been determined that there is a potential for approximately an 84.5% reduction in cooling load and an 82.8% reduction in discomfort hours. For example, in the optimal result 6.4, it is predicted that cooling load will decrease by 65.3%, hours of thermal discomfort will decrease by 34.8%, and energy consumption for cooling will decrease by 65.3%. In the other example optimal result 6.5, it is stated that cooling load will decrease by 19.6%, and discomfort hours will decrease by 82.8%. With these optimum results, high cooling load and discomfort hours caused by overheating problems will decrease.

As a result of all scenarios, optimum results that reduce both objective functions were achieved in scenarios 3 and 6. The optimal results that reduce both objective functions are examined in Tables 4.24 and 4.25.

As a result of the third scenario, the optimum results that both reduce discomfort hours and energy consumption are listed in Table 4.24. In these optimum solutions, the window-to-wall ratio of the living room varies between 29% and 78%. Currently, the window-to-wall ratio of the living room is 19.5%. By improving other variables, even if the window-to-wall ratio of the living room was increased, discomfort hours and energy consumption decreased.

Glass type appears as the 13th option in all optimum results. This option is the option with 12mm argon gas between 4mm low-emissivity glasses. The U value of this option is 1.172 $W/m^2.K$ and the SHGC value is 0.534. In the base case, 4 mm clear glass with 12 mm argon gas between it was used. In the base case, the U value of the glass type is 2.554 $W/m^2.K$ and the SHGC value is 0.742. From these results, as the U and SHGC values of the glass type decrease, the solar energy and heat coming from outdoor will enter the indoor less. In this way, overheating problems, energy consumption, and thermal discomfort hours will be reduced.

As for the shading type, the option where the angle is 0 and 5 degrees is most frequently seen in optimum results. In the base case, there is no shading element. The use of shading elements in this south-facing residential building with wide openings has reduced the problem of overheating.

In the base case, window-to-wall ratio of the bedroom and study room is 66.8%. For optimum results, window to wall ratios for the study room vary between 26% and 62%. The most common rate is seen to be between 26% and 32%. Optimum results for bedroom window-to-wall ratio are between 36% and 78%. It is noticed that the rates 36%

and 37% are most frequently used. While these rates are very high in the base case, it is seen that these window-to-wall ratios are reduced for optimum results.

The infiltration rate is 0.3 ac/h for all optimum solutions. For the base case, it was determined as 0.65 ac/h during the calibration process. In addition, in the sensitivity analysis, the fact that the infiltration rate design variable is one of the variables with high sensitivity for both thermal discomfort hours and energy consumption shows that the infiltration rate plays an important role in the retrofit scenario.

As for the external wall type, no insulation was applied in the base case, 19 cm pumice blocks were used. In the base case, the U value of the wall is 0.564 W/m^2.K. It is seen that wall types 9, 12, 15, 18, 23, 29, and 34 are used for optimum results. Table 4.23 lists these wall types and their properties. While no insulation is used in the base case, it is noticed that insulation is used in all selected wall types with optimum results. In addition, in all selected wall types, the U value decreased compared to the base case.

Table 4.23. List of external wall types for optimal results

External Wall Option List	Insulation Material	Material	U value (W/m^{2}K)
External wall-9	Stone wool (3cm)	Aerated concrete (30cm)	0.264
External wall-12	Stone wool (3cm)	BIMS (30cm)	0.292
External wall-15	Stone wool (5cm)	Aerated concrete (25cm)	0.259
External wall-18	Stone wool (5cm)	BIMS (25cm)	0.281
External wall-23	EPS (3cm)	Aerated concrete (30cm)	0.266
External wall-29	EPS (5cm)	Aerated concrete (25cm)	0.263
External wall-34	EPS (5cm)	Horizontal Perforated Brick(19cm)	0.378

The set point temperature for the cooling system was chosen to be 24 °C in all optimal results. The same value is specified for this set point temperature in ASHRAE Guideline 13 (2005). The heating set point temperature is 21 °C in many solutions. Additionally, solutions are using 22.5 °C and 20.5 °C. 21 °C are recommended in TS2164 for the heating set point temperature (TS 2164 1983).

Natural ventilation has been actively selected in line with the specified schedule in all optimum solutions. Since overheating is a problem in these types of houses, especially in spring, autumn, and summer, natural ventilation will be a helpful solution. Because generally, the indoor temperature will be higher than the outdoor temperature.

For the cooling system operating schedule, the option that is open throughout the year is generally chosen. The option that will only be active during the summer months is not an optimum solution. The reason for this is that high thermal discomfort hours and energy consumption are observed in these types of residential buildings due to

overheating, not only in summer but also in spring and autumn. For this reason, the optimum solutions include options that are active throughout the year or options that are active between April and October.

As a result of the sixth scenario, the optimum results that reduce both the cooling load and thermal discomfort hours are listed in Table 4.25. In these samples, window-to-wall ratios vary between 30% and 70% for the living room, between 25% and 69% for the study room, and between 26% and 61% for the bedroom. For the living room, values of 50% and 70% are most common. The most common values are 61% for the study room and 31% for the bedroom.

For the glass type design variable, type-15 is the most common. The most common degrees for the angle of the shading type are 5, 15, 25 and 50 degrees.

The most frequently used type in optimum solutions for the external wall type design variable is type-32. 25-centimeter BIMS was used in the external wall type-32, insulation was provided with 5-cm EPS. The infiltration rate was chosen as 0.3 ac/h for each optimum solution. The infiltration rate is chosen as 0.3 ac/h in all optimum solutions. It shows that the infiltration rate must be reduced according to the current situation to reduce the overheating problem.

The cooling set point is 24 °C in each optimal solution. For the heating set point, temperatures of 21, 21.5, 22, 22.5 °C are the most used solutions. The operating schedule of the cooling system has been chosen to be active throughout the year or between April and October. For the operating schedule of the cooling system, options were chosen to be active throughout the year or between April and October for both scenarios. Only the summer months are not seen in the optimum solutions. It shows that the cooling need is high in the spring months as well as the summer months.

Table 4.24. Optimum results in which both energy consumption and discomfort hours are reduced compared to the base case

Iteration	Generation	Total site energy (kWh)	Discomfort hours (h)	Energy cons. for cooling (kWh)	WWR living room (%)	Glazing type	Shading type	WWR study room (%)	WWR bedroom (%)	External wall type	Infiltration (ac/h)	Cooling set-point	Heating set-point	Nat. Vent	Cooling operation schedule
2454	90	1270.17	97.96	1216.6	78	Type-13	Angle:0	62	78	Type-34	0.3	24	21	Active	On 24/7
2343	86	1119.35	101.43	1073.45	77	Type-13	Angle:0	38	74	Type-18	0.3	24	21	Active	On 24/7
2259	83	1093.33	111.9	952.59	68	Type-13	Angle:0	55	53	Type-12	0.3	24	22.5	Active	On 24/7
2508	92	976.47	116.24	920.1	63	Type-13	Angle:0	41	60	Type-18	0.3	24	21	Active	On 24/7
2440	89	943.69	127.8	883.66	61	Type-13	Angle:0	38	58	Type-18	0.3	24	21	Active	On 24/7
2600	95	926.23	128.15	867.92	59	Type-13	Angle:0	35	57	Type-23	0.3	24	21	Active	On 24/7
1979	73	915.78	137.36	855.68	58	Type-13	Angle:0	45	47	Type-18	0.3	24	21	Active	On 24/7
2438	89	877.53	143.81	812.92	54	Type-13	Angle:0	32	55	Type-9	0.3	24	21	Active	On 24/7
2505	92	867.42	148.86	802.92	51	Type-13	Angle:0	37	50	Type-23	0.3	24	21	Active	On 24/7
1938	72	861.77	155.13	795.22	49	Type-13	Angle:0	42	45	Type-18	0.3	24	21	Active	On 24/7
1168	44	855.41	155.53	787.99	48	Type-13	Angle:0	41	45	Type-18	0.3	24	21	Active	On 24/7
2540	93	852.87	156.65	777.04	57	Type-13	Angle:5	32	54	Type-9	0.3	24	21	Active	On 24/7
2460	90	827.49	157.95	758.58	48	Type-13	Angle:0	32	47	Type-9	0.3	24	21	Active	On 24/7
2699	99	810.35	169.06	739.57	45	Type-13	Angle:0	36	41	Type-23	0.3	24	21	Active	On 24/7
1515	57	796.95	172.31	724	42	Type-13	Angle:0	35	41	Type-23	0.3	24	21	Active	On 24/7
2011	75	785.96	180.77	709.85	39	Type-13	Angle:0	32	43	Type-23	0.3	24	21	Active	On 24/7
1936	72	774.96	184.37	698.76	42	Type-13	Angle:0	31	39	Type-9	0.3	24	21	Active	On 24/7
1851	69	757.8	200.79	667.53	41	Type-13	Angle:5	32	40	Type-9	0.3	24	21	Active	On 24/7
1596	60	752.27	210.13	661.51	43	Type-13	Angle:5	32	37	Type-9	0.3	24	21	Active	April-October

(cont. on the next page)

Table 4.24 (cont.)

2132	79	730.12	217.03	643.84	35	Type-13	Angle:0	26	37	Type-15	0.3	24	21	Active	On 24/7
1350	51	729.99	229.59	631.19	37	Type-13	Angle:5	29	37	Type-9	0.3	24	21	Active	April-October
2589	95	719.41	237.31	614.61	34	Type-13	Angle:5	27	37	Type-29	0.3	24	21	Active	On 24/7
1750	66	710.46	240.91	603.98	32	Type-13	Angle:5	26	37	Type-15	0.3	24	21	Active	On 24/7
2547	93	706.26	250.16	597.13	30	Type-13	Angle:5	26	37	Type-15	0.3	24	21	Active	On 24/7
1982	74	705.09	270.91	580.79	29	Type-15	Angle:5	32	37	Type-9	0.3	24	21	Active	April-October
2551	93	703.52	277.55	576.09	31	Type-13	Angle:10	27	36	Type-15	0.3	24	21	Active	On 24/7
2335	86	693.31	280.2	561.57	29	Type-15	Angle:5	26	37	Type-15	0.3	24	21	Active	On 24/7
2612	95	686.09	328.77	605.67	33	Type-13	Angle:5	27	36	Type-9	0.3	24	20.5	Active	April-October
1927	72	681.54	335.25	598.85	32	Type-13	Angle:5	26	36	Type-29	0.3	24	20.5	Active	April-October
2512	92	677.11	376.38	619.99	35	Type-13	Angle:5	28	37	Type-9	0.3	24	20	Active	April-October
2606	95	671.79	378.51	613.23	34	Type-13	Angle:5	27	37	Type-29	0.3	24	20	Active	On 24/7
2320	85	671.15	382.96	612.63	34	Type-13	Angle:5	27	37	Type-29	0.3	24	20	Active	April-October
2172	80	670.93	384.26	612.59	33	Type-13	Angle:5	28	37	Type-29	0.3	24	20	Active	April-October
2424	89	660.66	391.1	601.41	32	Type-13	Angle:5	26	37	Type-15	0.3	24	20	Active	April-October

Table 4.25. Optimum results in which both cooling load and discomfort hours are reduced compared to the base case

Iteration	Generation	Cooling load (kWh)	Discomfort hours (h)	Energy cons. for cooling (kWh)	WWR living room (%)	Glazing type	Shading type	WWR study room (%)	WWR bedroom (%)	External wall type	Infiltration (ac/h)	Cooling set-point	Heating set-point	Nat. Vent	Cooling operation schedule
2206	94	1555.85	400.37	444.529	30	Type-12	Angle:55	25	31	Type-18	0.3	24	21.5	Active	On 24/7
942	42	1561.42	398.81	446.12	35	Type-14	Angle:55	30	30	Type-23	0.3	24	22.5	Active	April-October
2195	94	1562.9	379.62	446.56	30	Type-9	Angle:50	30	26	Type-9	0.3	24	21.5	Active	On 24/7
2088	90	1597.18	377.2	456.33	31	Type-12	Angle:50	30	29	Type-32	0.3	24	22	Active	April-October
1245	55	1598.98	374.93	456.85	32	Type-12	Angle:50	27	30	Type-32	0.3	24	22.5	Active	April-October
2288	98	1606.48	359.58	458.99	40	Type-11	Angle:45	30	30	Type-23	0.3	24	21.5	Active	April-October
1196	86	1637.75	353.28	467.92	36	Type-12	Angle:45	27	31	Type-32	0.3	24	22	Active	April-October
1940	83	1654.47	347.71	472.7	37	Type-12	Angle:45	29	31	Type-18	0.3	24	22	Active	April-October
2268	97	1690.51	329.62	483	43	Type-9	Angle:50	30	32	Type-18	0.3	24	22	Active	April-October
2291	98	1691.18	326.04	483.19	37	Type-12	Angle:45	29	31	Type-18	0.3	24	23	Active	April-October
2273	97	1732.8	323.55	495	33	Type-14	Angle:30	37	31	Type-26	0.3	24	22.5	Active	April-October
1820	79	1745.29	315.53	498.65	40	Type-12	Angle:40	34	32	Type-12	0.3	24	22	Active	April-October
1855	80	1753.78	300.67	501.08	70	Type-15	Angle:50	28	32	Type-32	0.3	24	21.5	Active	April-October
1893	82	1760.7	297.36	503.05	70	Type-15	Angle:50	28	32	Type-32	0.3	24	22	Active	April-October
1916	83	1776.84	285.51	507.66	51	Type-13	Angle:50	31	35	Type-32	0.3	24	22	Active	April-October
1517	66	1812.7	277.47	517.95	37	Type-10	Angle:20	34	32	Type-12	0.3	24	22.5	Active	April-October
2125	91	1828.64	261.65	522.46	49	Type-11	Angle:25	33	31	Type-12	0.3	24	21.5	Active	On 24/7
2260	97	1834.36	227.8	524.1	50	Type-15	Angle:25	30	30	Type-23	0.3	24	22.5	Active	April-October
1954	84	1949.46	215.49	556.9	50	Type-15	Angle:25	44	31	Type-32	0.3	24	22	Active	On 24/7

(cont. on the next page)

Table 4.25 (cont.)

Iteration	Generation	Cooling load (kWh)	Discomfort hours (h)	Energy cons. for cooling (kWh)	WWR living room (%)	Glazing type	Shading type	WWR study room (%)	WWR bedroom (%)	External wall type	Infiltration (ac/h)	Cooling set-point	Heating set-point	Nat. Vent	Cooling operation schedule
1825	79	1951.07	215.22	557.48	36	Type-8	Angle:15	34	32	Type-12	0.3	24	22.5	Active	April-October
1947	84	1952.93	213.53	557.98	36	Type-8	Angle:15	34	32	Type-12	0.3	24	22.5	Active	On 24/7
2253	96	1986.35	211.39	567.52	50	Type-15	Angle:25	44	37	Type-32	0.3	24	21.5	Active	April-October
2176	93	2005.79	210.52	573.08	50	Type-11	Angle:20	42	34	Type-14	0.3	24	22	Active	On 24/7
2193	94	2017.39	199.88	576.39	70	Type-15	Angle:25	33	34	Type-14	0.3	24	22	Active	On 24/7
2063	89	2022.01	196.97	577.71	50	Type-15	Angle:25	44	37	Type-28	0.3	24	22.5	Active	April-October
2061	88	2042.74	189.46	583.64	35	Type-14	Angle:10	43	34	Type-9	0.3	24	22.5	Active	On 24/7
2163	93	2119.17	188.22	605.47	50	Type-15	Angle:25	61	32	Type-32	0.3	24	22.5	Active	April-October
2098	90	2135.32	186.5	610.09	52	Type-9	Angle:25	42	42	Type-22	0.3	24	22	Active	On 24/7
2084	89	2148.78	170.47	613.93	50	Type-9	Angle:15	40	31	Type-32	0.3	24	22	Active	On 24/7
2142	92	2203.7	169.76	629.63	34	Type-9	Angle:10	47	31	Type-12	0.3	24	22.5	Active	April-October
1170	52	2222	165.01	634.86	39	Type-12	Angle:20	51	41	Type-26	0.3	24	23	Active	On 24/7
2071	89	2227.48	150.9	636.42	60	Type-15	Angle:15	41	34	Type-14	0.3	24	22	Active	On 24/7
1961	94	2320.1	149.14	662.88	31	Type-15	Angle:5	61	30	Type-32	0.3	24	22.5	Active	April-October
1790	77	2323	147.18	663.71	31	Type-15	Angle:5	61	30	Type-32	0.3	24	22.5	Active	On 24/7
2272	97	2332.24	138.52	666.35	60	Type-15	Angle:15	52	34	Type-32	0.3	24	22	Active	April-October
2298	98	2335.31	138.07	667.23	60	Type-15	Angle:15	52	34	Type-32	0.3	24	22	Active	On 24/7
2293	98	2474.9	125.89	707.14	60	Type-15	Angle:15	52	45	Type-11	0.3	24	22.5	Active	April-October
2198	94	2478.92	120.98	708.26	60	Type-15	Angle:15	52	45	Type-11	0.3	24	22.5	Active	On 24/7
2179	93	2488.12	108.24	710.89	70	Type-15	Angle:5	44	31	Type-32	0.3	24	22	Active	On 24/7

(cont. on the next page)

Table 4.25 (cont.)

Iteration	Generation	Cooling load (kWh)	Discomfort hours (h)	Energy cons. for cooling (kWh)	WWR living room (%)	Glazing type	Shading type	WWR study room (%)	WWR bedroom (%)	External wall type	Infiltration (ac/h)	Cooling set-point	Heating set-point	Nat. Vent	Cooling operation schedule
1869	81	2516.07	102.64	718.87	70	Type-15	Angle:5	38	37	Type-28	0.3	24	22.5	Active	On 24/7
2137	92	2729.91	96.99	779.97	70	Type-15	Angle:5	61	32	Type-32	0.3	24	22.5	Active	April-October
2269	97	2949.27	84.63	842.64	70	Type-15	Angle:5	61	53	Type-12	0.3	24	21.5	Active	April-October
2324	99	2995.7	76.88	855.91	70	Type-15	Angle:5	61	53	Type-23	0.3	24	22.5	Active	April-October
1364	60	2995.9	72.2	855.97	70	Type-15	Angle:5	61	53	Type-25	0.3	24	22.5	Active	On 24/7
2263	97	4240.58	69.09	1211.59	65	Type-2	Angle:0	69	61	Type-17	0.3	24	22.5	Active	April-October

CHAPTER 5

CONCLUSION

In this thesis study, retrofit scenarios are investigated for south-facing residential flats designed without paying attention to the orientation located in the Mediterranean climate zone. First, a comprehensive literature review was conducted with the keywords 'multi-objective optimization, uncertainty and sensitivity analysis, thermal comfort, energy consumption, Mediterranean climate, overheating'. In the literature review, the design variables and objective functions used in the research were analyzed, and the flow chart for retrofit scenarios was examined. In the light of this research, the thesis methodology, uncertainty sensitivity analysis, and multi-objective optimization method were determined. A south-facing case residential flat located in the Mediterranean climate zone was selected. Indoor and outdoor temperature and relative humidity values were monitored for eight months. A psychrometric chart was created with indoor monitoring data in line with ASHRAE-55 standards, and thermal discomfort hours were calculated. Climate data was created with hourly outdoor monitoring data. With this monitoring data, the model was calibrated.

The results obtained from the model and the number of discomfort hours calculated with monitoring data for the months of May and December were compared. It was calculated that all hours are thermally discomfort, especially in the summer months. In May, September, and October, high hours of thermal discomfort due to overheating are also observed. Objective functions and design variables were determined in light of the results obtained from the model and the literature review. Since the overheating problem was observed, the objective functions were determined as thermal comfort, energy consumption and cooling load. Design variables are window-to-wall ratios, glass type, external wall type, partition wall type, infiltration, window frame type, set points of heating and cooling systems, shading type, operating schedule of heating and cooling systems, efficiency of heating system, coefficient of performance of the cooling system and natural ventilation.

In the next step, uncertainty analysis was performed to determine possible deviations in the objective function and sensitivity analysis was performed to examine the sensitivities of the design variables on the objective functions. According to the

determined upper and lower values of the design variables or options, it is calculated that the thermal discomfort hours will be a minimum of 184.2 h, a maximum of 2605.6 h, and an average of 1301.3 h. For energy consumption, it is calculated that the minimum will be 588.3 kWh, the maximum will be 3298.7 kWh, and the average will be 1603.9 kWh.

In the sensitivity analysis, design variables were examined separately for each objective function. Since some variables were dominant in the first sensitivity analysis, the p-values of some of the other variables were high, which reduced the reliability of the result. For this reason, the dominant variables for both objective functions were removed, and the second sensitivity analysis was performed. In line with these analyses, the variables with high sensitivity for thermal comfort are heating set point (SRC: -0.4113), cooling set point (SRC: 0.8342), shading type (SRC: 0.5855), infiltration (SRC: 0.359), bedroom window-to-wall ratio (SRC: -0.3014), study room window-to-wall ratio (SRC: -0.2767) and living room window-to-wall ratio (SRC: -0.4763). The variables with medium sensitivity for thermal comfort were glass type (SRC: 0.1453), natural ventilation (SRC: -0.0815), and cooling system operating schedule (SRC: 0.1079). The variables with low sensitivity for thermal comfort are external wall type (SRC: -0.022), heating system operating schedule (SRC: 0.0503), cooling system performance coefficient (SRC: 0.012), heating system efficiency (SRC: -0.0127), partition wall type (SRC: 0.0466), window frame type (SRC: -0.0063).

Design variables with high sensitivity for energy consumption are cooling set point (SRC: -0.2571), heating set point (SRC: 0.4799), shading type (SRC: 0.1957), glazing type (SRC: -0.4241), infiltration (SRC: 0.6201). , bedroom window-to-wall ratio (SRC: 0.6049), study room window-to-wall ratio (SRC: 0.6125), and living room window-to-wall ratio (SRC: 0.5144). Design variables with medium sensitivity to energy consumption are external wall type (SRC: -0.114), while design variables with low sensitivity are heating system operating schedule (SRC: -0.0009), cooling system performance coefficient (SRC: -0.0373), natural ventilation (SRC). : -0.0351), heating system efficiency (SRC: -0.0084), partition wall type (SRC: 0.0042), window frame type (SRC: -0.0061), and cooling system operating schedule (SRC: -0.0106).

It is aimed to identify low-sensitivity design variables and eliminate these variables in multi-objective optimization. In this regard, it was determined that the design variables with low sensitivity for both objective functions were window frame type, heating system efficiency, cooling system performance coefficient, heating system

operating schedule, and partition wall type. These variables are not considered in multi-objective optimization.

Multi-objective optimization was performed with six scenarios. In the first and fourth scenarios, building envelope features, in the second and fifth scenarios, HVAC features, and in the third and sixth scenarios, all the design variables are considered. In the first three scenarios, it is aimed to minimize energy consumption and thermal discomfort hours, and in the other scenarios, it is aimed to minimize the cooling load and thermal discomfort hours. The convenience of these scenarios has been tested to solve the overheating problem. Only in the third and sixth scenarios were optimal solutions found that reduced both objective functions. In these two scenarios, both active and passive design variables are considered.

When these optimal solutions were evaluated, it was determined that the infiltration rate must be reduced. When the external wall types selected in optimal solutions are evaluated, it is seen that wall types with lower U values are preferred compared to the bas case. Similarly, it was determined that the selected glass types had lower U values compared to the base case.

Window-to-wall ratios and degree of shading element are selected differently in optimal solutions.

The cooling set point was chosen as 24 °C in all optimal solutions as specified in ASHRAE standards. Values between 21 and 22.5 °C are generally chosen for the heating set point. The need for cooling is seen not only in summer but also in spring and autumn. For this reason, the operating schedule of the cooling system was chosen to be active throughout the year or between April and October.

- What are the design variables and objective functions evaluated in optimization studies in the field of architecture?

In the field of architecture, various objective functions and design variables have been examined to develop retrofit scenarios for buildings or to make decisions at the design stage. It has been determined that the most frequently researched design variables are glass type, wall type, roof type, window-to-wall ratio, floor type, building orientation, infiltration rate, and shading type. The most frequently researched objective functions are energy consumption, carbon emissions, thermal comfort, and cost. Objective functions are determined according to the problems seen in the building or building types examined. For example, for a building with overheating problems, it would be a good choice to

address thermal comfort, energy consumption or cooling load. Because the overheating problem causes high thermal discomfort hours, energy consumption and cooling load.

- What are the sensitive design variables for thermal comfort and energy consumption in residential buildings located in the Mediterranean climatic region?

It is aimed to determine sensitive variables for residential buildings located in regions with a Mediterranean climate by using the sensitivity analysis method for thermal comfort and energy consumption objective functions. It has been determined that heating-cooling set points, shading type, infiltration rate, and window-to-wall ratios are highly sensitive variables for thermal comfort output. For energy consumption output, it has been analyzed that heating-cooling set points, shading type, glass type, infiltration rate, and window-to-wall ratios are sensitive variables. It was determined that the heating system operating schedule, the performance coefficient of the cooling systems, the efficiency of the heating system, the partition wall type, and the window frame type were low-sensitive variables compared to other variables. The sensitivities of the design variables for the two objective functions were evaluated together, and design variables with low sensitivity were not evaluated in the multi-objective optimization. These variables were window frame type, heating system efficiency, cooling system performance coefficient, heating system operating schedule, and partition wall type.

- What are the current thermal comfort level and annual energy consumption in a studio-type flat in an existing residential building in Izmir?

It has been determined that the thermal comfort condition of the existing building cannot provide thermal comfort conditions at all hours during the summer months. During the summer months and September and October, dissatisfaction rates are 100%. In the south-facing residential building designed without paying attention to orientation, there is an overheating problem due to the high window-to-wall ratios. Due to the overheating problem, energy consumption and thermal discomfort hours are also high.

- Is it possible to solve the overheating problem seen in residential buildings in the Mediterranean climatic region only with precautions on the building envelope?

In the first and fourth scenario of multi-objective optimization, the suitability of the precautions to be taken in the building envelope to reduce energy consumption, cooling load and thermal discomfort hours for residential flats located in the Mediterranean climate region. As a result of these scenarios, it has been determined that it may not be possible to reduce both objective functions with measures to be taken only on the building

envelope. However, it has been calculated that there is still a potential to reduce energy consumption by 68.1% by improving the building envelope properties.

- Can high thermal discomfort hours and energy consumption be reduced with improvement solutions considering the properties of heating and cooling systems?

The number of variables that can be considered regarding the properties of heating and cooling systems is limited. In this study, the operating schedule of the heating system, heating system efficiency, heating system set point, cooling system operating schedule, cooling system performance coefficient, and cooling system set point are discussed. Heating system operating schedule, heating system efficiency, and cooling system performance coefficient variables were determined to be low-sensitivity variables for thermal comfort and energy consumption and were not evaluated in multi-objective optimization. An optimum result that could reduce both objective functions could not be found with the cooling set point, heating set point, and cooling operating schedule design variables. However, the potential of this scenario to reduce energy consumption by 49.1% and thermal discomfort hours by 53.7% has been determined.

- How much can energy consumption and thermal discomfort hours be reduced by implementing solutions both on the building envelope and heating and cooling system requirements? Can the overheating problem be overcome with these related design variables?

In the third and sixth scenario, both the heating and cooling system and its features and the building envelope and its features are considered as design variables. In these scenario, 99 and 115 optimum results were found. In 34 of 99 and 45 of 115, both thermal discomfort hours and energy consumption are reduced. By considering these design variables, the goal of reducing thermal discomfort hours and energy consumption together has been achieved, and the overheating problem has been overcome with these design variables.

5.1. Future Studies

Studies that can be considered for future research: In this thesis study, optimum results were determined with multi-objective optimization, and retrofit potentials for energy consumption and thermal discomfort hours were analyzed. In further studies, costs and payback periods can be calculated to choose among optimum results. A feasibility

report can be prepared for each of the optimal results. These reports will make it easier for the customer to make a choice.

This study focused on a south-facing residential flat. It has become a guide for retrofit scenarios for south-facing flats. In future studies, optimum solutions can be found for different directions to serve as examples of improvement scenarios for flats facing other directions.

Other south-facing studio-type residential buildings that do not consider orientation into account can be examined. The results obtained for each building or flat can be compared and analyzed.

REFERENCES

Abdou, Nawal, El Mghouchi, Said Hamdaoui, Najat El Asri, and Mhamed Mouqallid. 2021. "Multi-Objective Optimization of Passive Energy Efficiency Measures for Net-Zero Energy Building in Morocco." *Building and Environment* 204 (October): 108141. https://doi.org/10.1016/j.buildenv.2021.108141.

Acar, Ugur, Onder Kaska, and Nehir Tokgoz. 2021. "Multi-Objective Optimization of Building Envelope Components at the Preliminary Design Stage for Residential Buildings in Turkey." *Journal of Building Engineering* 42, (October): 102499. https://doi.org/10.1016/j.jobe.2021.102499.

Adams, Matthew, Victoria Burrows, Stephen Richardson. 2024. "Bringing Embodied Carbon Upfront." Accessed April 29, 2024. https://worldgbc.org/article/bringing-embodied-carbon-upfront/.

Akgül, Sevim. 2013. "Turkey Electric Energy Demand Forecasting With Artificial Neural Networks and Comparative Analysis With Other Methods." PhD diss., University of Atatürk.

Aksoy, Yazgı. 2016. "Sürdürülebilir Toplu Konut Yerleşmesi Tasarımı İçin Pareto Genetik Algoritmaya Dayalı Bir Model Önerisi: SSPM." Thesis, Istanbul Technical University.

Alam, Fasihul Mohammed, Ken McNaught, and Trevor Ringrose. 2004. "A Comparison of Experimental Designs in the Development of a Neural Network Simulation Metamodel." *Simulation Modelling Practice and Theory* 12, no. 7–8 (November): 559–78. https://doi.org/10.1016/j.simpat.2003.10.006.

Albatayneh, Aiman. 2021. "Optimisation of Building Envelope Parameters in a Semi-Arid and Warm Mediterranean Climate Zone." *Energy Reports* 7, (November): 2081–93. https://doi.org/10.1016/j.egyr.2021.04.011.

Anderson, Dave, and George McNeill. 1992. *Artificial neural networks technology.* New York: Kaman Sciences Corporation.

Arıkan Kargı, Vesile Sinem. 2013. “Artificial Neural Network Models and An Application at a Textile Firm.” PhD diss., University of Uludağ.

Asadi, Ehsan, Manuel Gameiro Silva, Carlos Henggeler Antunes, Luís Dias, and Leon Glicksman. 2014. “Multi-Objective Optimization for Building Retrofit: A Model Using Genetic Algorithm and Artificial Neural Network and an Application.” *Energy and Buildings* 81 (October): 444–56. https://doi.org/10.1016/j.enbuild.2014.06.009.

Ascione, Fabrizio, Nicalo Bianco, Claudio De Stasio, Gerardo Maria Mauro, Giuseppe Peter Vanoli. 2017. “A new compherensive approach for cost-optimal building design integrated with the multi-objective model predictive control of HVAC systems.” *Sustainable Cities and Society* 31 (May): 136-150. https://doi.org/10.1016/j.scs.2017.02.010.

Ascione, Fabrizio, Nicalo Bianco, Gerardo Maria Mauro, and Giuseppe Peter Vanoli. 2019. “A new compherensive framework fort he multi-objective optimization of building energy design: Harlequin.” *Applied Energy* 241, (May): 331-361. https://doi.org/10.1016/j.apenergy.2019.03.028.

Ascione, Fabrizio, Nicola Bianco, Claudio De Stasio, Gerardo Maria Mauro, and Giuseppe Peter Vanoli. 2016. “Multi-stage and multi-objective optimization for energy retrofitting a developed hospital reference building: A new approach to assess cost-optimality.” *Applied Energy* 174, (July): 37-68. https:// doi:10.1016/j.apenergy.2016.04.078.

Ascione, Fabrizio, Nicola Bianco, Rosa De Masi, Gerardo Maria Mauro, and Giuseppe Peter Vanoli. 2015. “Design of the Building Envelope: A Novel Multi-Objective Approach for the Optimization of Energy Performance and Thermal Comfort.” *Sustainability* 7, no. 8 (August): 10809–36. https://doi.org/10.3390/su70810809.

Ascione, Fabrizio, Nicola Bianco, Teresa Iovane, Gerardo Maria Mauro, Davide Ferdinando Napolitano, Antonio Ruggiano, and Lucio Viscido. 2020. “A Real Industrial Building: Modeling, Calibration and Pareto Optimization of Energy Retrofit.” *Journal of Building Engineering* 29 (May): 101186. https://doi.org/10.1016/j.jobe.2020.101186.

Ascione, Fabrizio, Rosa Francesca De Masi, Valentino Festa, Gerardo Maria Mauro, and Giuseppe Peter Vanoli. 2023. “Optimizing Space Cooling of a Nearly Zero Energy Building via Model Predictive Control: Energy Cost vs Comfort.” *Energy and Buildings* 278 (January): 112664. https://doi.org/10.1016/j.enbuild.2022.112664.

ASHRAE Guideline 13. 2015. “Specifying Building Automation Systems.” Accessed March 9, 2024. https://www.ashrae.org/technical-resources/bookstore/ashrae-guideline-13-2015-specifying-building-automation-systems.

ASHRAE Guideline 14. 2002. “Measurement of Energy And Demand Savings.” Accessed March 9, 2024. https://webstore.ansi.org/standards/ashrae/ashraeguideline142002#:~:text=ASHRAE%20Guideline%2014%20includes%20the,%2C%20commercial%2C%20and%20industrial%20buildings.

ASHRAE Standard 55. 2004. “Thermal EnvironmentalConditions for Human Occupancy.” Accessed March 18, 2024. https://www.ashrae.org/file%20library/technical%20resources/standards%20and%20guidelines/standards%20addenda/55-2004_ad55d_e_f_g.pdf.

Badeche, Mounira, and Yasmina Bouchahm. 2020. “Design Optimization Criteria for Windows Providing Low Energy Demand in Office Buildings in Algeria.” *Environmental and Sustainability Indicators* 6 (June): 100024. https://doi.org/10.1016/j.indic.2020.100024.

Bagheri-Esfeh, Hamed, and Mohammad Reza Dehghan. 2022. “Multi-Objective Optimization of Setpoint Temperature of Thermostats in Residential Buildings.” *Energy and Buildings* 261 (April): 111955. https://doi.org/10.1016/j.enbuild.2022.111955.

Baghoolizadeh, Mohammadreza, Mohammad Rostamzadeh-Renani, Reza Rostamzadeh-Renani, and Davood Toghraie. 2023. “Multi-Objective Optimization of Venetian Blinds in Office Buildings to Reduce Electricity Consumption and Improve Visual and Thermal Comfort by NSGA-II.” *Energy and Buildings* 278 (January): 112639. https://doi.org/10.1016/j.enbuild.2022.112639.

Bayır, Fırat. 2006. “An Application on Artificial Neural Networks and Predictive Modeling.” Thesis, University of İstanbul.

Bayraktar, Meltem, Baret Binatlı, and Tuğçe Üzümoğlu. 2023. “Türkiye Bina Sektörü Karbonsuzlaşma Yol Haritası.” Aralık. https://webdosya.csb.gov.tr/db/meslekihizmetler/menu/turkiye_bina_sektoru_karbonsuzlasma_yol_haritasi_-v1_20231218095757.pdf

Besbas, Soumaya, Francesco Nocera, Noureddine Zemmouri, Mohamed Amine Khadraoui, and Asma Besbas. 2022. “Parametric-Based Multi-Objective Optimization Workflow: Daylight and Energy Performance Study of Hospital Building in Algeria.” *Sustainability* 14, no. 19 (October): 12652. https://doi.org/10.3390/su141912652.

Boyd, Stephen, and Lieven Vandenberghe. 2004. *Convex Optimization.* Cambridge, United Kingdom: Cambridge University Press,

Bre, Facundo, and Víctor Fachinotti. 2017. “A Computational Multi-Objective Optimization Method to Improve Energy Efficiency and Thermal Comfort in Dwellings.” *Energy and Buildings* 154 (November): 283–94. https://doi.org/10.1016/j.enbuild.2017.08.002.

Bre, Facundo, Arthur Santos Silva, Enedir Ghisi, and Víctor Fachinotti. 2016. “Residential Building Design Optimisation Using Sensitivity Analysis and Genetic Algorithm.” *Energy and Buildings* 133 (December): 853–66. https://doi.org/10.1016/j.enbuild.2016.10.025.

Carpino, Cristina, Roberto Bruno, V. Carpino, and Natale Arcuri. 2022. “Improve Decision-Making Process and Reduce Risks in the Energy Retrofit of Existing Buildings through Uncertainty and Sensitivity Analysis.” *Energy for Sustainable Development* 68 (June): 289–307. https://doi.org/10.1016/j.esd.2022.04.007.

Carpino, Cristina, Roberto Bruno, V. Carpino, and Natale Arcuri. 2022. “Uncertainty and Sensitivity Analysis to Moderate the Risks of Energy Performance Contracts in Building Renovation: A Case Study on an Italian Social Housing District.” *Journal*

of Cleaner Production 379 (December): 134637. https://doi.org/10.1016/j.jclepro.2022.134637.

Chaudhuri, Tanaya, Yeng Chai Soh, Hua Li, and Lihua Xie. 2019. "A Feedforward Neural Network Based Indoor-Climate Control Framework for Thermal Comfort and Energy Saving in Buildings." *Applied Energy* 248 (August): 44–53. https://doi.org/10.1016/j.apenergy.2019.04.065.

Chen, Jiandong, Shulei Cheng, and Malin Song. 2017. "Decomposing Inequality in Energy-Related CO2 Emissions by Source and Source Increment: The Roles of Production and Residential Consumption." *Energy Policy* 107 (August): 698–710. https://doi.org/10.1016/j.enpol.2017.05.003.

Chen, Ruijun, and Yaw-Shyan Tsay. 2022. "Carbon Emission and Thermal Comfort Prediction Model for an Office Building Considering the Contribution Rate of Design Parameters." *Energy Reports* 8 (November): 8093–8107. https://doi.org/10.1016/j.egyr.2022.06.012.

Chen, Ruijun, Yaw-Shyan Tsay, and Shiwen Ni. 2022. "An Integrated Framework for Multi-Objective Optimization of Building Performance: Carbon Emissions, Thermal Comfort, and Global Cost." *Journal of Cleaner Production* 359 (July): 131978. https://doi.org/10.1016/j.jclepro.2022.131978.

Chen, Zhengshu, Yanqiu Cui, Haichao Zheng, and Qiao Ning. 2024. "Optimization and Prediction of Energy Consumption, Light and Thermal Comfort in Teaching Building Atriums Using NSGA-II and Machine Learning." *Journal of Building Engineering* 86 (June): 108687. https://doi.org/10.1016/j.jobe.2024.108687.

Choi, Younhee, Doosam Song, Sungmin Yoon, and Junemo Koo. 2021. "Comparison of Factorial and Latin Hypercube Sampling Designs for Meta-Models of Building Heating and Cooling Loads." *Energies* 14, no. 2 (January): 512. https://doi.org/10.3390/en14020512.

City Multi, n.d., Mitsubishi Electric Klima Sistemleri, 2014.

Crick, M.J., and Hill, M.D. “The role of sensitivity analysis in assessing uncertainty.” Uncertainty analysis for performance assessments of radioactive waste disposal systems (1987).

D’Agostino, Diana, Federico Minelli, and Francesco Minichiello. 2023. “New Genetic Algorithm-Based Workflow for Multi-Objective Optimization of Net Zero Energy Buildings Integrating Robustness Assessment.” *Energy and Buildings* 284 (April): 112841. https://doi.org/10.1016/j.enbuild.2023.112841.

Delmastro, Chiara. 2022. “Buildings.” *International Energy Agency.*

DesignBuilder Software LTD – Home. Accessed March 5, 2024. https://designbuilder.co.uk/.

Ekici, Berk, Ioannis Chatzikonstantinou, Sevil Sariyildiz, M. Fatih Tasgetiren, and Quan-Ke Pan. 2016. “A Multi-Objective Self-Adaptive Differential Evolution Algorithm for Conceptual High-Rise Building Design.” *2016 IEEE Congress on Evolutionary Computation (CEC)* (July). https://doi.org/10.1109/cec.2016.7744069.

Encinas, Felipe, and André De Herde. 2013. “Sensitivity Analysis in Building Performance Simulation for Summer Comfort Assessment of Apartments from the Real Estate Market.” *Energy and Buildings* 65 (October): 55–65. https://doi.org/10.1016/j.enbuild.2013.05.047.

EnergyPlus, n.d., Accessed March 5, 2024. https://energyplus.net/.

Ergül, Engin Ufuk. 2010. “Multi-objective genetic algorithms: Fundamentals and applications.” PhD diss., University of Ondokuz Mayıs.

Escandón, Rocío, Fabrizio Ascione, Nicola Bianco, Gerardo Maria Mauro, Rafael Suárez, and Juan José Sendra. 2019. “Thermal Comfort Prediction in a Building Category: Artificial Neural Network Generation from Calibrated Models for a Social Housing Stock in Southern Europe.” *Applied Thermal Engineering* 150 (March): 492–505. https://doi.org/10.1016/j.applthermaleng.2019.01.013.

European Commissions, “New rules to boost energy performance of buildings,” *An official website of the European Union*, December 7, 2023, https://ec.europa.eu/commission/presscorner/detail/en/IP_23_6423.

Eurostat. 2024. “Heating and Cooling Degree Days – Statistics.” Accessed March 25, 2024. https://ec.europa.eu/eurostat/statistics-explained/index.php?title=Heating_and_cooling_degree_days_-_statistics#Heating_and_cooling_degree_days_at_EU_level.

Fanger, Povl Ole. 1986. "Thermal Environment—Human Requirements." E*nvironmentalist* 6.4: 275-278.

Gao, Bo, Xiaoyue Zhu, Jing Ren, Jingyu Ran, Moon Keun Kim, and Jiying Liu. 2023. “Multi-Objective Optimization of Energy-Saving Measures and Operation Parameters for a Newly Retrofitted Building in Future Climate Conditions: A Case Study of an Office Building in Chengdu.” *Energy Reports* 9 (December): 2269–85. https://doi.org/10.1016/j.egyr.2023.01.049.

General Directorate of Meteorology. 2022. “Resmi İstatistikler.” Accessed March 3, 2024. https://www.mgm.gov.tr/veridegerlendirme/il-ve-ilceler-istatistik.aspx?k=A

General Directorate of Meteorology. 2024. “Isıtma ve Soğutma Gün Dereceleri.” Accessed March 3, 2024. https://www.mgm.gov.tr/veridegerlendirme/gun-derece.aspx?g=merkez&m=35-00&y=2023&a=12.

Gercek, Mumine, and Zeynep Durmuş Arsan. 2019. “Energy and Environmental Performance Based Decision Support Process for Early Design Stages of Residential Buildings under Climate Change.” *Sustainable Cities and Society* 48 (July): 101580. https://doi.org/10.1016/j.scs.2019.101580.

Google Earth. “Fabrika Loft +1.” Accessed March 24, 2024. https://earth.google.com/web/search/Fabrika+Loft+%2b1/@38.4487563,27.1903816,6.24267272a,805.93712719d,35y,300.75835639h,45t,0r/data=CnoaUBJKCiUweDE0Yjk2M2RhNjQ2MWU4NzM6MHhiOTMyNGM0MzI3NWFlY2EyGd4vsNhwOUNAIZnCOdm8MDtAKg9GYWJyaWthIExvZnQgKzEYAiABIiYKJAn85vkS0DlDQBG2EYG3tDhDQBk5Iq3cbjI7QCH4o7bb3C87QDoDCgEw.

Google Maps. 2024. “Fabrika Loft +1.” Accessed March 24, 2024. https://www.google.com/maps/place/Fabrika+Loft+%2B1/@38.4487559,27.1801033,15z/data=!3m1!4b1!4m6!3m5!1s0x14b963da6461e873:0xb9324c43275aeca2!8m2!3d38.4487563!4d27.1903816!16s%2Fg%2F11fmy_c9tp?entry=ttu.

Gou, Shaoqing, Vahid Nik, Jean-Louis Scartezzini, Qun Zhao, and Zhengrong Li. 2018. “Passive Design Optimization of Newly-Built Residential Buildings in Shanghai for Improving Indoor Thermal Comfort While Reducing Building Energy Demand.” *Energy and Buildings* 169 (June): 484–506. https://doi.org/10.1016/j.enbuild.2017.09.095.

Hamby, David. 1994. “A review of techniques for parameter sensitivity analysis of environmental models.” *Environmental Monitoring and Assessment*, 32: 135–154. doi:10.1007/bf00547132.

Harvey, Danny. 2020. “Using modified multiple heating-degree-day (HDD) and cooling-degree-day (CDD) indices to estimate building heating and cooling loads.” *Energy and Buildings*, 229: 110475. doi:10.1016/j.enbuild.2020.110475.

Hawila, Abed Al Waheed, and Abdelatif Merabtine. 2021. “A Statistical-Based Optimization Method to Integrate Thermal Comfort in the Design of Low Energy Consumption Building.” *Journal of Building Engineering* 33 (January): 101661. https://doi.org/10.1016/j.jobe.2020.101661.

Haykin, Simon. 2009. *Neural Networks and Learning Machines.* New Jersey: Pearson Education.

Hegazy, Tarek, and Amr Ayed. 1998. “Neural Network Model for Parametric Cost Estimation of Highway Projects.” *Journal of Construction Engineering and Management* 124, no. 3 (May): 210–18. https://doi.org/10.1061/(asce)0733-9364(1998)124:3(210).

Helton, Jon, Jay Johnson, Cedric Sallaberry, and Curtis Storlie. 2006. “Survey of Sampling-Based Methods for Uncertainty and Sensitivity Analysis.” *Reliability Engineering & System Safety* 91, no. 10–11 (October): 1175–1209. https://doi.org/10.1016/j.ress.2005.11.017.

Hensen, Jan L. 2004. “Towards more effective use of building performance simulation in design,” in *Proceedings of the 7th International Conference on Design & Decision Support Systems in Architecture and Urban Planning,* (July), 2-5.

HOBO Temperature/Relative Humidity Data Logger. 2024 “HOBO Temperature/Relative Humidity Data Logger.” Accessed March 5, 2024. https://www.onsetcomp.com/products/data-loggers/u12-011.

Huang, Huilan, Wan Iman Binti Wan Mohd Nazi, Yiqun Yu, and Yaodong Wang. 2020. “Energy Performance of a High-Rise Residential Building Retrofitted to Passive Building Standard – a Case Study.” *Applied Thermal Engineering* 181 (November): 115902. https://doi.org/10.1016/j.applthermaleng.2020.115902.

Huo, Haie, Xiaoxue Deng, Yanhuan Wei, Zhibo Liu, Mingrong Liu, and Liu Tang. 2024. “Optimization of Energy-Saving Renovation Technology for Existing Buildings in a Hot Summer and Cold Winter Area.” *Journal of Building Engineering* 86 (June): 108597. https://doi.org/10.1016/j.jobe.2024.108597.

Hwang, C. L., and Masud Abu Syed M. *Multiple objective decision making, methods and applications: A state-of-the-art survey*. Berlin: Springer-Verlag, 1979.

Hwang, Ruey-Lung, and Wei-An Chen. 2022. “Creating Glazed Facades Performance Map Based on Energy and Thermal Comfort Perspective for Office Building Design Strategies in Asian Hot-Humid Climate Zone.” *Applied Energy* 311 (April): 118689. https://doi.org/10.1016/j.apenergy.2022.118689.

Ilbeigi, Marjan, Mohammad Ghomeishi, and Ali Dehghanbanadaki. 2020. “Prediction and Optimization of Energy Consumption in an Office Building Using Artificial Neural Network and a Genetic Algorithm.” *Sustainable Cities and Society* 61 (October): 102325. https://doi.org/10.1016/j.scs.2020.102325.

Intergovernmental Panel on Climate Change. 2018. “IPCC Special Report on Global Warming of 1.5ºC.” https://www.birbucukderece.com/bilimsel-kaynaklar/ipcc-1-5-c-raporu.

Ioannou, Anastasios, and Laure Itard. 2015. “Energy Performance and Comfort in Residential Buildings: Sensitivity for Building Parameters and Occupancy.” *Energy and Buildings* 92 (April): 216–33. https://doi.org/10.1016/j.enbuild.2015.01.055.

Izmir Development Agency. *İzmir İli Kırsal ve Kentsel Alanlarının Tespitine Yönelik Analiz Çalışması.* İzmir: eValue, 2021. https://izka.org.tr/wp-content/uploads/2021/10/kirsal_kentsel_alanlarinin_tespiti.pdf.

Kabakçı, Oğuz Kürşat. “Binalarda Enerji Verimliliği.” *Ministry of Energy and Natural Resources,* 2017. https://www.dunyaenerji.org.tr/wp-content/uploads/2019/11/21112019Sunum.pdf.

Kang, Yiting, Dongjie Zhang, Yu Cui, Wei Xu, Shilei Lu, Jianlin Wu, and Yiqun Hu. 2024. “Integrated Passive Design Method Optimized for Carbon Emissions, Economics, and Thermal Comfort of Zero-Carbon Buildings.” *Energy* 295 (May): 131048. https://doi.org/10.1016/j.energy.2024.131048.

Khani, Ali, Mehdi Khakzand, and Mohsen Faizi. 2022. “Multi-Objective Optimization for Energy Consumption, Visual and Thermal Comfort Performance of Educational Building (Case Study: Qeshm Island, Iran).” *Sustainable Energy Technologies and Assessments* 54 (December): 102872. https://doi.org/10.1016/j.seta.2022.102872.

Konak, Abdullah, David Coit, and Alice Smith. 2006. “Multi-Objective Optimization Using Genetic Algorithms: A Tutorial.” *Reliability Engineering & System Safety* 91, no. 9 (September): 992–1007. https://doi.org/10.1016/j.ress.2005.11.018.

Köppen, Wladimir, Esther Volken, and Stefan Brönnimann. 2011. “The thermal zones of the earth according to the duration of hot, moderate and cold periods and to the impact of heat on the organic world (Translated from: Die Wärmezonen der Erde, nach der Dauer der heissen, gemässigten und kalten Zeit und nach der Wirkung der Wärme auf die organische Welt betrachtet, Meteorol Z 1884, 1, 215-226).” *Meteorologische Zeitschrift* 20: 351-360.

Koutsoyiannis, A., Ümit Şenesen, and Gülay Günlük-Şenesen.1989. *Ekonometri Kuramı: Ekonometri Yöntemlerinin tanıtımına giriş*. Ankara: Verso.

Krarti, Moncef. 2023. “Optimal Energy Performance of Dynamic Sliding and Insulated Shades for Residential Buildings.” *Energy* 263 (January): 125699. https://doi.org/10.1016/j.energy.2022.125699.

Kristiansen, Tobias, Faisal Jamil, Ibrahim A. Hameed, and Mohamed Hamdy. 2022. “Predicting Annual Illuminance and Operative Temperature in Residential Buildings Using Artificial Neural Networks.” *Building and Environment* 217 (June): 109031. https://doi.org/10.1016/j.buildenv.2022.109031.

Levenberg, Kenneth. 1944. "A method for the solution of certain non-linear problems in least squares." *Quarterly of applied mathematics* 2.2: 164-168.

Loeppky, Jason, Jerome Sacks, and William J. Welch. 2009. “Choosing the sample size of a computer experiment: A practical guide.” *Technometrics* 51: 366–376. doi:10.1198/tech.2009.08040.

Long, Luong Duc. 2023. “An AI-Driven Model for Predicting and Optimizing Energy-Efficient Building Envelopes.” *Alexandria Engineering Journal* 79 (September): 480–501. https://doi.org/10.1016/j.aej.2023.08.041.

Lu, Shuai, Jingyu Li, and Borong Lin. 2020. “Reliability Analysis of an Energy-Based Form Optimization of Office Buildings under Uncertainties in Envelope and Occupant Parameters.” *Energy and Buildings* 209 (February): 109707. https://doi.org/10.1016/j.enbuild.2019.109707.

Lv, You, Jizhen Liu, and Tingting Yang. 2013. “Comparative Studies of Model Performance Based on Different Data Sampling Methods.” *2013 25th Chinese Control and Decision Conference (CCDC)*. https://doi.org/10.1109/ccdc.2013.6561406.

Ma, Xiangmeng, Yunlei Guan, Rui Mao, Simi Zheng, and Qun Wei. 2021. “Modeling of Lead Removal by Living Scenedesmus Obliquus Using Backpropagation (BP) Neural Network Algorithm.” *Environmental Technology & Innovation* 22 (May): 101410. https://doi.org/10.1016/j.eti.2021.101410.

Magnier, Laurent, and Fariborz Haghighat. 2010. “Multiobjective Optimization of Building Design Using TRNSYS Simulations, Genetic Algorithm, and Artificial Neural Network.” *Building and Environment* 45, no. 3 (March): 739–46. https://doi.org/10.1016/j.buildenv.2009.08.016.

Mara, Thierry A. and Stefano Tarantola. 2008. “Application of global sensitivity analysis of model output to building thermal simulations.” *Building Simulation 1*: 290–302. doi:10.1007/s12273-008-8129-5.

Marquardt, Donald. 1963. "An algorithm for least-squares estimation of nonlinear parameters." *Journal of the society for Industrial and Applied Mathematics* 11.2: 431-441.

MathWorks. 2024. “Choose Neural Network Input-Output Processing Functions.” Accessed March 12, 2024. https://ch.mathworks.com/help/deeplearning/ug/choose-neural-network-input-output-processing-functions.html

Mckay, M. D., Richard J. Beckman, and William Conover. 2000. “A Comparison of Three Methods for Selecting Values of Input Variables in the Analysis of Output from a Computer Code.” *Technometrics* 42, no. 1 (February): 55. https://doi.org/10.2307/1271432.

Miettinen, Kaisa. 1999. “Nonlinear Multiobjective Optimization.” PhD diss., University of Jyvaskyla.

Mitsubishi Klima. 2020. “Cop Ve Eer Nedir? Klimalardaki İşlevi ve Değerleri Nedir?” Accessed May 9, 2024. https://www.iklimplus.com/cop-nedir/#:~:text=G%C3%BCn%C3%BCm%C3%BCz%20teknolojisinde%20%C3%BCretilen%20klimalarda%20COP,elektrik%20harcayarak%20%C3%A7ok%20%C4%B1s%C4%B1tma%20sa%C4%9Flar.

Mostafazadeh, Farzad, Saeed Jalilzadeh Eirdmousa, and Mehdi Tavakolan. 2023. “Energy, Economic and Comfort Optimization of Building Retrofits Considering Climate Change: A Simulation-Based NSGA-III Approach.” *Energy and Buildings* 280 (February): 112721. https://doi.org/10.1016/j.enbuild.2022.112721.

Mukkavaara, Jani, and Farshid Shadram. 2021. “An Integrated Optimization and Sensitivity Analysis Approach to Support the Life Cycle Energy Trade-off in Building Design.” *Energy and Buildings* 253 (December): 111529. https://doi.org/10.1016/j.enbuild.2021.111529.

Nejat, Payam, Fatemeh Jomehzadeh, Mohammad Madri Taheri, Mohammad Gohari, Muhd Zaimi Abd. Majid. 2015. “A global review of energy consumption, CO2 emissions and policy in the residential sector (with an overview of the top ten CO2 emitting countries).” *Renewable and Sustainable Energy Reviews*, 43 (March): 843-862. doi:10.1016/j.rser.2014.11.066.

Nguyen, Anh-Tuan, Sigrid Reiter, and Philippe Rigo. 2014. “A Review on Simulation-Based Optimization Methods Applied to Building Performance Analysis.” *Applied Energy* 113 (January): 1043–58. https://doi.org/10.1016/j.apenergy.2013.08.061.

Ouanes, Sara, and Leila Sriti. 2024. “Regression-Based Sensitivity Analysis and Multi-Objective Optimisation of Energy Performance and Thermal Comfort: Building Envelope Design in Hot Arid Urban Context.” *Building and Environment* 248 (January): 111099. https://doi.org/10.1016/j.buildenv.2023.111099.

Özerol, Gizem, and Semra Arslan Selçuk. 2023. “Bioclimatic Façade Design Based on Daylight Parameter and Optimization of Alternatives through Genetic Algorithms: An Office Building in Ankara.” *PLANARCH - Design and Planning Research* (March). https://doi.org/10.5152/planarch.2023.221940.

Rabani, Mehrdad, Habtamu Bayera Madessa, and Natasa Nord. 2021. “Achieving Zero-Energy Building Performance with Thermal and Visual Comfort Enhancement through Optimization of Fenestration, Envelope, Shading Device, and Energy Supply System.” *Sustainable Energy Technologies and Assessments* 44 (April): 101020. https://doi.org/10.1016/j.seta.2021.101020.

Rasouli, Mohammad, Gaoming Ge, Carey James Simonson, and Robert William Besant. 2013. “Uncertainties in Energy and Economic Performance of HVAC Systems and Energy Recovery Ventilators Due to Uncertainties in Building and HVAC Parameters.” *Applied Thermal Engineering* 50, no. 1 (January): 732–42. https://doi.org/10.1016/j.applthermaleng.2012.08.021.

Rosso, Federica, Virgilio Ciancio, Jacopo Dell'Olmo, and Ferdinando Salata. 2020. "Multi-Objective Optimization of Building Retrofit in the Mediterranean Climate by Means of Genetic Algorithm Application." *Energy and Buildings* 216 (June): 109945. https://doi.org/10.1016/j.enbuild.2020.109945.

Sainlez, Matthieu, and Georges Heyen. 2011. "Recurrent Neural Network Prediction of Steam Production in a Kraft Recovery Boiler." *Computer Aided Chemical Engineering*: 1784–88. https://doi.org/10.1016/b978-0-444-54298-4.50135-5.

Saltelli, Andrea. 1999. "Sensitivity Analysis: Could Better Methods Be Used?" *Journal of Geophysical Research: Atmospheres* 104, no. D3 (February): 3789–93. https://doi.org/10.1029/1998jd100042.

Saltelli, Andrea. 2007. *Sensitivity analysis in practice: A guide to assessing scientific models*. Chichester: John Wiley & Sons.

Saryazdi, Seyed Mohammad, Alireza Etemad, Ali Shafaat, and Ammar M. Bahman. 2022. "Data-Driven Performance Analysis of a Residential Building Applying Artificial Neural Network (ANN) and Multi-Objective Genetic Algorithm (GA)." *Building and Environment* 225 (November): 109633. https://doi.org/10.1016/j.buildenv.2022.109633.

Saurbayeva, Assemgul, Shazim Ali Memon, and Jong Kim. 2023. "Sensitivity Analysis and Optimization of PCM Integrated Buildings in a Tropical Savanna Climate." *Journal of Building Engineering* 64 (April): 105603. https://doi.org/10.1016/j.jobe.2022.105603.

Si, Binghui, Jianguo Wang, Xinyue Yao, Xing Shi, Xing Jin, and Xin Zhou. 2019. "Multi-Objective Optimization Design of a Complex Building Based on an Artificial Neural Network and Performance Evaluation of Algorithms." *Advanced Engineering Informatics* 40 (April): 93–109. https://doi.org/10.1016/j.aei.2019.03.006.

Storlie, Curtis B., Laura P. Swiler, Jon C. Helton, and Cedric J. Sallaberry. 2009. "Implementation and Evaluation of Nonparametric Regression Procedures for Sensitivity Analysis of Computationally Demanding Models." *Reliability*

Engineering & System Safety 94, no. 11 (November): 1735–63. https://doi.org/10.1016/j.ress.2009.05.007.

T.C. İzmir Valiliği, Doğayla Dost. Accessed April 13, 2024. http://www.izmir.gov.tr/cografi-bilgiler-bitki-ortusu-ve-ormanlar.

Tabassum, Mujahid, and Kuruvilla Mathew. 2014. "A Genetic Algorithm Analysis towards Optimization Solutions." *International Journal of Digital Information and Wireless Communications* 4, no. 1: 124–42. https://doi.org/10.17781/p001091.

The Merriam-Webster Dictionary, s.v. "Optimization (n.)," accessed May 4, 2024, https://www.merriam-webster.com/dictionary/optimization.

Tian, Wei. 2013. "A Review of Sensitivity Analysis Methods in Building Energy Analysis." *Renewable and Sustainable Energy Reviews* 20 (April): 411–19. https://doi.org/10.1016/j.rser.2012.12.014.

TUIK. 2023. "Energy Accounts, 2021." Accessed April 16, 2024. https://data.tuik.gov.tr/Bulten/Index?p=Energy-Accounts-2021-49751&dil=2

TUIK. 2023. "TUIK Veri Portalı." Accessed March 3, 2024. https://data.tuik.gov.tr/Search/Search?text=n%C3%BCfus.

Tunç, Ömer. 2021. "Türkiye'deki Bina Sayıları (The Number of Buildings in Turkey)." Accessed April 16,2024. https://www.researchgate.net/publication/349829931_Turkiye'deki_Bina_Sayilari_The_Number_of_Buildings_in_Turkey.

Turkish Standard. 2024. "TS 2164 Principles For the Prefaration of the Projects of the Central Heating Systems." Accessed March 9, 2024. https://intweb.tse.org.tr/standard/standard/Standard.aspx?081118051115108051104119110104055047105102120088111043113104073101109106079048112048122052117048.

Ulukavak Harputlugil, Gülsu. 2009. "Enerji Performansı Öncelikli Mimari Tasarım Sürecinin İlk Aşamasında Kullanılabilecek Tasarıma Destek Değerlendirme Modeli," PhD diss., University of Gazi.

Wan, Kevin K.W., Danny H. W. Li, Dalong Liu and Joseph C. Lam. 2011. “Future trends of building heating and cooling loads and energy consumption in different climates.” *Building and Environment,* 46, pp. 223-234. doi: 10.1016/j.buildenv.2010.07.016.

Wang, Yuanping, Lang Hu, Lingchun Hou, Weiguang Cai, Lin Wang, and Yu He. 2023. “Study on Energy Consumption, Thermal Comfort and Economy of Passive Buildings Based on Multi-Objective Optimization Algorithm for Existing Passive Buildings.” *Journal of Cleaner Production* 425 (November): 138760. https://doi.org/10.1016/j.jclepro.2023.138760.

Wetter, Michael, and Jonathan Wright. 2004. “A Comparison of Deterministic and Probabilistic Optimization Algorithms for Nonsmooth Simulation-Based Optimization.” *Building and Environment* 39, no. 8 (August): 989–99. https://doi.org/10.1016/j.buildenv.2004.01.022.

Wu, Chengjin, Haize Pan, Zhenhua Luo, Chuan Liu, and Hulongyi Huang. 2024. “Multi-Objective Optimization of Residential Building Energy Consumption, Daylighting, and Thermal Comfort Based on Bo-XGBoost-NSGA-II.” *Building and Environment* 254 (April): 111386. https://doi.org/10.1016/j.buildenv.2024.111386.

Xu, Luyi, Junjie Liu, Jingjing Pei, and Xu Han. 2013. “Building Energy Saving Potential in Hot Summer and Cold Winter (HSCW) Zone, China—Influence of Building Energy Efficiency Standards and Implications.” *Energy Policy* 57 (June): 253–62. https://doi.org/10.1016/j.enpol.2013.01.048.

Xu, Yizhe, Chengchu Yan, Guanqun Wang, Jingfeng Shi, Kai Sheng, Jun Li, and Yanlong Jiang. 2023. “Optimization Research on Energy-Saving and Life-Cycle Decarbonization Retrofitting of Existing School Buildings: A Case Study of a School in Nanjing.” *Solar Energy* 254 (April): 54–66. https://doi.org/10.1016/j.solener.2023.03.006.

Yandex Maps. 2024. “375 Sok., No:1.” Accessed March 24, 2024. https://yandex.com.tr/harita/115715/bornova/house/375_sok_1/Zk4Ydw5gSkMHQF1ifXh1eXtrZQ==/?ll=27.191954%2C38.447705&z=16.62.

Yaşar, Yalçın, and Kübra Sumer Haydaraslan. 2023. “Evaluation of Building Design Strategies According to the Effects of Climate Change by Simulation-Based Optimisation: A Case Study for Housing in Different Climate Regions.” *International Journal of Global Warming* 30, no. 1: 33. https://doi.org/10.1504/ijgw.2023.10055641.

Yigit, Sadik. 2021. “A Machine-Learning-Based Method for Thermal Design Optimization of Residential Buildings in Highly Urbanized Areas of Turkey.” *Journal of Building Engineering* 38 (June): 102225. https://doi.org/10.1016/j.jobe.2021.102225.

Yıldız, Yusuf, and Zeynep Durmuş Arsan. 2011. “Identification of the Building Parameters That Influence Heating and Cooling Energy Loads for Apartment Buildings in Hot-Humid Climates.” *Energy* 36, no. 7 (July): 4287–96. https://doi.org/10.1016/j.energy.2011.04.013.

Yildiz, Yusuf, Koray Korkmaz, Türkan Göksal Özbalta, and Zeynep Durmus Arsan. 2012. “An Approach for Developing Sensitive Design Parameter Guidelines to Reduce the Energy Requirements of Low-Rise Apartment Buildings.” *Applied Energy* 93 (May): 337–47. https://doi.org/10.1016/j.apenergy.2011.12.048.

Yu, Wei, Baizhan Li, Hongyuan Jia, Ming Zhang, and Di Wang. 2015. “Application of Multi-Objective Genetic Algorithm to Optimize Energy Efficiency and Thermal Comfort in Building Design.” *Energy and Buildings* 88 (February): 135–43. https://doi.org/10.1016/j.enbuild.2014.11.063.

Yüzük, Feyyaz. 2019. “Çoklu Regresyon Analizi ve Yapay Sinir Ağları ile Türkiye Enerji Talep Tahmini.” PhD diss., University of Sivas Cumhuriyet.

Zhang, Lei, Guochen Sang, Xiaoling Cui, and Weixiao Han. 2022. “Design Optimization of Rural Building in Dry-Hot and Dry-Cold Area Using a Back Propagation (BP) Neural Network.” *Energy and Buildings* 259 (March): 111899. https://doi.org/10.1016/j.enbuild.2022.111899.